ISTANBUL TECHNICAL UNIVERSITY ★ EURASIA INSTITUTE OF EARTH SCIENCES

RECONSTRUCTION OF THE PALEOCLIMATE ON DEDEGÖL MOUNTAIN WITH PALEOGLACIAL RECORDS AND NUMERICAL ICE FLOW MODELS

M.Sc. THESIS

Adem CANDAŞ

Department of Solid Earth Sciences

Geodynamics Programme

JUNE 2017

ISTANBUL TECHNICAL UNIVERSITY ★ EURASIA INSTITUTE OF EARTH SCIENCES

RECONSTRUCTION OF THE PALEOCLIMATE ON DEDEGÖL MOUNTAIN WITH PALEOGLACIAL RECORDS AND NUMERICAL ICE FLOW MODELS

M.Sc. THESIS

Adem CANDAŞ
(602151009)

Department of Solid Earth Sciences

Geodynamics Programme

Thesis Advisor: Assoc. Prof. Dr. Mehmet Akif SARIKAYA

JUNE 2017

İSTANBUL TEKNİK ÜNİVERSİTESİ ★ AVRASYA YER BİLİMLERİ ENSTİTÜSÜ

ESKİ BUZUL KAYITLARI VE SAYISAL BUZUL AKIŞ MODELLERİYLE DEDEGÖL DAĞI PALEOİKLİM REKONSTRÜKSÜYONU

YÜKSEK LİSANS TEZİ

Adem CANDAŞ
(602151009)

Katı Yer Bilimleri Anabilim Dalı

Jeodinamik Programı

Tez Danışmanı: Doç. Dr. Mehmet Akif SARIKAYA

HAZİRAN 2017

Adem CANDAŞ, a M.Sc. student of ITU Eurasia Institute of Earth Sciences 602151009 successfully defended the thesis entitled "RECONSTRUCTION OF THE PALEO-CLIMATE ON DEDEGÖL MOUNTAIN WITH PALEOGLACIAL RECORDS AND NUMERICAL ICE FLOW MODELS", which he prepared after fulfilling the requirements specified in the associated legislations, before the jury whose signatures are below.

Thesis Advisor :   **Assoc. Prof. Dr. Mehmet Akif SARIKAYA**   ....
Istanbul Technical University

Jury Members :   **Prof. Dr. Ömer Lütfi ŞEN**   ....
Istanbul Technical University

Assist. Prof. Dr. Cihan BAYRAKDAR   ....
Istanbul University

Date of Submission :   **May 5, 2017**
Date of Defense :   **June 8, 2017**

"...to my lovely wife Eda"

FOREWORD

I would like to thank my advisor, Mehmet Akif Sarıkaya, who encouraged me to study on paleoglaciers and glacier modeling. This work would not be come into being without his countless assistance and unconditional help. I also would like to thank Attila Çiner for his guiding comments on glacier modeling. I will never forget his teachings in my first field study at Dedegöl Mountain. I owe great appreciation to Ömer Lütfi Şen, who provided valuable assistance and advice in climatic reconstructions. His suggestions and comments on climate modeling were very helpful to the study.

Many people have also provided valuable assistance and advice in completing this work. I would like to thank Oğuzhan Köse for his friendship in the field and his dedicated work in preparing maps used in this study. I also would like to thank Salih Gülşen for his helping on generating codes. My recognitions are also due to Constantine Khroulev and PSIM team members who provided invaluable assistance and expertise about using Parallel Ice Sheet Model. Thanks to Nüzhet Dalfes, who provided precious comments on ice flow model. I thank my thesis committee member Cihan Bayrakdar from Istanbul University for sharing with me his comments and advice. Special thanks to Pınargözü Hostel and its personnel who greatly host us during our visits to Yenişarbademli. I also would like to thank Kurucuova residents for their help and logistic support in the field.

Finally, I am deeply grateful to my wife, my mother and my friends for their endless support and patience during my studies in Eurasia Institute of Earth Sciences.

June 2017   Adem CANDAŞ
                                                                           (Mechanical Engineer)

x

TABLE OF CONTENTS

ABBREVIATIONS

BP   : Before Present
DEM   : Digital Elevation Model
ELA   : Equilibrium Line Altitude
GIS   : Geographic Information Systems
GPS   : Global Positioning System
lat, lon   : Latitude and Longitude
LGM   : Last Glacial Maximum
M, N   : Number of Grids on x and y axis
prec   : Precipitation
PDD   : Positive Degree Day
PISM   : Parallel Ice Sheet Modeling
SIA   : Shallow Ice Approximation
SSA   : Shallow Shelf Approximation
x, y   : 2-D Coordinate axes

SYMBOLS

A	: Coefficient for velocity due to ice deformation
acc	: Yearly accumulation
abl	: Yearly ablation
B	: Coefficient for velocity due to ice sliding
bheatflx	: Basal Heat Flux
ddfi	: Degree Day Factor for Ice
ddfs	: Degree Day Factor for Snow
f	: Deformation and sliding parameter
g	: Gravitational acceleration
h	: Ice surface elevation
H	: Glacier thickness
k	: Non-linear conductance coefficient
iarea	: Glacier area
ivol	: Glacier volume
M	: Mass balance
q	: Ice flux
$\mathbf{u_d}$	: Column integrated ice velocity deformation component
$\mathbf{u_s}$	: Column integrated ice velocity sliding component
pamp	: Precipitation Multiplier
ρ	: Ice density
rf	: Refreeze Factor
σ	: Standard deviation with respect to the monthly mean temperature
surtemp	: Ice Surface Temperature
$\mathbf{T_{mon}}$	: Monthly mean ice surface temperature
τ	: Basal shear stress
thk	: Glacier Thickness in PISM
toffset	: Temperature Offset
topg	: Topography on 2-D Coordinate System
ye	: End year of simulation
ys	: Start year of simulation

LIST OF TABLES

LIST OF FIGURES

RECONSTRUCTION OF THE PALEOCLIMATE ON DEDEGÖL MOUNTAIN WITH PALEOGLACIAL RECORDS AND NUMERICAL ICE FLOW MODELS

SUMMARY

The current glaciers in Anatolia have been gradually disappearing with the ongoing climate changes. There are geological proxies left behind from the ice, which is an indication of paleoclimate changes. It is known that the glaciers carry large amounts of sediments in their life cycles. After they retreat, these sediments remain where they were. They are called as moraine, which has been well preserved in some Anatolia mountains. In this study, the paleoglaciers that existed in the Late Quaternary period on the Dedegöl Mountain were reconstructed under the prescribed paleoclimatic conditions. The main idea is to recreate paleoglaciers under different climatic conditions; it is the recreation of the paleoclimate. This approach, in a sense, is aimed at understanding the past-term climate. Thus the proxies left behind by the glaciers have been used as an important proxy to estimate the paleoclimate conditions.

Dedegöl Mountain is located within the boundaries of Konya and Isparta provinces. The maximum elevation of the mountain is 2997 m above the sea level. Beyşehir Lake is located about 15 km to the east of the study area. 30 $m \times 30$ m resolution digital elevation model of Dedegöl Mountain was used. The model domain is covering 37.5670 - 37.7237 North latitudes and 31.2100 - 31.3667 East longitudes. The model area is about 16.92 $km \times 16.92$ $km = 286$ km^2.

Glacial mass balance was calculated with today's climatic conditions. Then the paleoclimate was modeled. A two-dimensional numerical glacier flow model was written in MATLAB to reconstruct the flow of glaciers under different paleoclimatic conditions. An open source glacier flow model software named Parallel Ice Sheet Model (PISM) was also used.

The glacier valleys in the area are identified during two field studies in the summer months of 2015 and 2016. The Sayacak Glacial Valley on the north, the Elmadere Glacial Valley on the east, the Muslu and Karagöl and the Karçukuru Glacier Valleys in the south and the Kisbe Glacial Valley in the north-west were studied. The moraine crests positions were identified and paleoglacier boundaries were determined. Then, paleoclimatic conditions of that fit the modeled glacier extent were determined.

Positive Degree Days approach was used to calculate the ablation of a glacial. This approach is briefly based on the idea that there is a correlation between the sum of all the temperatures above the melting point and melting of snow (or ice) at the same location over a year. A decrease in glacial mass occurs for days with a temperature higher than 2°C. In the calculation of the accumulation mass, the amount of precipitation in the area is used. If the precipitation occurs at a temperature higher than 0°C degrees, all precipitation occurs as rain. The accumulation linearly increases between 2 and 0°C and it contributes to the annual mass balance. The precipitation

is considered to be entirely snow below 0°C air temperature. Therefore, glacier's annual budget is based on the difference between accumulation and ablation. It is thus possible to establish a direct relationship between the amount of ice in a particular area and climate conditions. In these calculations, factors such as surface energy mass, the cloudiness, and the wind effect can be also used, but these factors are not included in this study.

Previous studies in the region have indicated that paleoclimate was cooler and wetter than present-day climate during the Last Glacial Maximum period. It is stated that the temperatures were 8 to 11°C lower than today, with the precipitation being 20% higher. In this study, temperatures in the model of paleoglaciers were decreased by 8, 9, and 10°C. Precipitation values were increased by 0%, 25% and 50% than today.

The best way as a glacial flow model is to solve the Full Stokes equations. However, the solution of these equations is not efficient in terms of processor requirements and time. Different models have been developed for the flow of glaciers moving. In this work, open source software named Parallel Ice Sheet Model (PISM) was used. However, a two-dimensional time-dependent glacial flow model has also been developed. The results obtained in these two models were discussed. PISM uses the netCDF file type as input. In this file, data such as temperature, precipitation, glacial thickness were stored. Within the scope of the thesis, a code was developed to provide appropriate data input for PISM. This code calculates the glacial mass balance under the paleoclimatic conditions and then transforms this data into an input for PISM.

The results obtained from the study include: (1) although the Parallel Ice Sheet Model (PISM) has been developed for modeling larger-scale ice sheets, it is proved it can be also used as a model for valley glaciers, such as Dedegöl Glacier Valleys (2) a temperature depression between 10°C with an increase in precipitation of 25%, and 9°C with 25% for LGM and Early Holocene respectively, (3) existing digital elevation data used in the models may cause some degradation of glacier reconstruction because they contain moraine deposits of different glacial periods, (4) the results obtained from the models indicate that the moraine deposits formed at different times should be evaluated with different climatic conditions.

There are various sources of uncertainty in the model. Firstly, the resolution of the climate models is 570 m. The digital elevation model resolution is 30 m, so this dismatching can create some uncertainty. However, sudden elevation changes in the digital elevation model can lead to high slopes. From the past, it can be assumed that the boundaries of the changing structure with erosional processes created uncertainty. Moreover, seasonal fluctuations in climate data can create uncertainty in the model.

In further studies, the removal of the moraine deposits to reconstruct the digital elevation model will positively affect the ice flow. This is because these obstacles prevent the glaciers to advance to the past moraines. The glacier flow and climate models applied in this study can be used in other paleoglacial areas in the region which can increase the proxy data about Turkey's paleoclimatic conditions.

ESKİ BUZUL KAYITLARI VE SAYISAL BUZUL AKIŞ MODELLERİYLE DEDEGÖL DAĞI PALEOİKLİM REKONSTRÜKSYONU

ÖZET

Anadolu'da bulunan eski buzullar değişen iklim koşullarıyla beraber giderek yok olmaktadır. İklim değişimlerine karşı oldukça hassas olan buzullardan geriye bazı jeolojik izler kalmıştır. Buzulların ilerlemeleri sırasında kendileriyle birlikte büyük miktarda sediman taşıdıkları bilinmektedir. Geri çekilmeleri sırasında bu yapılar oldukları yerde kalırlar. Türkiye'de iyi saklanmış örneklerine rastlanılan bu yapılara moren adı verilir. Bu çalışmada Türkiye'nin güney batısında yer alan Dedegöl Dağları'nda geç Kuvaterner döneminde var olan buzulların, eski iklim koşulları altında rekonstrüksiyonu yapılan modelleri ile moren depoları eşleştirilmiştir. Burada ana fikir, geçmiş buzulların farklı iklim koşulları altında rekonstrüksiyonu; dolasıyla geçmiş iklimin yeniden yaratılmasıdır. Bu yaklaşım, bir anlamda geçmiş dönem iklimini anlama amacı taşımaktadır. Böylece buzulların geriye bıraktığı izler, geçmiş iklim koşulları hakkında önemli bir proksi verisi olarak kullanılabilir.

Bu çalışmada Anadolu'da Orta Toroslar'ın bir parçası olan Dedegöl Dağı'nın 30 $m \times$ 30 m çözünürlüklü sayısal yükseklik modeli kullanılmıştır. 37.5670 - 37.7237 Kuzey enlemleri ve 31.2100 - 31.3667 Doğu boylamları koordinatları arasında yer alan modelin kapladığı alan 16.92 $km \times$ 16.92 $km = 286\ km^2$ 'dir. Dağın en yüksek noktası denizden 2997 m yüksekliktedir. 15 km doğusunda Beyşehir Gölü bulunmaktadır. Alanın büyük bir kısmı Isparta; bir kısmı ile Konya il sınırları içinde bulunmaktadır.

Modellemede kullanmak amacıyla önce günümüz iklim koşullarıyla, buzulun kütle dengesi hesaplanmış, ardından bölge ikliminin geçmişteki hali modellenmiştir. Geçmiş iklim koşulları altında oluşan buzulların akışı için de 2 boyutlu sayısal buzul akış modeli geliştirilmiştir. Bununla beraber, Parallel Ice Sheet Model (PISM) isimli açık kaynak kodlu bir buzul akış modeli yazılımı aynı amaç için kullanılmıştır.

2015 ve 2016 yaz aylarında gerçekleştirilen iki saha çalışmasında, bölgedeki buzul vadileri incelenmiştir. Buna göre çalışılan vadiler kuzeyde Sayacak Buzul Vadisi, doğuda Elmadere Buzul Vadisi, güney doğuda ve Muslu ve Karagöl, batıda Karçukuru Buzul Vadisi, kuzey batıda ise Kisbe Buzul Vadileridir. Değişen iklim koşulları altında geri çekilmeye başlayan buzullar sonucunda konumları belirli moren depoları ile modellemelerden elde edilen buzul ilerlemelerinin eşleştirilmesi sonucunda söz konusu buzulların ulaştıkları en fazla ilerlemenin hangi iklim koşulları altında olduğu belirlenmiştir.

İklim modelinde, bir buzulun yıllık yüzey kütle dengesi hesabı yapılmaktadır. Yıl boyunca, farklı mevsimlerdeki kar yağışlar, buzulun yıllık bütçesinde artış meydana getirirken; buzulun erimesi, kopan buzul parçaları, buzul tabanı akışları gibi etkenler de azalma meydana getirmektedir. Erime yoluyla meydana gelen azalmanın hesaplanmasında Pozitif Dereceli Günler yaklaşımı uygulanmıştır. Bu yaklaşım özetle erime noktasının üzerindeki tüm sıcaklıkların toplamı ile belli bir periyot boyunca

aynı yerde kar veya buzun erimesi arasında bir korelasyon olduğu fikrine dayanır. Buna göre yıl içinde sıcaklığı 0°C dereceden yüksek olan günler için buzul kütlesinde azalma oluşmaktadır. Buzul kütlesindeki birikimin hesaplanmasında ise, meydana gelen yağışın miktarı kullanılmaktadır. Yağışın 2°C dereceden yüksek sıcaklıkta meydana gelmesi durumunda kütle dengesine ekleme yapılmamaktadır. 0 ile 2°C derece arasında ise doğrusal bir şekilde arttırılan kütle dengesi, 0°C'nin altında ise tamamen kar olarak yıllık buzul bütçesine katkı sağlamaktadır. Bir başka ifadeyle yüzey kütle dengesi hesabında, 0°C sıcaklığın altında gerçekleşen yağışlar tamamen kar olarak kabul edilmektedir. Buzulun yıllık bütçesi, buzul kütlesindeki birikimin ve azalımın farkı alınarak bulunmaktadır. Böylece belirli bir alandaki buzulun miktarı ile iklim koşulları arasında doğrudan bir ilişki kurmak mümkündür. Bu hesaplamalarda, yüzey enerji dengesi, buzul alanındaki bulutluluk oranı ve rüzgar etkisi gibi faktörler de bulunmaktadır, ancak bu çalışmada bu etmenlere yer verilmemiştir.

Önceki çalışmalarda belirtilen geçmiş iklim modelleri Son Buzul Maksimum dönemi boyunca iklimin günümüz ikliminden daha soğuk ve daha yağışlı olduğunu ortaya koymaktadır. Sıcaklıkların günümüzden 8 ile 11°C derece daha düşük olduğu, bununla beraber yağışın %20 daha fazla olduğu belirtilmektedir. Bu çalışmada, geçmiş dönem buzullarının modellemesinde sıcaklıklar günümüze göre 8, 9 ve 10°C derece azaltılmış; yağış değerleri ilk durumda sabit tutulmuş, ardından %25 ve %50 artırılmıştır.

Buzul akış modeli olarak en iyi yöntem Tam Stokes Denklemlerini çözmektir. Ancak bu denklemlerin çözümü işlemci gereksinimleri ve zaman açısından verimli değildir. Yarı katı, yarı akışkan hamurumsu bir yapıda hareket eden buzulların akışı için farklı modeller geliştirilmiştir. Bu çalışmada Parallel Ice Sheet Model isimli açık kaynak kodlu yazılım kullanılmıştır. Bununla beraber 2 boyutlu, zamana bağlı bir buzul akış modeli de geliştirilmiştir. Bu iki modelden elde edilen sonuçlar birbirine yakınlık göstermektedir. PISM girdi olarak netCDF dosya türünü kullanmaktadır. Bu dosya içinde, sıcaklık, yağış, buzul kalınlığı gibi veriler saklanmaktadır. Tez kapsamında, PISM için uygun veri girişini sağlamak amacıyla bir kod geliştirilmiştir. Bu kod önce belirtilen iklim koşulları altında buzul kütle dengesini hesaplamakta, ardından bu verileri PISM için bir girdi haline dönüştürmektedir.

Çalışma sonucunda Dedegöl Dağı geçmiş dönem buzullarının sayısal modellemesi yapılmıştır. Buna göre elde edilen sonuçlar, (1) Parallel Ice Sheet Model (PISM) daha büyük boyutlu buz kalkanlarının modellemesi için geliştirilmiş olmasına rağmen, vadi buzullarının modellemesinde de kullanılabilir, (2) günümüze göre 10°C derece sıcaklık düşüşü ve buna eşlik eden %25 yağış artımı ile 9°C derece sıcaklık düşüşü ve %25 yağış artımı sırasıyla LGM ve Erken Halosen dönem iklimleri için elde edilen sonuçlardır, (3) modellerde kullanılan mevcut sayısal yükseklik verileri, farklı buzul dönemlerine ait moren depolarını içermeleri nedeniyle, buzulların yeniden oluşturulmasında bazı farklar yaratabilir, (4) modellerden elde edilen sonuçlar, farklı zamanlarda oluşan moren depolarının, farklı iklim koşulları ile değerlendirilmeleri gerektiğini göstermektedir, buna göre Son Buzul Maksimum'dan bu yana farklı buzul zamanları oluşmuştur.

Modelde çeşitli belirsizlik kaynakları mevcuttur. Bunlardan ilki, kullanılan iklim parametrelerinin çözünürlüğünün 570 m olmasıdır. Sayısal yükseklik modelinin 30 m olduğu düşünülürse, bunun bir belirsizlik yarattığı söylenebilir. Bununla beraber, sayısal yükseklik modelindeki ani yükseklik değişimleri yüksek eğimler meydana

getirebilir. Bu bağlamda, geçmişten bu güne erozyonal süreçlerle yapısı değişen alanın, bir belirsizlik yarattığı düşünülebilir. Bunlarla beraber iklim verilerindeki mevsimsel dalgalanmalar, modelde belirsizlik yaratabilir.

Gelecek çalışmalarda, nispeten daha genç buzulların taşıdığı çökellerin oluşturduğu moren depolarının sayısal yükseklik modelinden kaldırılması model sonuçlarına olumlu yansıyacaktır. Çünkü bu yapılar, bir vadide ilerleyen buzulların daha geçmişte oluşan morenlere ilerlemelerine engel teşkil etmektedirler. Bölgede bulunan diğer eski buzul alanlarında bu çalışmada kullanılan yöntemlerle uygulanacak buzul ve iklim modellemeleri, Türkiye'nin geçmiş iklim koşulları hakkındaki verileri arttıracaktır.

1. INTRODUCTION

The glacial geomorphic features such as moraines and trimlines, provide a valuable data to rebuild a paleoglacial construction [1]. When a glacier advances to its final position, it transports deposits to the terminal position. After retreating of the glacier, the deposited sediments keeps their final positions. This formation gives the maximum advance of the paleoglacier. Practically, the advances and retreat of the glacier are used to reconstruct the paleoglaciers. Because the trimlines and moraines are direct proxies for glacier movement. The evidence of their final positions can be observed in the field. Because a glacier is a quite sensitive proxy for the climatic fluctuations, the extend of the glacier is directly changed with the related climatic changes [2]. For that reason, paleoglaciers can be used to estimate climatic variations over time. These variations record the temperature and precipitation changes from the past to present. Moreover, these data can be considered as input to a model of the paleoglaciers.

It is briefly explained that the transported sediments which can be observed at the present time in mountains can be used to understand the climatic effects. The extend of the glacier depends on the positive or negative changes in the glacier mass balance in a local area. The mass balance of a glacier can be calculated with using different temperature and precipitation conditions. The calculated mass balance with a proper ice flow model is used to find the terminus position of the paleoglacier. As long as the appropriate mass balance should be calculated compatible with the paleoclimatic conditions, the paleoclimatic conditions can be reconstructed. If the different terminus position of the paleoglacier in the field are thoroughly defined, the paleotemparature and precipitation conditions can be modeled by means of paleoglaciers.

The Late Quaternary climate changes shaped the glaciations on Mountains of Turkey [3]. The locations of the paleoglaciers of Turkey can be seen in Figure 1.1 [4]. It was stated that glaciers are retreating at accelerating rates on Turkish mountains [3]. It is a fact that, the changing climate caused the ablation of glaciers in Anatolia and the Eastern Mediterranean.
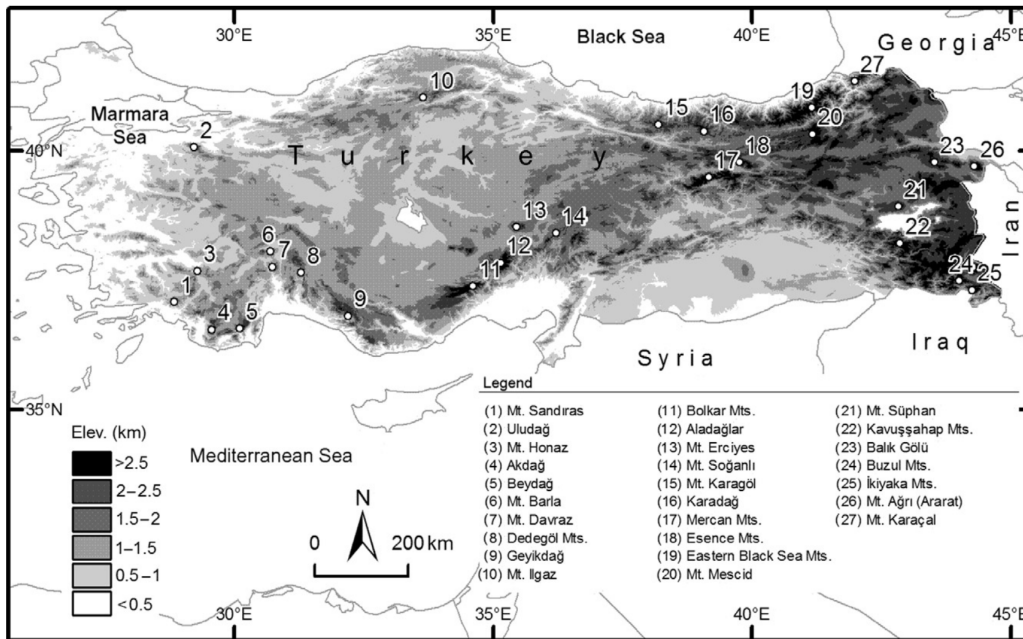
Figure 1.1 : Glaciated mountains in Turkey [4].

However, not only well-preserved moraines as a proxy can be found, but also several mountains preserve current glaciers in Turkey. Ağrı Mountain (5137 *m*) and Cilo Mountain (4135 *m*), have recent glaciers up to 1.5 *km* in length. Kaçkar Mountains (3932 *m*) and Erciyes Mountains (3917 *m*) have also glaciers today [3]. In this study, the paleoglaciers of the Dedegöl Mountain is reconstructed with surface mass balance and two-dimensional ice flow model. Finally, the climatic conditions simulated from paleoglacier will give a comparison of present and paleoclimate over time.

1.1 Purpose of the Thesis

The main idea of this thesis is a reconstruction of the paleoglaciers with using climatic proxies. As a matter of fact that, this rebuilding can be considered as an estimation of the paleoclimate conditions. For this purpose, the maximum glacial extends on Dedegöl Mountains are detected and glacial boundaries are defined. After simulation of the mass balance and ice flow models on computer environment, the simulation results and the glacial boundaries are compared. As a result of that, the matched climatic conditions with field studies give the Late Quaternary climatic conditions around Dedegöl Mountain. It also gives a practical approach to determine climate conditions during the times where geochronological data exist.

The previous dating studies [5], and also ongoing cosmogenic dating projects can give the dating of the associated moraines in Turkish Mountains. In that matter, dating results and simulation results provide glacial maximum extends over defined time, in Anatolian Mountains.

1.2 Literature Review

There were many studies on Anatolian glaciers [6–8]. In the decades, Quaternary glacier studies have been further advanced by applying the cosmogenic surface dating method [9]. Studies on glacier geomorphology and Quaternary geology in the Dedegöl Mountains have started in 1970's [10]. The sedimentological properties of terminal and lateral moraines in the Karagöl and Muslu Valleys were investigated in the south of Beyşehir Lake [10]. The glacier and karst relations were studied in Dedegöl Mountains and investigated the effect of karstification in the development of the glacier geomorphology of the region [11, 12]. The moraine complex were dated in the Muslu Glacier Valley in the southern part of the mountain using ^{10}Be and ^{26}Al isotopes due to the presence of quartz containing volcanic and they found that the LGM glaciers had progressed 29.6 ± 1.9 thousand years ago before present (BP) and started to retreat 21.5 ± 1.5 thousand years ago [5]. In the Muslu Valley, glaciers were started to retreat in the Late Glacial period, 15.2 ± 1.1 thousand years ago.

The morphological evidence of glaciers such as glacier valleys, circuses, truncated surfaces, moraine deposits were well identified in Dedegöl Mountain [12–14]. As a result of the reconstruction of the Dedegöl Mountain glaciers, the Equilibrium Line Altitude (ELA) found as 2230 *m*, the glaciers cover 21.2 *km* and the glaciers extend to 1500 *m* from the top of the mountain [13]. Moreover, from 7 samples taken from the moraine deposits in the region, OSL ages ranges from 148 ± 13 ka and 2.6 ± 0.1 ka. In Dedegöl Mountain, the current ELA at 3400-3500 *m* level has descended to approximately 2230 *m* level in Pleistocene [13, 15]. The products of the glaciations in the study area took its present shape with the effect of the karst formation topography. Especially due to the tectonic and karstic processes that occur in the glaciation area, the valleys are far from typical U-shape valley profiles. Moreover, there are elevation differences between the ends of glacier valleys. A highly complex structure has been developed in the glacial fields due to karstification, tectonic and periglacial factors [13].

Data from field studies and glacial modeling approach can be combined. The previous models were generated to simulate glacier in a certain area. The reconstruction of mean annual temperature and precipitation changes from present, was used to advance to their LGM extends in the North Island of New Zealand [16]. The best simulation results are from the temperature decreasing are between 5.1 and 6.3°C, and also decrease in precipitation of up to 25% from the present. In the same area, there are different modeling approach to simulate glacier flow. The modified Paterson-Budd flow law was employed in a polythermal model experiments related changes in strain rate (softening) of ice under certain circumstances [17]. In that model, there are some consequences of changing strain rates. 'Softer' ice flows faster than 'stiffer' ice. Because paleoflow rates can not be adjusted correctly, the flow parameter should be tuned carefully to achieve as close as possible match to geomorphological evidence [17]. In the same study, the Parallel Ice Sheet Model (PISM) was used to numerically reproduce the Last Glacial Maximum (LGM) ice extend with 500 m resolution. The LGM cooling is stated as at least 6-6.5°C cooler than today to bring about valley glaciers that extend beyond the mountains. The associated precipitation regime is up to 25% drier than today [17]. An another paper using the PISM shows that the LGM temperature in Alpine ice cap 12°C cooler and precipitation is about 53% - 80% drier compared to present values [18].

The coupled surface energy mass balance and flow modeling approach was defined and improved in previous studies [19–21]. Using of 2-D flow model approach is suitable where topographic influence on glacier mass balance may be a significant factor [1]. The steady state glacier extend in a certain area can be obtained under some climatic conditions which remain relatively stable for a long time period [1]. In this study, the main approach to simulate the paleoglacier depends on that idea. The reconstruction of paleoglacier in the Bishop Creek drainage basin in the eastern Sierra Nevada, USA, shows that paleoclimatic conditions are 6°C colder and 10% wetter than modern climate [1]. The same method applied in the Wasatch and southern Uinta Mountains, USA, was used to regenerate paleoglacier [1]. This study shows that mountains were 6-7°C colder and precipitation multiplier is about 1-3 times greater than present conditions [22].

1.3 Study Area: Dedegöl Mountain

Dedegöl Mountain (Dede means grandfather, göl means lake in Turkish) (37.6°N 31.3°E, 2997 *m* above mean sea level) is the part of the Western Taurus Mountains in Anatolian Peninsula (Figure 1.2) [14]. It is located about 15 *km* west of Beyşehir Lake. The study area is located in the Lakes Region (Göller Yöresi in Turkish). A large part of the mountain remains within the borders of the province of Isparta, while a small eastern part is in the province of Konya.
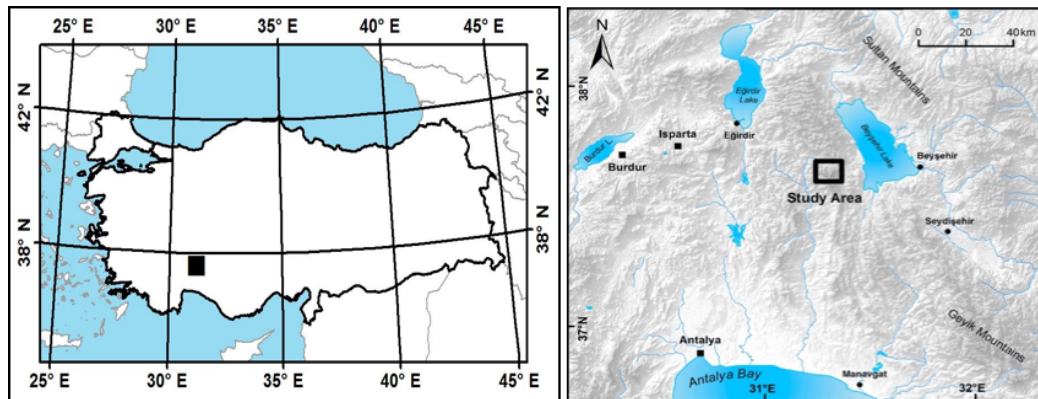
Figure 1.2 : Study Area - Dedegöl Mountain [14].

The highest point of the study area is the Dedegül Peak (2997 *m*). The width and length of the area are 16.9 *km* in both directions. Although it has been referred to as Dedegül Tepe in the topography maps, the former name Dedegöl has been named in many previous studies. The name Dedegöl will be used in this study to avoid confusion. Nowadays, the glaciers do not exist in the mountain, because the maximum elevation of Dedegöl Mountains is lower than present snowline 2230 *m*. There are many examples of the Quaternary glacial erosion and accumulation in the area. This shows that temperatures and the ELA have decreased in the Dedegöl Mountains especially during the cold periods of the Quaternary. The glacier flow directions and the lowest levels reached by the glaciers were identified and the limits of the study area were established. Thus, the survey area with an approximate of 286 km^2 is limited to latitudes of 37.5670 - 37.7237°N and longitudes 31.2100 - 31.3667°E. ASTER GDEM numerical elevation model (DEM) with a resolution of 30 *m* was used for the main data source for the topography (Figure 1.3). 1/25,000 scale topography maps and 1/100,000 scale geological maps (MTA, 2010) were also used. ArcGIS 10.3, was used for mapping as Geographic Information Systems (GIS) software; Panoply 4.7.0 and Google Earth Pro were used to plot and visualize the netCDF datasets.
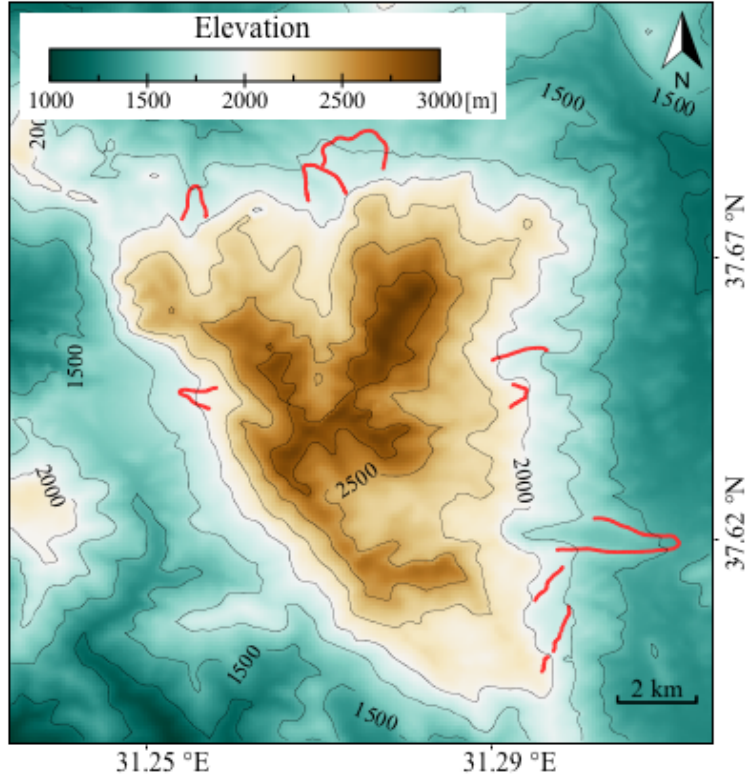
Figure 1.3 : Dedegöl Mountain Digital Elevation Model with 30 *m* resolution. Red lines show paleoglacial ice extend from the moraine locations [12-14].

The glacial extension areas in the study area are the Kisbe and Sayacak glacial valleys in the northern side, the Elmadere glacial area in the north-eastern side, the Karagöl and Muslu glacial areas in the eastern side, and the Karçukuru glacial area in the western side.

1.3.1 Physical geography and geology

The detailed studies on the geology of the region were carried out by other studies [23, 24]. There were several studies have revealed in detail the stratigraphic and structural elements of the region [25–28]. There are allochtone units, which offer various stratigraphic and structural features in the region. The autochthon units usually consist of platform type limestones. The allochtone units are represented by Antalya Naps, which is composed of oceanic crust, slope and rift reefs. Tertiary and Quaternary sediments are found as stratigraphic conglomerates on autochthonic-allochtonic massifs [27]. The 1/100,000 scale geological maps of the region (Isparta M26) was prepared by the MTA [29, 30].

According to that, in general, Beydağları autochthon, Anamas-Akseki autochthon, Antalya Naps and Beyşehir-Hoyran-Hadim Naps and Miocene-Quaternary rock units are exposed in the region [29].

The Dedegöl Mountains are mostly located in the Anamas-Akseki autochthon. The Anamas-Akseki autochthon, which covers wide areas in the Central Taurus Mountains, is represented by overlapping blocks of platform type rocks deposited between the Cambrian-Middle Eocene [29]. The Dipoyraz Formation, which supplies glacial sediments in these, is generally represented by dolomite, dolomitic limestone, and reefal limestones. The Dipoyraz Formation includes massive, thick-bedded, gray, dark gray, terrestrial black, red and pink colored reef limestones and dolomitic limestone, dolomite and dolomite-limestone breccia [26]. Dipoyraz formation has been deposited in the carbonate shelf environment and has a maximum of 1400 m thickness [29].

1.3.2 Present climate conditions

Today's climate in southwest Turkey is characterized by dry/hot summers and wet/temperate winters [31]. Winters are moderately wet [2]. The average summer temperature (June, July and, August; JJA) on the southwest Mediterranean coast of Turkey is about 26°C and average winter temperature (December, January, and February; DJF) is about 10°C [2]. In this area, 60% of average 900 mm annual precipitation falls in winter months (DJF) because of the penetration of depressions that bring moisture from either the Atlantic Ocean or the Mediterranean Sea [32]. These storm tracks which bring most of the rainfall in the winter, tend to move east along the Mediterranean [31, 33]. The summers are dry, opposed to winters'. Only 2% of the annual rain falls during the summer months (JJA) due to the prevailing northerly winds [31].

These values are somewhat different in the study area due to its high elevation. In Dedegöl Mountain, the average summer temperature is 17.6°C and the average winter temperature is -1.2°C. The yearly temperature average in the study area is about 8.2°C according to data which is obtained from WorldClim [34]. Moreover, 42% of average 646 mm annual precipitation falls in winter months (DJF) in the study area.

The present annual precipitation and annual average temperature distribution can be seen in Figure 1.4 a and b, respectively.
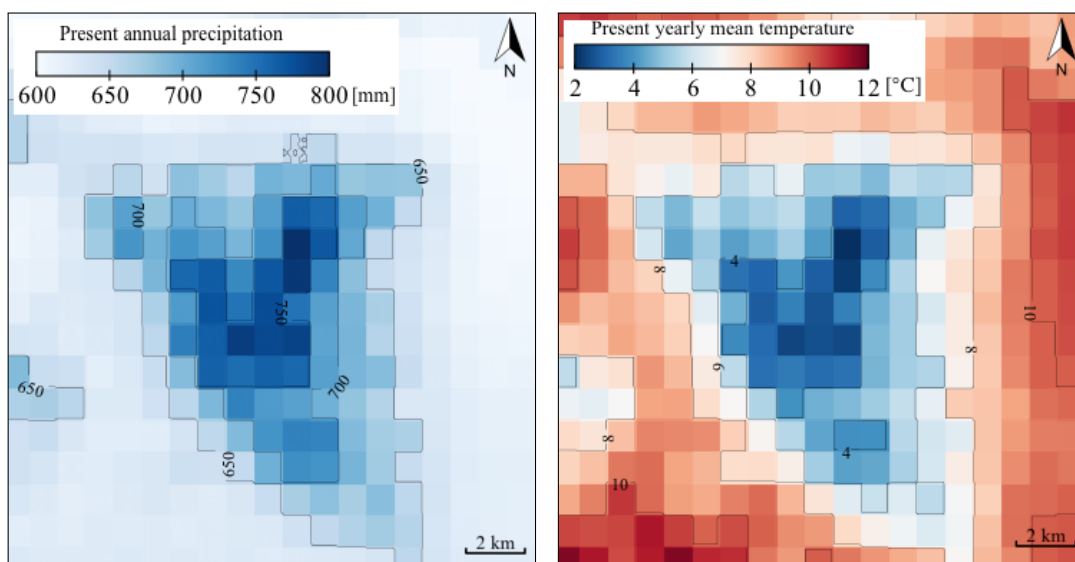
Figure 1.4 : **a)** Present annual precipitation. **b)** Present mean annual temperature on Dedegöl Mountain (Please see the Figure 1.3 for the spatial coordinates).

1.3.3 Paleoclimate conditions

Present climate data were used in order to reconstruct the paleoclimatic conditions. Present temperature and precipitation data are obtained from WorldClim 1.4 [34]. These data show the average of the temperature and precipitation values for each month during a year.[1]

It is a fact that the Last Glacial Maximum climate is colder and wetter than today's climate. It was stated that LGM glaciers were the most extensive ones in Turkey in the last 22 ka (ka=thousands years), and they were closely correlated with the global LGM chron (between 19 and 23 ka) according to the ^{36}Cl cosmogenic exposure ages of moraines show [3]. This cosmogenic dating results showed that LGM glaciers started retreating 21.3±0.9 ka ago on Erciyes Mountain, central Turkey, and 20.4±1.3 ka ago on Sandıras Mountain, southwest Turkey. It was also stated that glaciers showed changes by 14.6±1.2 ka ago (Late Glacial) on Erciyes Mountain and 16.2±0.5 ka ago on Sandıras Mountain [3]. Aladağlar Mountain, south-central Turkey, large Early Holocene glaciers were active. They reached their maximum extend at 10.2±0.2 ka and retreated by 8.6±0.3 ka, and they retreated by 9.3±0.5 ka on Erciyes Mountain [3].

---

[1]The input climate data of study area can be found in CD, Appendix C.

Paleoclimate proxy data and 1-D glacier modeling were used to reconstruct the paleoclimate [3]. Temperature was 8-11°C colder than today during LGM and wetter up to 2 times on the southwestern mountains, drier by about 60% on the northeastern ones and approximately the same as present in the interior regions [3]. The Early Holocene was 2.1°C to 4.9°C colder on Erciyes Mountain and up to 9°C colder on Aladağlar, based on doubled precipitation rates. The Late Holocene was 2.4-3°C colder than today and the precipitation was close to the modern levels [3].

2. METHODOLOGY

2.1 Field Studies

On August 2015, the first detailed fieldwork was carried out in Dedegöl Mountain, by Prof. Dr. Attila Çiner (researcher), Assoc. Prof. Dr. Mehmet Akif Sarıkaya (thesis adviser), the thesis student Adem Candaş and geographer Oğuzhan Köse. In the field study, lateral, terminus, and piedmont moraines were found in the glacial areas at about 1800-2400 *m*. The locations of moraines were measured using 1/25,000 scale topography maps and GPS, and the maps containing sample points were produced. The moraine deposits which are evidence of paleoglaciers are identified with help of the satellite images and field surveys.

Sampling for cosmogenic dating and obtaining glacial geochronology are a subject of Oğuzhan Köse's study [14] in the same study area. However, these procedures will be explained to help to understand the this study's scope. When choosing the samples in the field, original surfaces showing minimum complications after sedimentation were chosen. The samples of about 500 grams were taken from the top surface of the biggest blocks which are not easy to overturn, from a depth of 2-3 cm (Figure 2.1).

Figure 2.1 : Sayacak Valley sampling studies [14].

During the sampling process, non-rooted overturned blocks within the matrix have been avoided. The moraine deposits in the region are thought to be minimally affected by the anthropogenic degradation processes, mostly due to the barren nature of the carbonate rocks. All data required (eg. coordinates, height, sample thickness, horizon angles, photographs, etc.) were recorded when sampling was done in the field. A total of 20 samples were taken from the moraines identified in the glacial areas; 7 from Karagöl glacier area, 8 from Sayacak glacier valley and 5 from Kisbe glacier valley.

The second fieldwork was carried out for four days on July, 2016. In this study, the detailed maps of glacier geomorphology were reviewed in Dedegöl Mountain. The Northern paleoglaciation valleys were illustrated in Figure 2.2 [14] .
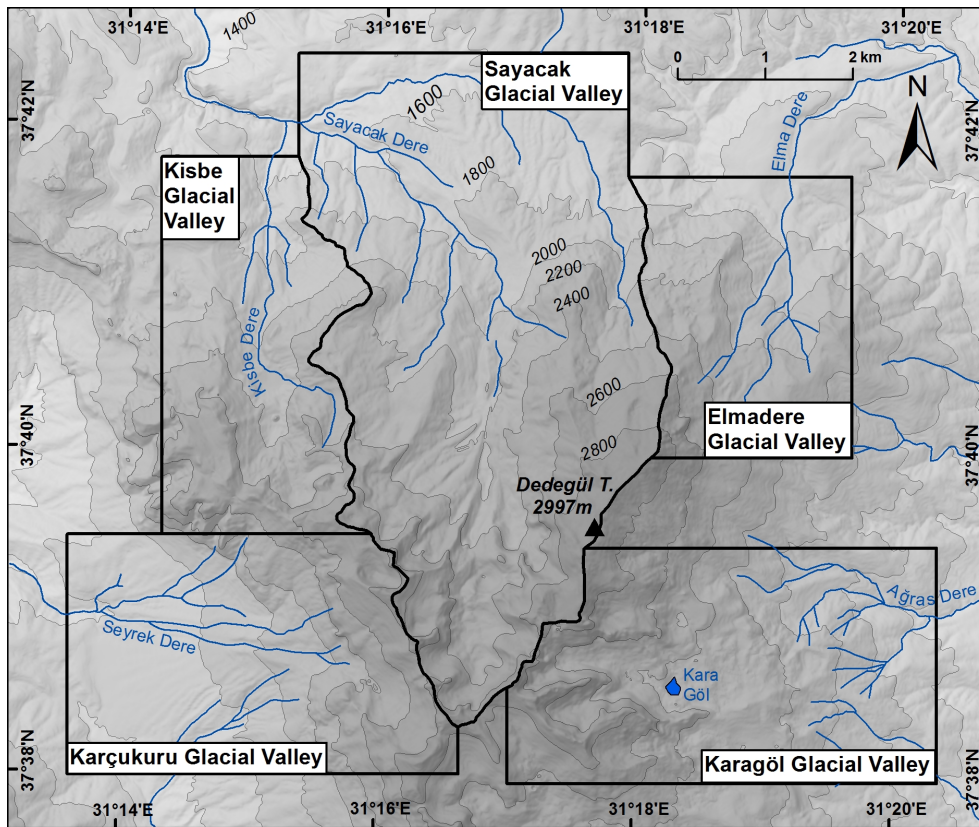
Figure 2.2 : Dedegöl Mountain northern paleoglacial valleys [14].

The Global Positioning System (GPS), 1/25,000 scale topography maps and pre-plotted glacier geomorphology maps were used to better understand ground shapes of the glacier geomorphology, determine their location and make detailed mapping. In order to fully understand the structure of moraines and to determine the boundaries of large moraines, photographs and videos were recorded and mapped using an airborne drone.

2.2 Climate Data Input

Climate data for PISM consist of two main parameters: (1) average monthly mean temperatures [°C] and (2) average monthly precipitation [mm]. All climate data were downloaded from the WorldClim Global Climate Data website [35]. They were all provided in APPENDIX D in ASCII format.

WorldClim is a set of global climate layers (gridded climate data) with a spatial resolution of about 1 km^2 [34]. It has average monthly climate data for minimum, mean, and maximum temperature and for precipitation for 1960-1990. The data layers were generated through interpolation of average monthly climate data from weather stations on a 30 arc-second resolution grid (about 1 km^2 resolution) [34].

2.3 Paleoclimate Modeling

In this study, different temperature and precipitation values are used to reconstruct paleoclimate conditions. Paleotemperature changes may vary depending on the season. Some studies have shown that the change in the warmest months may be greater than the change in the coldest months [36, 37]. Therefore, a model can be used to add seasonality effect to the temperature change. In the mentioned articles, the difference between the summer temperatures in the Eastern Mediterranean and the winter temperatures can be up to 5°C. In order to study the effect of this seasonality on the glacial mass balance, some coefficients were used which made the temperature offset. These coefficients and temperature offset values (ΔT^m) are shown in Table 2.1.

Table 2.1 : The coefficients used to offset temperature depending on the seasonal effect. The default ΔT =-9°C.

Months	1	2	3	4	5	6	7	8	9	10	11	12
Coefficients	0.65	0.65	0.7	0.75	0.8	0.9	1	1	0.9	0.8	0.75	0.7
ΔT^{new} [°C]	-7.3	-7.3	-7.9	-8.4	-9.0	-10.1	-11.3	-11.3	-10.1	-9.0	-8.4	-7.9

The following calculation was made to keep the temperature changing constant over a year while temperature changes depending on the season (equation 2.1).

$$\Delta T^{new}(m) = \frac{\Delta T^{default} \times 12}{\sum_{n=1}^{12} coeff_n} \times coeff^m, \quad m = 1...12 \tag{2.1}$$

13

where $\Delta T^{default}$ is the default offset value. Each month has different offset values (ΔT^{new}) as seen in Table 2.1.

Figure 2.3 shows the seasonal dependent and independent temperature depressions.
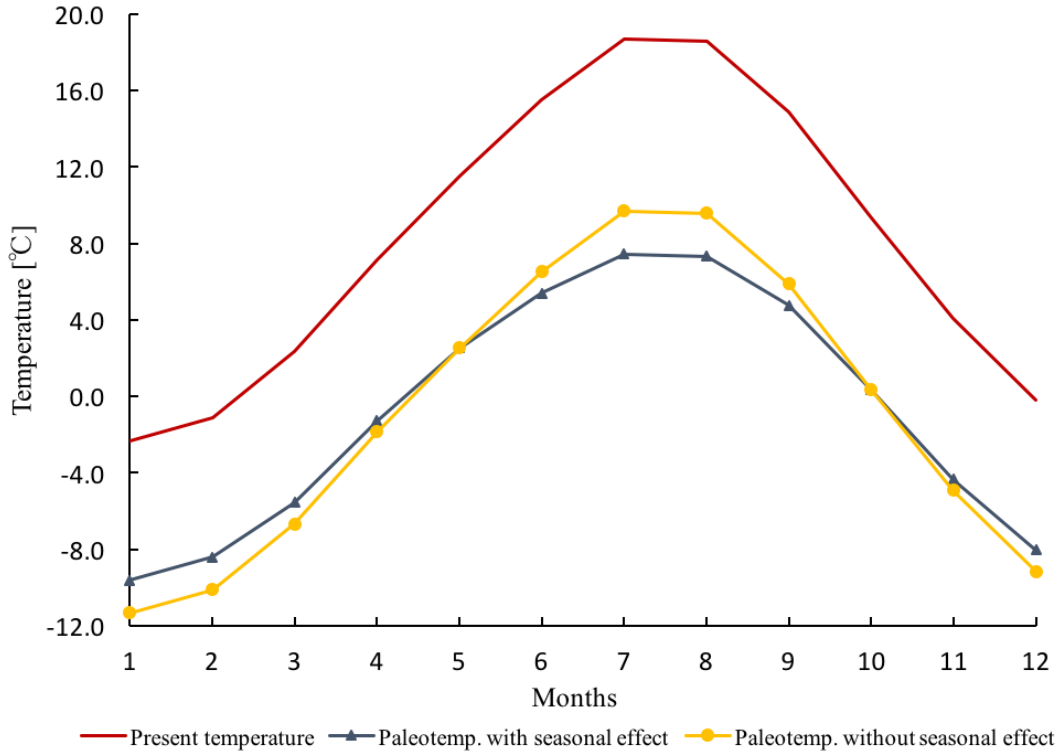
Figure 2.3 : -9°C temperature depression comparision between seasonal effect and without seasonal effect.

As seen in Figure 2.3, a model has been proposed in which the decreasing in summer paleotemperatures is greater than the winter temperatures. According to this model, when the seasonal distribution is applied, the mass balance is affected in a positive way. If the seasonal effect is not applied, the maximum mass balance is 639 mm/yr, in the case of a -9°C temperature depression and 25% precipitation increase; with the seasonal distribution, this value rises to 874 mm/yr. Similarly, the minimum mass balance increases from -4858 mm/yr to -4293 mm/yr.

Three precipitation values were used in simulations. The first precipitation condition was the present values. The other conditions were increased by 25% and 50% with regard to the present. The temperature was ranged from -8 to -10°C with regard to present temperature.

The comparison of present and a paleoclimate conditions can be seen in Figure 2.4. In that case, temperature was depressed by 9°C with precipitation 25% increased.
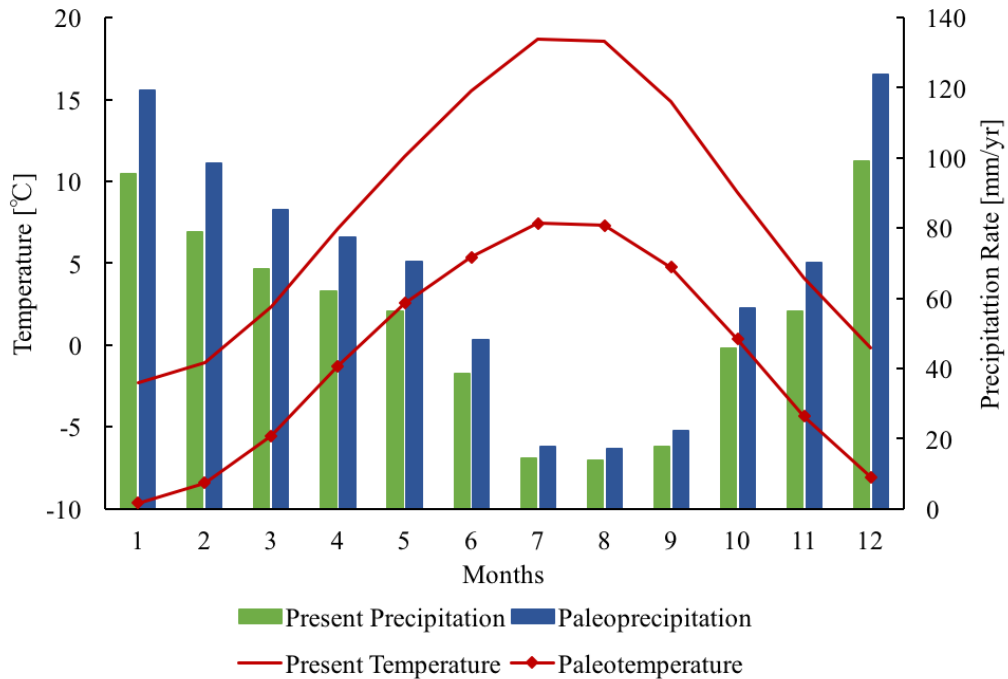
Figure 2.4 : Temperature and precipitation during the present and paleoclimatic conditions with -9°C colder and 25% more precipitation values. Temperature offsets vary with months because of seasonal effect.

2.4 Glacier Modeling

In this study, the coupled surface mass balance and two-dimensional flow modeling approach are used to regenerate extensions of paleoglaciers. Temperature and precipitation are the most important climatic parameters. They are used in mass balance calculations. Although cloudiness and wind speed affect mass balance, they are inherited in the mass balance calculation [1]. Surface mass balance is calculated under present temperature and precipitation data. Different cases which can be fitted to paleoclimate climatic conditions were created. In order to determine which condition is the best fitted to field signs, temperature and precipitation values were changed according to present values. Therefore, paleoclimatic surface mass balances are used to simulate in different cases. The second step to simulate the paleoglacier is modeling the flowing of ice. 1-D (along with a flow line) models generally neglect topographic effects and they are used to analyze temporary glacier fluctuations [1].

The paleoglacier area where mass balance is depending on topography should be modeled with a 2-D approach.

2.4.1 Equilibrium line altitude

Equilibrium line altitude (ELA) divides accumulation and ablation zones on a glacier. Above the ELA, the glacier gathers snow or ice as mass and below the ELA ablation processes are dominant rather than accumulation processes (Figure 2.5) [38]. At that altitude, accumulation of snow is exactly balanced by ablation. This term is important for the mass balance calculations and glacier modeling. If ELA rises, mass balance of a glacier increases. Fall of ELA causes mass balance decreases. Therefore, this relationship has a significant effect on the modeling of paleoglacier. ELA is an important climatic indicator and it can change with time. It was about 2300-3000 *m* in Anatolian mountains, and around 2500-2600 on Dedegöl Mountains during the Last Glacial Maximum (LGM, 21,000 calendar years ago), [2].
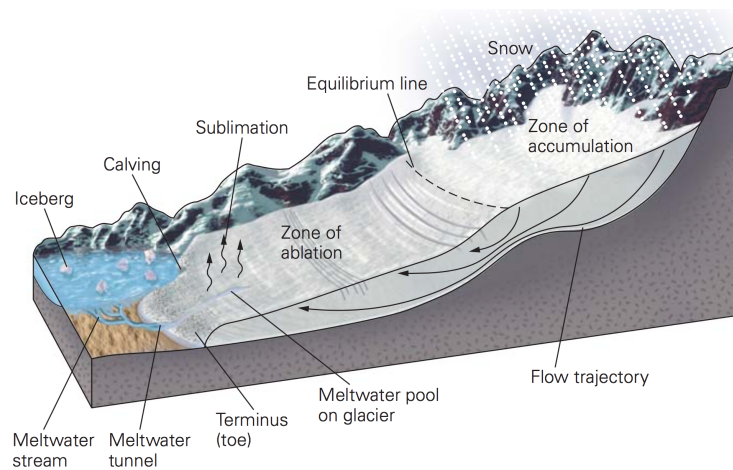
Figure 2.5 : The equilibrium line separates the zone of accumulation from the zone of ablation. As indicated by arrows, ice flows down in the zone of accumulation and up in the zone of ablation [37].

2.4.2 Surface mass balance

The surface mass balance (also called the glacial yearly budget) is the difference between the accumulation and ablation of ice of a certain location and time (equation 2.2). It is essentially an accounting of the input/output relationship of snow, firn, and ice over a certain time interval.

16

$$M = \sum acc - \sum abl. \tag{2.2}$$

where *M* is surface mass balance, *acc* is accumulation and, *abl* is ablation during a year. This term is related to the mechanical response of glaciers and the geomorphic work they accomplish [39]. The accumulation term is used to define adding the water equivalent of ice and snow to a glacier. The accumulation's primary source are snowfall, rain, water that freezes on the surface, avalanches from the valley walls, and the freeze of meltwater at the base of the glacier. The other term is ablation which removes snow or ice. It includes melting, evaporation, wind erosion, and sublimation. Also, calving is a type of abrasion, which means that huge masses break from the ice in an ocean or marine areas. This is not applicable to the study site.

The time interval for the mass balance calculations is defined as the budget year. Accumulation and ablation on a certain area depend on temperature and precipitation relations. If the accumulation is greater than the ablation process, terminus or toe of the glacier advances to unglaciated areas (Figure 2.6). This process is called as *glacial advance*. During the advances, terminus moves downslope in mountain glaciers.
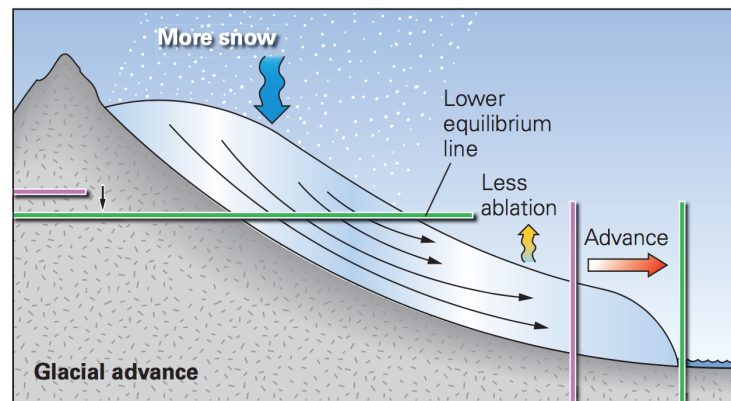
Figure 2.6 : The glacier advances if accumulation exceeds ablation. The terminus moves farther from the origin and the ice is thickening [37].

In an equilibrium state, the rate of ablation and accumulation are equal over the entire glacier. The position of the terminal is not changed seen as in Figure 2.7. The glacier mass balance is in equilibrium. Although the glacier continues to flow, the terminus position is not changed because of the ablation.

The third case is which the rate of accumulation is less than ablation's. In that case, the position of terminus moves back toward the origin of the glacier. The term used for that situation is *glacial retreat* as can be seen in Figure 2.8 [38].
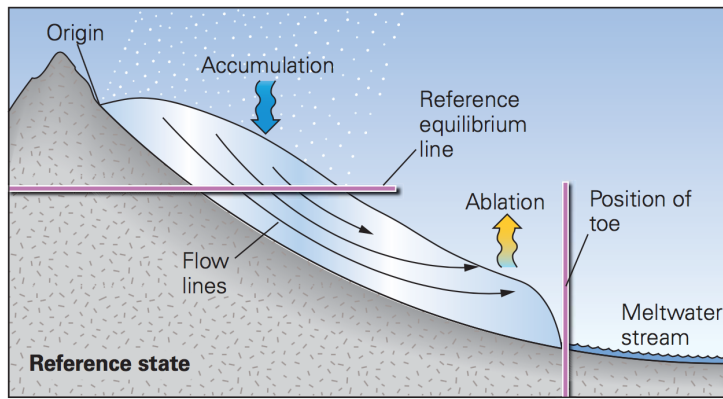
Figure 2.7 : The position of the terminus represents a balance between addition by accumulation and loss by ablation [37].

When the glacier retreats, terminus moves back toward the origin. Ice flow continues toward the terminus toward downslope because of gravitation.
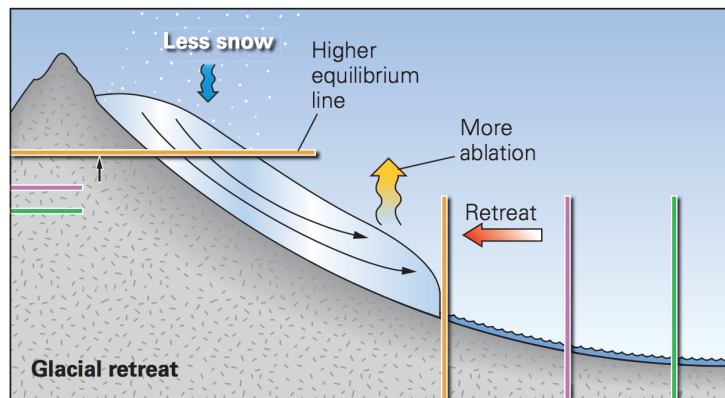
Figure 2.8 : The glacier retreats and thins if ablation exceeds accumulation. The toe moves back, even though ice continues to flow toward the terminus [37].

As a result, if a glacier has a positive mass balance, more accumulation is occurred than ablation during a budget year. The negative mass balance indicates the excess of ablation. The equality between ablation and accumulation can be observed with a mass balance is zero.

2.4.3 Formation of moraines

In the accumulation zone, ice gradually moves down toward the base of the glacier, because accumulation process increases the amount of snow which eventually turn into firn and ice. In ablation zone, ice moves upward from beneath to the surface of the glacier, because of the ablation. Thus, ice volumes follow curved trajectories seen in Figures 2.6, 2.7 and, 2.8. Moving glaciers carry out the sediments to lateral and terminus position of the glacier (Figure 2.9).

The sediment load incorporated into the moving ice can be fallen from bordering cliffs or gets plucked and lifted from the substrate [38]. The sediments accumulating on the end of the glacier is called as the moraine. These landforms give the maximum extend of the glacier. In that matter, glacier moves like a conveyor belt, moving sediment toward the terminus of the glacier [38].
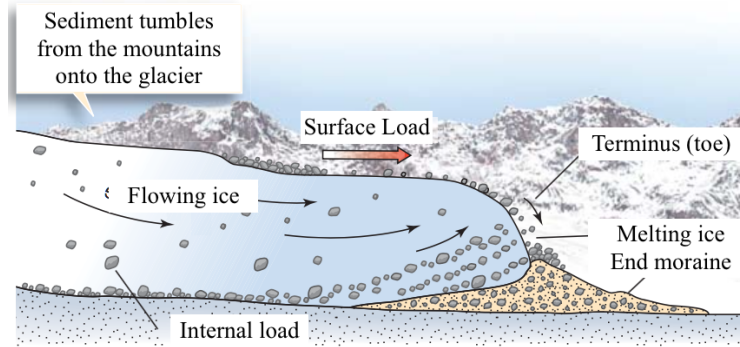
Figure 2.9 : Sediment falls on a glacier from bordering mountains and gets plucked up from below [37].

2.4.4 Positive degree day factor

Positive Degree Day (PDD) is a widely used method to predict glacier ablation calculations [40]. It depends on the idea that there is a correlation between the sum of all temperatures above the melting point and melting of snow or ice at the same place over a certain period [41]. It basically means that air temperature is one of the most important factors for glacier melting. In this method, cumulative temperature above melting point of ice is a parameter for correlating with the observed melt via the degree day factor. It links the ablation to the air temperature. The yearly sum of positive degree days at the surface can give the melting rate empirically. In the equation (2.3), expected sum of positive degree days (EPPD) can be evaluated as [42]:

$$EPDD = \sigma \int_0^{12} 30.4 \left[0.3989 \exp \left(-1.58 \left| \frac{T_{mon}}{\sigma} \right|^{1.1372} \right) + \max \left(0, \frac{T_{mon}}{\sigma} \right) \right] dt.$$

(2.3)

where T_{mon} is the surface temperature of each month. σ is the standard deviation of monthly temperature account for the daily cycle [42]. It was taken as $2°C$ in this study. It was assumed that monthly precipitation is uniformly distributed and the temperature is normally distributed [1].

Expected number of positive degree days is corresponding to melting of snow and ice. The default positive degree day factors were chosen as 3.0 $mmd^{-1}{}^{\circ}C^{-1}$ for snow and 8.0 $mmd^{-1}{}^{\circ}C^{-1}$ for ice as suggested in [41]. These values were obtained from the observations in central west Greenland [41]. A sensitivity analysis of factors and standard deviation are run and the results are given in Chapter 4.5. The refreezing factor was chosen as 0.6 which means that 60% percent of melt water refreezes. The sensitivity analysis was also run for it. In retention process, rain is considered as fully run off and is not accounted for retention process [42].

2.4.5 Basal heat flux

Basal heat flux $[mW/m^2]$ affects the basal ice temperatures of a glacier. It is measured at the Earth's surface and related to the temperatures of the Earth's crust and upper mantle. The heat flux distribution of the study area is gathering from the global dataset [43]. These flux values are used as an input for PISM. The study area heat flux is approximately 70.42 mW/m^2 based on study [43].

2.4.6 Two-dimensional diffusion equation and glacier flow

The velocity of a glacier generally is in between 10 and 300 m/yr. Nevertheless, all parts of a glacier do not flow at the same rate. The friction between rock and ice decelerates the movement of ice, therefore the center of a valley glacier moves faster than its side boundaries. The glacier surface moves faster than its base (Figure 2.10).
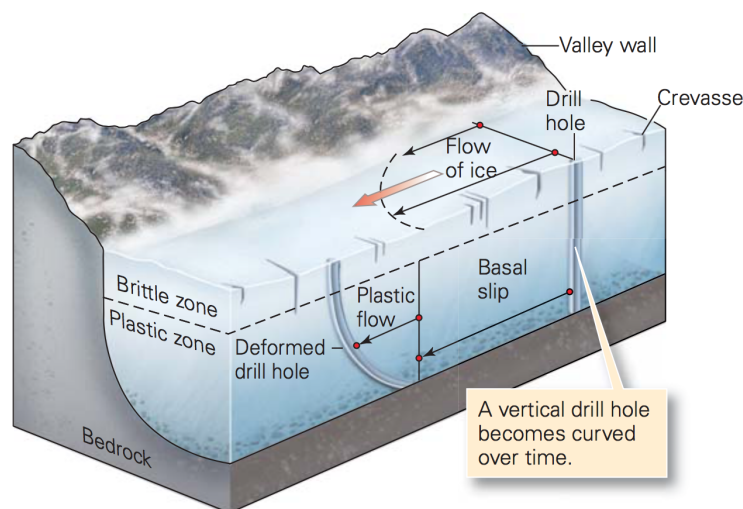
Figure 2.10 : A glacier flows with velocity differentiation due to friction with the substrate [37].

Two-dimensional time dependent continuity equation was suggested to model glacier flow [44] [1]. The equation 2.4 gives ice surface elevation. Changing of the elevation of a glacier over time is dependent on the fluxes through x and y directions on a horizontal plane and governed by:

$$\frac{\partial h(x,y,t)}{\partial t} = M(x,y) - \nabla q(x,y). \tag{2.4}$$

where $h(x,y,t)$ is glacier elevation; $M(x,y)$ is mass balance (difference accumulation and ablation) and; $q(x,y)$ is glacier flow in direction x and y.

In the equation 2.5, it is stated that from a physical interpretation, the flux through x,y on a horizontal plane ($q(x,y)$), is given the product of column-averaged ice velocity (u) and ice thickness (H) [44]:

$$q(x,y) = uH = -k(x,y)\nabla h(x,y), \tag{2.5}$$

where u term states column-averaged ice velocity in m/yr, H glacier thickness in m; k non-linear conductance coefficient which is a function of ice thickness and ice surface slope.

The equation 2.6a shows that there are two component of the velocity: sliding (equation 2.5b) and internal deformation (equation 2.5c) [44]:

$$u = fu_s + (1-f)u_d, \tag{2.6a}$$

$$u_s = \left[\frac{\rho g H \nabla h}{B}\right]^m, \tag{2.6b}$$

$$u_d = \frac{2}{n+2}\left[\frac{\rho g H \nabla h}{A}\right]^n H, \tag{2.6c}$$

where, ρ is the density of ice in kg/m^3, g the gravitational acceleration in m/s^2, u_s the velocity due to the sliding in , u_d the velocity due to the internal friction in m/yr and f a parameter which varies between 0-1 to adjust which velocity component is dominant during movement of the ice. If it is close to the 0, the internal deformation is dominant, else, sliding is the major factor in flux. In this study, the f factor is chosen as 0.5. The exponents m and n are taken 2 and 3 respectively from the previous studies [44]. A is a coefficient for velocity due to deformation and B is for sliding. These parameters can be seen in APPENDIX C.

τ is the basal shear stress and expressed in equation 2.7:

$$\tau = \nabla \rho g H \tag{2.7}$$

The combination of equations 2.5 and 2.6a gives the equation 2.8:

$$UH = -k\nabla h = \left[fB(\rho g H \nabla h)^m + (1-f)\frac{2}{n+2}A(\rho g H \nabla h)^n H \right] H. \tag{2.8}$$

The conductance $k(x,y)$ can be defined as equation 2.9:

$$k(x,y) = fB(\rho g)^m H^{m+1}\nabla h^{m-1} + (1-f)\frac{2}{n+2}A(\rho g)^n H^{n+2}\nabla h^{n-1}. \tag{2.9}$$

Because $k(x,y)$ is depending on variables such as ice surface slope and ice thickness which are changing on a horizontal plane over time, the solution can proceed by an iterative solution. The final equation including h, M and, $k(x,y)$ is shown in equation 2.10. The finite difference method is used to solve this equation.

$$\frac{dh}{dt} = M - \nabla(k\nabla h) \tag{2.10}$$

2.4.7 Diffusion equation discretization

The finite difference method [45] is used to solve the equation 2.10. Firstly, non-linear conductance $k(x,y)$ is presumed as uniform on the horizontal plane. After, calculating the ice surface height h, and hence also ice thickness H, the new value of the conductance will be recalculated. In this process, changing of H will be getting smaller and a solution will be converging in a certain condition. This convergence is related to the initial uniform $k(x,y)$.

There are some preparation and assumptions should be defined before starting discretization. Firstly, a grid-point cluster is defined as seen in Figure 2.11. There is a central control volume of the point P. Points North N, South S, East E and, West W are the neighbors in direction of Center Point P. Dashed lines show that the control volume around P. The thickness of the control volume through z direction is defined as time. North and East directions represent to positive y,x directions respectively. Control volume borders are denoted by the lower case letters, such as n,s,e,w. Control volume is $\Delta x \times \Delta y \times 1$. δx and δy are the distance between two grid points. In this study, they are assumed to constant over a domain.
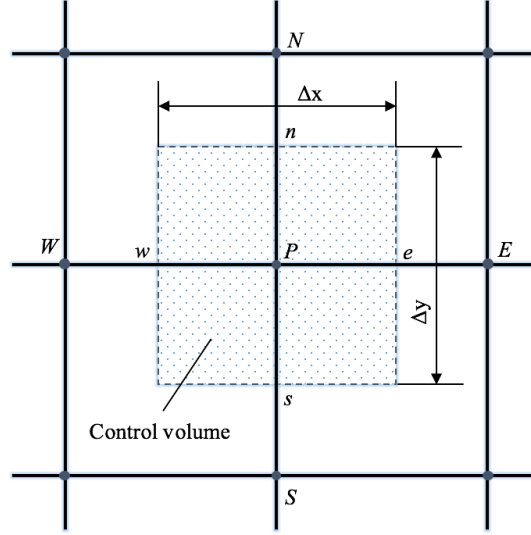
Figure 2.11 : Control volume structure for the two-dimensional discretization
(Reproduced from [44]).

Another assumption is that the value of h at a grid point is same over the control volume. Because this assumption defines the slope, for example, $\partial h/\partial x$, as zero at the borders of the control volume. So, linear interpolation functions should be used between the grid points for avoiding undefined areas. Therefore, the discretization equation will be obtained with evaluating the derivative $\partial h/\partial x$ from the piece-linear profile. The preparation and assumptions are shown in equation 2.11:

$$\frac{d}{dx}\left(k\frac{\partial h}{\partial x}\right) = \left(k_e\frac{\partial h}{\partial x}\right)_e - \left(k_w\frac{\partial h}{\partial x}\right)_w = \frac{k_e(T_E - T_P)}{(\delta x)_e} - \frac{k_w(T_P - T_W)}{(\delta x)_w} \qquad (2.11)$$

The equations are discretized in two-dimension according to equation 2.11. The solution will be calculated by progressing in time from an initial condition. h_P is the point located in the center of the control volume. If at time t it is donated by h_P^0 and it is called "old" (given) values of h_P; else at time $t + \Delta t$ donated by h_P^1 and called "new" (unknown). This notation is also applied on h_N, h_S, h_E and, h_W.

The first two-dimensional equation is derived by integrating the equation 2.10 over the control volume shown in Figure 2.11 and over the time interval. To handle the problem with the one-dimensional scheme is easier than the two-dimensional and due to this fact, problem was solved in 1-D first and then, transformed into 2-D equation:

$$\int_w^e \int_t^{t+\Delta t} \frac{\partial h}{\partial x}\,dt\,dx = \int_t^{t+\Delta t} \int_w^e \frac{\partial}{\partial x}\left(k\frac{\partial h}{\partial x}\right)\,dx\,dt. \qquad (2.12)$$

23

In that situation, it is assumed that h, the grid-point value is same on all control volume. So, it can be said that:

$$\int_w^e \int_t^{t+\Delta t} \frac{\partial h}{\partial x} \, dt \, dx = \Delta x (h_P^1 - h_P^0) \tag{2.13}$$

And, the equation is obtained before from equation 2.11:

$$\int_t^{t+\Delta t} \int_w^e \frac{\partial}{\partial x} \left(k \frac{\partial h}{\partial x} \right) dx \, dt = \int_t^{t+\Delta t} \left[\frac{k_e(h_E - h_P)}{(\delta x)_e} - \frac{k_w(h_P - h_W)}{(\delta x)_w} \right] dt, \tag{2.14}$$

And, the final version of the equation is:

$$\Delta x (h_P^1 - h_P^0) = \int_t^{t+\Delta t} \left[\frac{k_e(h_E - h_P)}{(\delta x)_e} - \frac{k_w(h_P - h_W)}{(\delta x)_w} \right] dt. \tag{2.15}$$

An assumption about how h_P, h_E and, h_W vary with time from t to $t + \Delta t$ is proposed below [45]:

$$\int_t^{t+\Delta t} h_p \, dt = (k h_P^1 + (1-k) h_P^0) \, \Delta t, \tag{2.16}$$

where k is a weighting factor between 0 and 1. Using similar formulas for the integrals h_E and h_E, derived from Eq. 2.15:

$$\frac{\Delta x}{\Delta t}(h_P^1 - h_P^0) = k \left[\frac{k_e(h_E^1 - h_P^1)}{(\delta x)_e} - \frac{k_w(h_P^1 - h_W^1)}{(\delta x)_w} \right] + (1-k) \left[\frac{k_e(h_E^0 - h_P^0)}{(\delta x)_e} - \frac{k_w(h_P^0 - h_W^0)}{(\delta x)_w} \right] \tag{2.17}$$

In this equation, if weighting factor $k = 0$ leads to the explicit scheme, $k = 0.5$ to the Crank-Nicolson scheme, and $k = 1$ to the fully implicit scheme.

For the explicit scheme ($k = 0$), Eq. 2.17 becomes

$$\frac{\Delta x}{\Delta t}(h_P^1 - h_P^0) = \frac{k_e(h_E^0 - h_P^0)}{(\delta x)_e} - \frac{k_w(h_P^0 - h_W^0)}{(\delta x)_w}. \tag{2.18}$$

The two-dimensional equation has N and S indices.

The final discretization equation in two-dimensional scheme after adding surface mass balance becomes

$$a_P h_P = a_E h_E^0 + a_W h_W^0 + a_N h_N^0 + a_S h_S^0 + (a_P - a_N - a_S - a_E - a_W) h_P^0 + M(x,y), \tag{2.19}$$

where,

$$a_N = \frac{k_n \Delta x}{(\delta y)_n}, \tag{2.20}$$

24

$$a_S = \frac{k_s \Delta x}{(\delta y)_s}, \tag{2.21}$$

$$a_E = \frac{k_e \Delta y}{(\delta x)_e}, \tag{2.22}$$

$$a_W = \frac{k_w \Delta y}{(\delta x)_w}, \tag{2.23}$$

$$a_P = \frac{\Delta x \Delta y}{(\Delta t)}. \tag{2.24}$$

$$a_S = \frac{k_s \Delta x}{(\delta y)_s},$$

3. GLACIER FLOW MODELS

3.1 Two-Dimensional Numerical Glacial Flow Code in MATLAB

Two-dimensional ice flow model was explained in Section 2. The final equation 2.10 cannot be solved by hand because of computational reasons. So, a new MATLAB code is written to solve that equation over even a long time and simulate the two-dimensional numerical flow model (APPENDIX A)[1]. The developed code simply works on a horizontal plane and generates glaciers on defined area under various climatic conditions. Firstly, positive degree days and surface mass balance are calculated by *smb_calc.m function* which can be found in APPENDIX B. It uses yearly precipitation and temperature values as input and generates an accumulation and ablation values. The output of this function is the surface mass balance. Simulations were carried out on a plane with the resolution of 30 m using 565×565 grid points. All input and output data are also given in APPENDIX D.

3.2 Parallel Ice Sheet Model (PISM)

In this study, the valley glaciers have been modeled and simulated with PISM with proper parameters. The paleoice extent of the Dedegöl Mountain glaciers is modeled with using the PISM under different constant climate conditions. Although PISM is generally used to simulate big scaled glaciers, like as ice sheet, it can be used with changing the half-width of the square bed elevation smoothing domain used by the bed roughness parameterization in smaller spatial scales, like Dedegöl Mountain. This parameterization is turned off by setting up **bed smoother range 0**.

Ice sheets are continent-size glaciers structures. They are acting like a fluid. The best way for modeling a glacier is the Stokes model [46]. On the other hand, using this model is not suitable according to computational efficiency [18]. The efficient way of modeling glacier was provided Parallel Ice Sheet Model (PISM).

---

[1]The MATLAB code can be found in CD, APPENDIX D.

27

It is used to simulate the movement of ice flow, its temperature etc. [47]. PISM has different sliding flow model for simulation, such as the Shallow Ice Approximation (SIA, Hutter, 1983), the Shallow Shelf Approximation (SSA, Morland, 1987) and also, *hybrid-type model*. The *hybrid-type model* is computationally less expensive than the Stokes equations which are the most physically accurate model for simulating glacier [18]. PISM applications have done before successfully in the New Zealand Southern Alps and European Alps [17, 18]. They are larger than Dedegöl Mountain paleoglaciers.

3.2.1 Preparing input data for PISM

PISM uses Network Common Data Form (NetCDF) as input file type. This is a machine-independent data format that supports the creation, access, and sharing of array-oriented scientific data [48]. In a $*.nc$ file, different variables can be defined, for example, temperature, precipitation, ice thickness etc. A code was written in MATLAB to create and modify to NetCDF files. All preprocessor codes can be found in APPENDIX B[2]. It consists of three functions. The *smb_calc.m function* uses the temperature and precipitation data as input and calculates surface mass balance over a year. The first section of code calculates the Positive Degree Days and accumulation as stated in Section 2. The input screen can be seen in Figure 3.1.
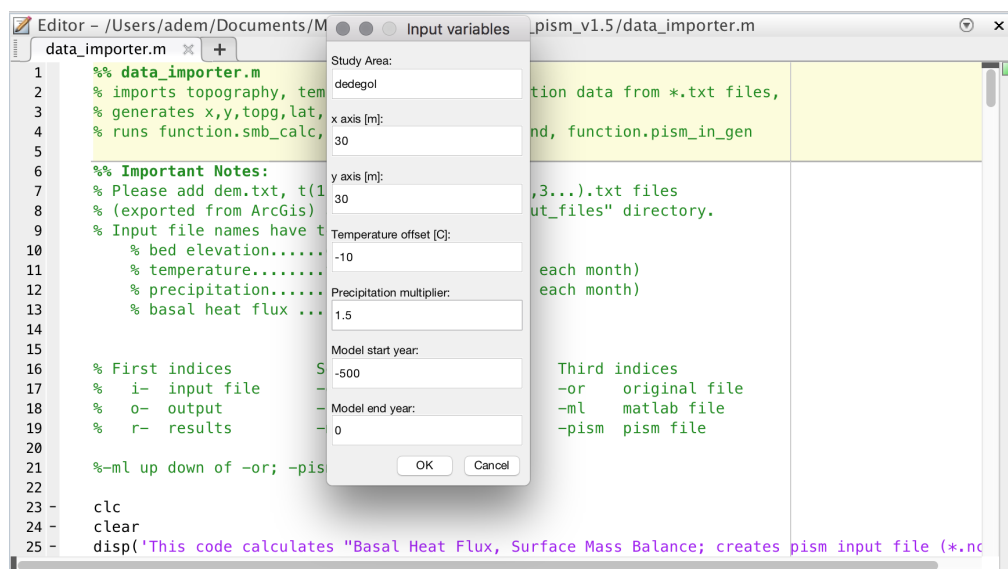
Figure 3.1 : The input screen to create NetCDF file for PISM. The study area, x and y axis resolution, climatic forcings (Temperature offset and precipitation multiplier), and model time can be defined.

---

[2]The MATLAB code can also be found in CD, APPENDIX D.

Paleoclimatic conditions have been created by changing the present temperature and precipitation data. The study area and spatial resolutions were defined on the input screen. Digital elevation data of Dedegöl Mountain were taken from ASTER Global Digital Elevation Model with 30 *m* spatial resolution. The climatic inputs are from WorldClim - Global Climate Data - Current Conditions with a spatial resolution of 1 km^2 [34]. The temperature above 2°C precipitation is considered as rain and neglected. Between 0 and 2°C, it is a transition zone with snow and rain. Below the 0°C whole precipitation was taken as snow. Then, the ablation is subtracted from accumulation. Therefore, a positive mass balance value means accumulation occurring in a defined cell and a negative mass balance value means ablation. The second part of the code is *pism_in_gen.m function* which creates a *.nc file, creates variables and, attributes. It also gives a code which can be used for running the PISM with generated file. The third function is *bheat flux.m* which import basal heat flux values from The Global Dataset of Heat Flow Measurements [43]. The heat flux value for Dedegöl Mountain is 70.42 mW/m^2.

The main code, *data_importer.m* starts with a user input screen and gets *study area*, *dx*, *dy*, *toffset*, *pamp*, *ye* and, *ys* into the program. *dx* and *dy* variables are spatial resolutions in *x* and *y*-direction respectively. In Dedegöl Mountain digital elevation model, the distance between two grids is the same for each direction: 30 *m*. *toffset* offsets the present temperature and *pamp* multiply the present precipitation; they are used to create paleoclimatic conditions. *ye* and *ys* are the starting and ending year of the simulation using by PISM as input. The main code and other functions calculate positive degree days, surface mass balance and create a *.nc input file for PISM[3].

PISM is run with a script[4] entered in a terminal screen on a Unix-based operating system. The script includes the input file, climatic and spatial variables, model time, output types etc. The Average running time for the program is about 72-96 hours.

---

[3]All PISM input files using in this study can be found in CD, APPENDIX D.

[4]mpiexec -n 8 pismr -i pism_dedegol_T9_P1.25.nc -bootstrap -Mx 565 -My 565 -Mz 11 -Lz 400 -bed_smoother_range 0 -ys -500 -ye 0 -surface given -ts_file ts_dedegol_T9_P1.25.nc -ts_times -500 yearly 0 -extra_file ex_dedegol_T9_P1.25.nc -extra_times -500 5 0 -extra_vars tempicethk_basal,bmelt,velsurf_mag,mask,thk,topg,lat,lon,usurf -o output_dedegol_T9_P1.25.nc &> run_dedegol_T9_P1.25.txt &

4. RESULTS

4.1 Field Evidence of Paleoglaciations in Dedegöl Mountain

The glacial valleys identified in the field studies were shown in Figure 4.1 and discussed in detail by [14]. In that study, the rock samples gathered from the crests were dated with cosmogenic dating method. In the figure, moraine crests in each valley were indicated with red lines. In this study, modeling of paleoglaciers was examined. Then, the paleoglacier models and moraine crests were matched to each other. Moreover, advances of the glaciers in the Sayacak Valley was investigated. The glacier thickness and velocity data were shown in Section 4.3.
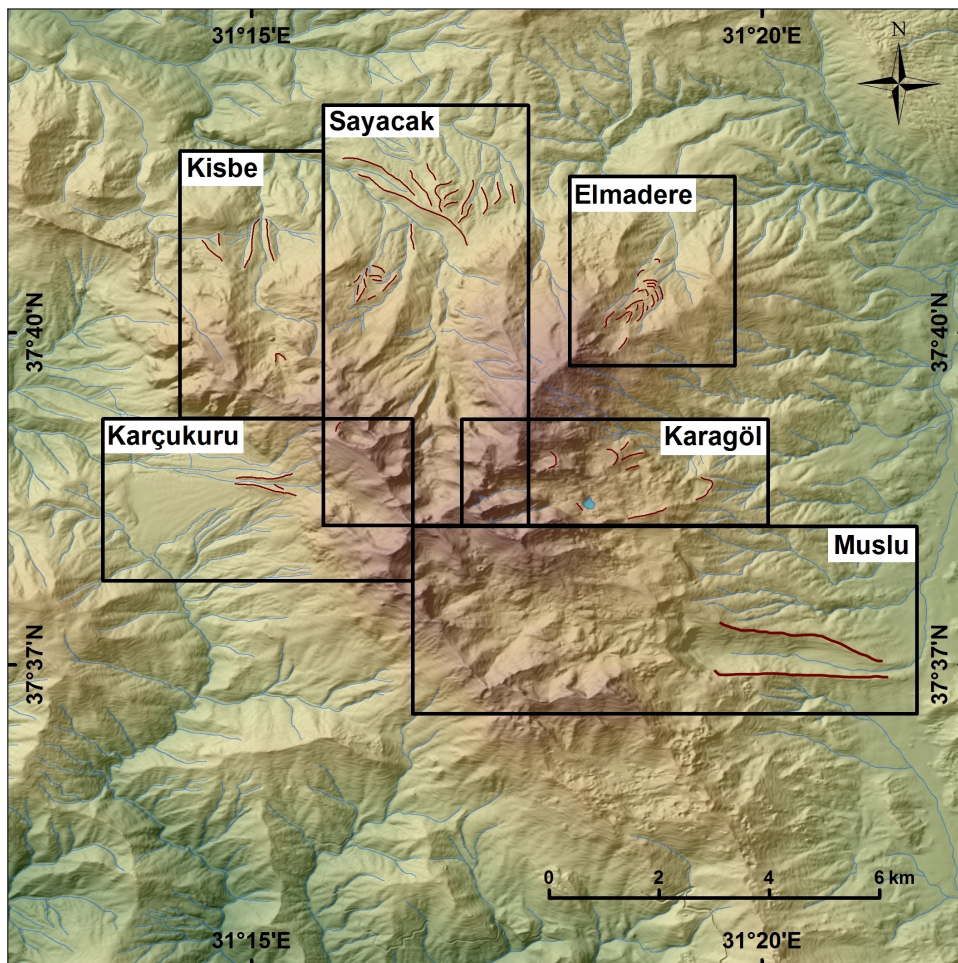
Figure 4.1 : Dedegöl Mountain paleoglacial valleys. Red lines show the moraine crests [14].

4.2 Paleoclimate Surface Mass Balance

The paleoclimatic surface mass balance data were recreated using the approach described in Section 2.2. The maximum surface mass balance values under the paleoclimate conditions used in the model are given in Table 4.1. The highest mass balance value occurred at -10°C offset and 50% precipitation increase than present time as expected. Low temperature and high precipitation increase the mass balance. Precipitation increase leads to a rise in the maximum value of the mass balance. For example, the maximum mass balance is 782 mm/yr when the precipitation rate is unchanged, 999 mm/yr at 25% precipitation increase and, 1217 mm/yr at 50% precipitation increase for 10°C colder than current conditions. The maximum mass balance values increase with temperature offset when precipitation is constant. Table 4.1 also shows the minimum mass balance values in parenthesis for each case. The minimum mass balance values appear at ΔT = -8°C and ΔP = unchanged condition. It means that, under this climatic condition, the glacier budget is minimum. So, the reconstructed glacier area will be smaller than the other conditions. When temperature offset is constant, increasing precipitation rates increase the minimum mass values. In the case, if precipitation remains constant, the decrease in temperature decreases the minimum values of mass balance.

Table 4.1 : Paleoclimatic surface mass balance maximum and minimum
(in parenthesis) values in mm/yr

ΔT	ΔP		
	unchanged	+ %25	+ %50
-8°C	504 (-5352)	705 (-5168)	906 (-4984)
-9°C	664 (-4488)	874 (-4293)	1084 (-4098)
-10°C	782 (-3686)	999 (-3486)	1217 (-3286)

The areal distribution is also very important as well as the minimum and maximum values of the mass balance. The changing mass balance values depending on the elevation are one of the most important factors in the advances of the valley glaciers. The graphical representation of mass balance values of different climate models can be seen in Figure 4.2.

(a) ΔT = -8°C, ΔP = 0%   (b) ΔT = -8°C, ΔP = +25%   (c) ΔT = -8°C, ΔP = +50%

(d) ΔT = -9°C, ΔP = 0%   (e) ΔT = -9°C, ΔP = +25%   (f) ΔT = -9°C, ΔP = +50%

(g) ΔT = -10°C, ΔP = 0%   (h) ΔT = -10°C, ΔP = +25%   (i) ΔT = -10°C, ΔP = +50%

-5500   -4150   -2800   -1450   -100   1250 [mm/yr]
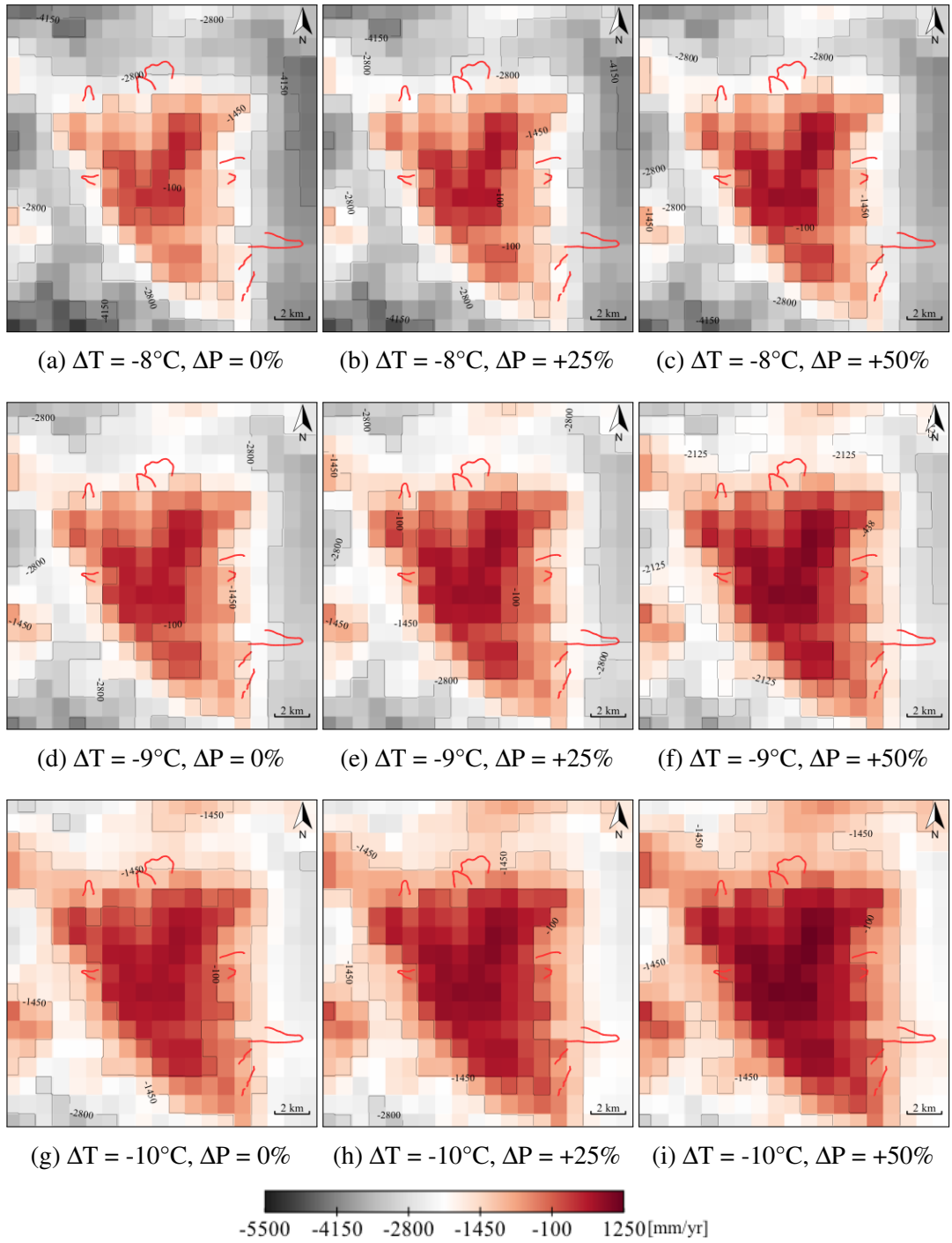
Figure 4.2 : Dedegöl Mountain paleoclimate surface mass balance values
in *mm/year*

It can be seen that the maximum mass balance distrubition is on (i) condition. In that case, the temperature offset (ΔT) is -10°C and the precipitation increase (ΔP) is +50%. The minimum mass balance values were in (a) condition, where ΔT is -8°C and ΔP is unchanged.

4.3 Paleoclimatic Reconstructions Using the PISM

The paleoglaciers of Dedegöl Mountain were modeled by using PISM. Table 4.2 showed Dedegöl Mountain paleoclimatic reconstruction results. The modeled study area is 286 km^2. The area of simulations varies between 15.85 and 94.44 km^2. The glacier area (*iarea*) and the glacial volume (*ivol*) were shown for each model. These two values were used to determine the steady state. A 500 year model time was enough for the largest model to pass the transient zone. After the changes of the *iarea* and *ivol* were minimal, the models were stopped.

Table 4.2 : Dedegöl Mountain paleoclimatic reconstruction. Maximum and Minimum Mass Balance (in parenthesis) (M) [mm/yr], Equilibrium Line Altitude (ELA) [m], Ice volume (*ivol*) [km^3], Ice area (*iarea*) [km^2], Maximum ice thickness (H) [m] were shown for each simulations.

ΔT		ΔP		
		unchanged	+ %25	+ %50
-8°C	M	504 (-5352)	705 (-5168)	906 (-4984)
	ELA	2642±132	2552±130	2444±126
	ivol	0.63	1.51	2.44
	iarea	15.85	27.08	42.51
	H	119	197	225
-9°C	M	664 (-4488)	874 (-4293)	1084 (-4098)
	ELA	2475±131	2343±115	2278±
	ivol	2.19	3.37	4.70
	iarea	37.98	55.56	72.56
	H	214	228	244
-10°C	M	782 (-3686)	999 (-3486)	1217 (-3286)
	ELA	2283±130	2133±113	2066±136
	ivol	4.40	6.14	8.06
	iarea	69.27	94.44	115.09
	H	234	239	255

The glacier geometries modeled with different climatic conditions were shown in Figure 4.3.

(a) ΔT = -8°C, ΔP = 0%   (b) ΔT = -8°C, ΔP = 25%   (c) ΔT = -8°C, ΔP = 50%

(d) ΔT = -9°C, ΔP = 0%   (e) ΔT = -9°C, ΔP = +25%   (f) ΔT = -9°C, ΔP = +50%

(g) ΔT = -10°C, ΔP = 0%   (h) ΔT = -10°C, ΔP = +25%   (i) ΔT = -10°C, ΔP = +50%
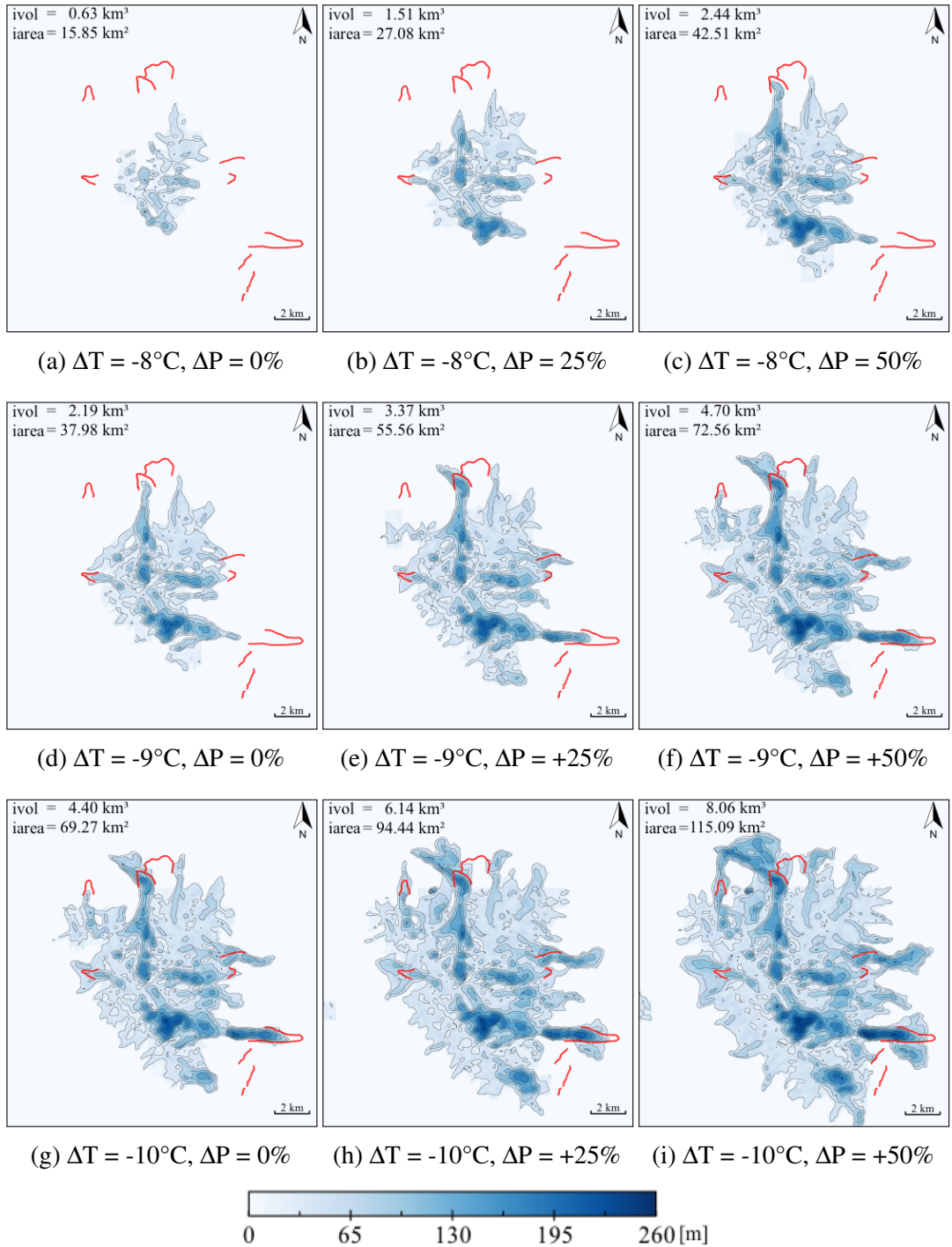
Figure 4.3 : Dedegöl Mountain paleoclimatic reconstruction. Ice thickness was shown in meters. Dark blue color expresses thick glaciers while light blue color indicates thinner glacier. The red continues lines indicate the moraine crests obtained from field studies.

The simulations in this figure were consistent with the mass balance figures which were shown in Figure 4.2. The increasing of surface mass balance extended the glaciers area and increased volume. The smallest ice area was observed in the condition ΔT = -8°C and ΔP = unchanged. The area increases when the precipitation increases. The area increases also with the temperature offset. The *iarea* was 15.85 km^2 at ΔT = -8°C, 37.98 km^2 at ΔT = -9°C and, 69.27 km^2 at ΔT = -10°C when the precipitation was unchanged. The biggest glacier area in the simulations is at ΔT = -10°C and ΔP = 25%. The ice volumes were also increased with temperature offset and precipitation increase.

The modeled glacier extend and moraine crests were matched in Sayacak Valley in the case ΔT = -9°C and ΔP = 25%. The moraines in the area were dated at Early Holocene time [14]. On the other hand, the glacier extent of condition ΔT = -9°C and ΔP = 25% was matched with the Muslu Valley moraine crests which was dated at Last Glacial Maximum.

The models also showed that the temperature decreases more than -10°C did not fit with Dedegöl Mountain moraine deposits.

The ELA values were also given in Figure 4.4. All ELAs were shown as weighted averages of minimum positive mass balance altitude with uncertainties at the 1-sigma level. ELAs were calculated with minimum positive mass balance altitudes. The means of these values with a $\pm 1\sigma$ standard deviation can be seen in Figure 4.4.
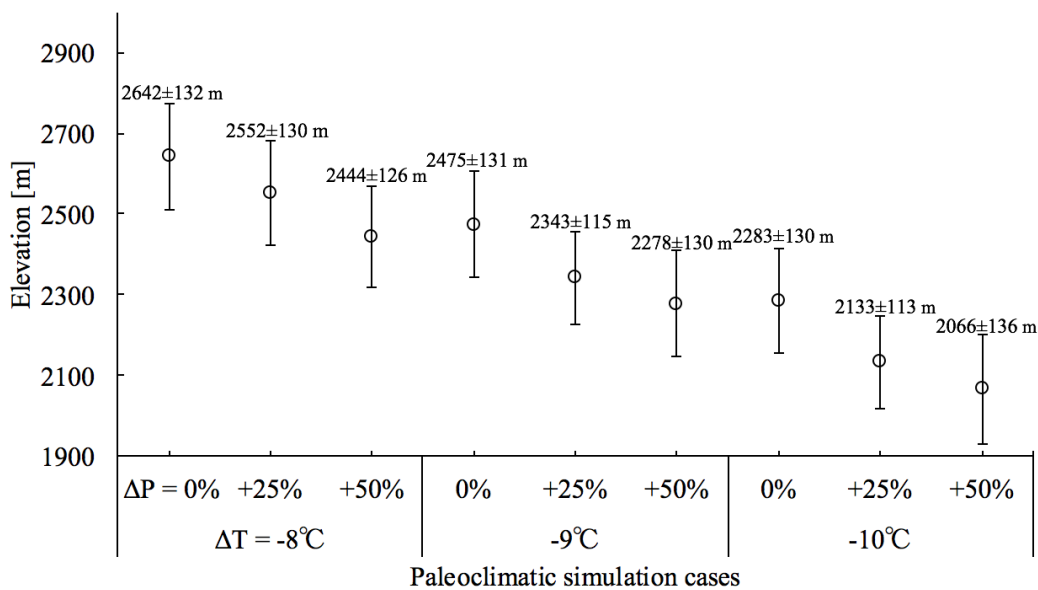
Figure 4.4 : Dedegöl Mountain paleoglacial ELAs with $\pm 1\sigma$.

Figure 4.5 showed the Sayacak Valley Google Earth image with the glacier thickness layer. The paleoclimatic conditions were ΔT = -9°C, ΔP = +25%. The cosmogenic ages were also shown over the moraine deposits. The modeled glacier reached to the front crest which were dated at Early Holocene. The yellow line is used to examine the glacier section along the valley. The black lines indicate that the step change of the glacier thickness.
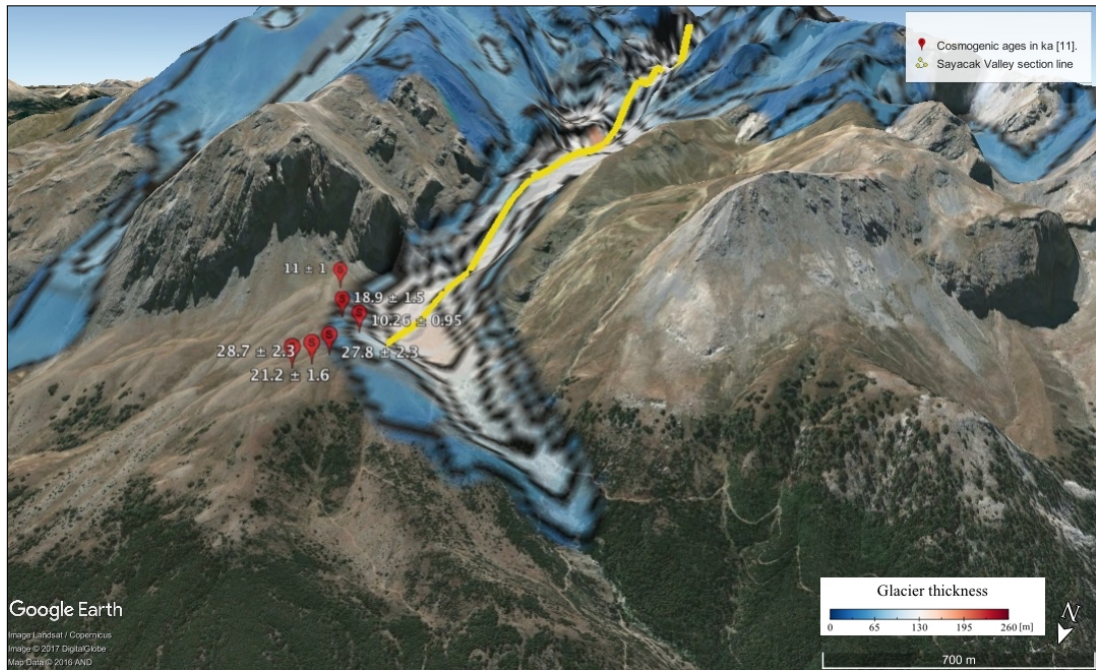
Figure 4.5 : Sayacak Valley Google Earth image with modeled paleoglacier extent layer. Cosmogenic ages of dated rock samples are shown [11]. Climatic conditions are ΔT = -9°C, ΔP = +25%. The yellow line is the section line of the valley.

The drone view image of Sayacak Valley and Google Earth image were shown in Figure 4.6 a and b, respectively. The photography was taken in the field study in July 2016. Google Earth image was recorded in May 2017.
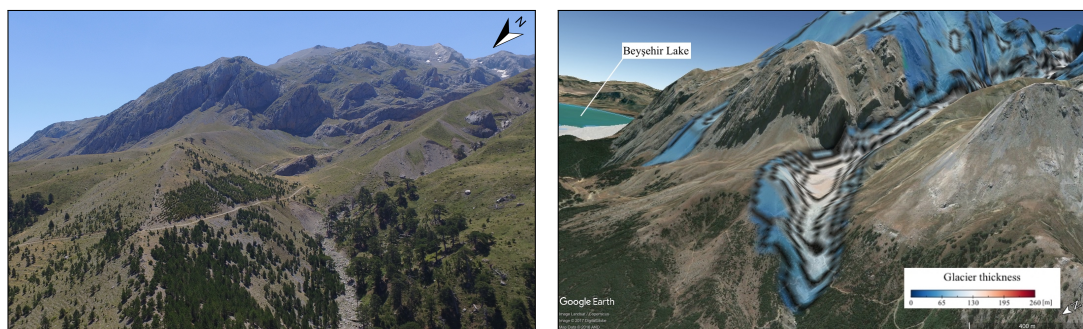
Figure 4.6 : **a)** Sayacak Valley drone view (July 2016) **b)** Google Earth image (May 2017). Climatic conditions are ΔT = -9°C, ΔP = +25%.

37

The sectional views of the Sayacak Valley are shown in Figure 4.7 and 4.8.
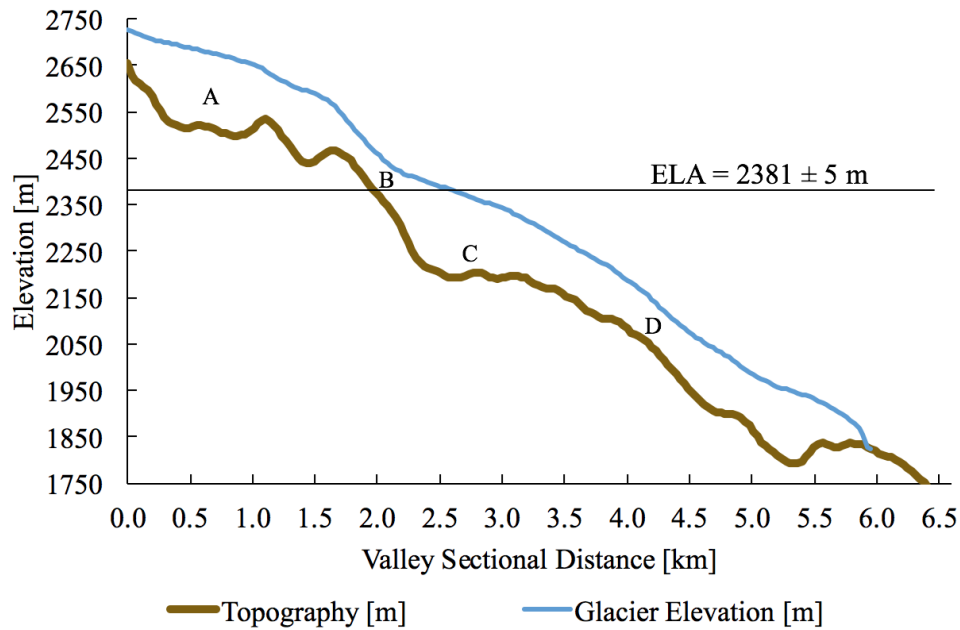
Figure 4.7 : Sayacak Valley sectional view under climatic conditions: ΔT = -9°C and ΔP = +25% (condition (e) in Figure 4.3). The brown continuous line shows bedrock topography for 6.57 *km*. The blue line shows glacier elevation along topography.
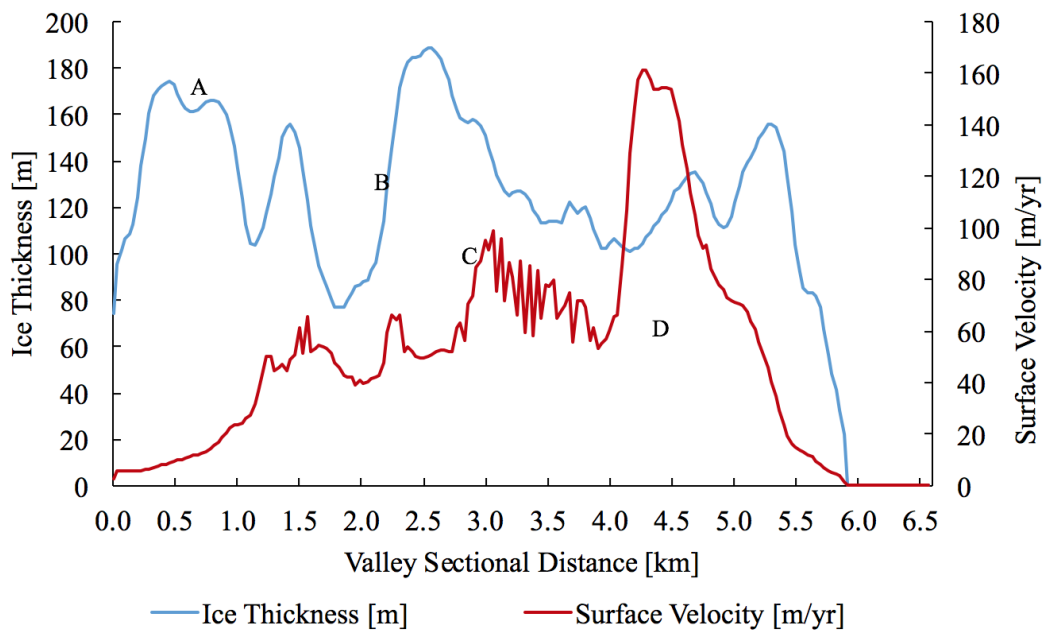
Figure 4.8 : Sayacak Valley sectional view under climatic conditions: ΔT = -9°C and ΔP = +25% (condition (e) in Figure 4.3). The red continuous line shows horizontal velocity at glacier surface. The blue line shows glacier along topography.

The A zone shows the accumulation area of the glacier where the valley glacier first formed. The zone B is the area where velocity is increased with increasing inclination.

38

The velocity of the glacier increases while thickness decreases because of high slope in this area. The thickness of glacier flowing from B to C increased due to the decreasing slope and the bulge at the end of C. As the glacier continues to advance from C to D, the thickness gradually decreases because of the decrease in mass. These results show the topography effect on the glacier movement. The changing of the slopes and the valley profile effect the velocity and thickness.

The ELA line is 2381 ± 5 m for the Sayacak Valley. The mass balance values above this line are positive; and opposite, it is negative. The ELA can be different in other valleys.

4.4 Sensitivity Analysis

The effects of the changes of rf (refreeze factor), ddfs (degree day factor for snow) and ddfi (degree day factor for ice) on the maximum and minimum values of the surface mass balance are shown in Figure 4.9. These parameters are used to calculate the surface mass balance and positive degree days. In the sensitivity analysis, each parameter has been changed from -50% to $+50\%$, with the others kept constant. The default values are $rf = 0.6$; $ddfs = 3$ $d^{-1}{}^{\circ}C^{-1}$ and; $ddfi = 8$ $d^{-1}{}^{\circ}C^{-1}$. So, the change in mass balance is observed. The varying of the parameters affect the maximum mass balance less than minimum mass balance values. The maximum mass balance values were not changed with ddfi. On the contrary, the increase in ddfi leads to an enormous decrease in the minimum mass balance values.

rf increment affects the maximum mass balance in a positive way as expected. The effect of rf on the minimum values is also significant.

The effect of the change of ddfs on the minimum mass balance values is less than the other parameters. On the other hand, with the increase of ddfs, the minimum of mass values is reduced.

The increase of mass balance values causes to extend glacier mass and area. The decrease of mass balance values has a negative effect on the glacier's mass and area.

It can be seen that rf, ddfs and, ddfi parameters are very important on mass balance change. So, these values directly affect the climate models. This makes climate models significantly dependent on mass changes.

These parameters need to be examined in more detail. The areal distribution of mass balance and the changing of each parameter can affect the mass balance values for different elevations.
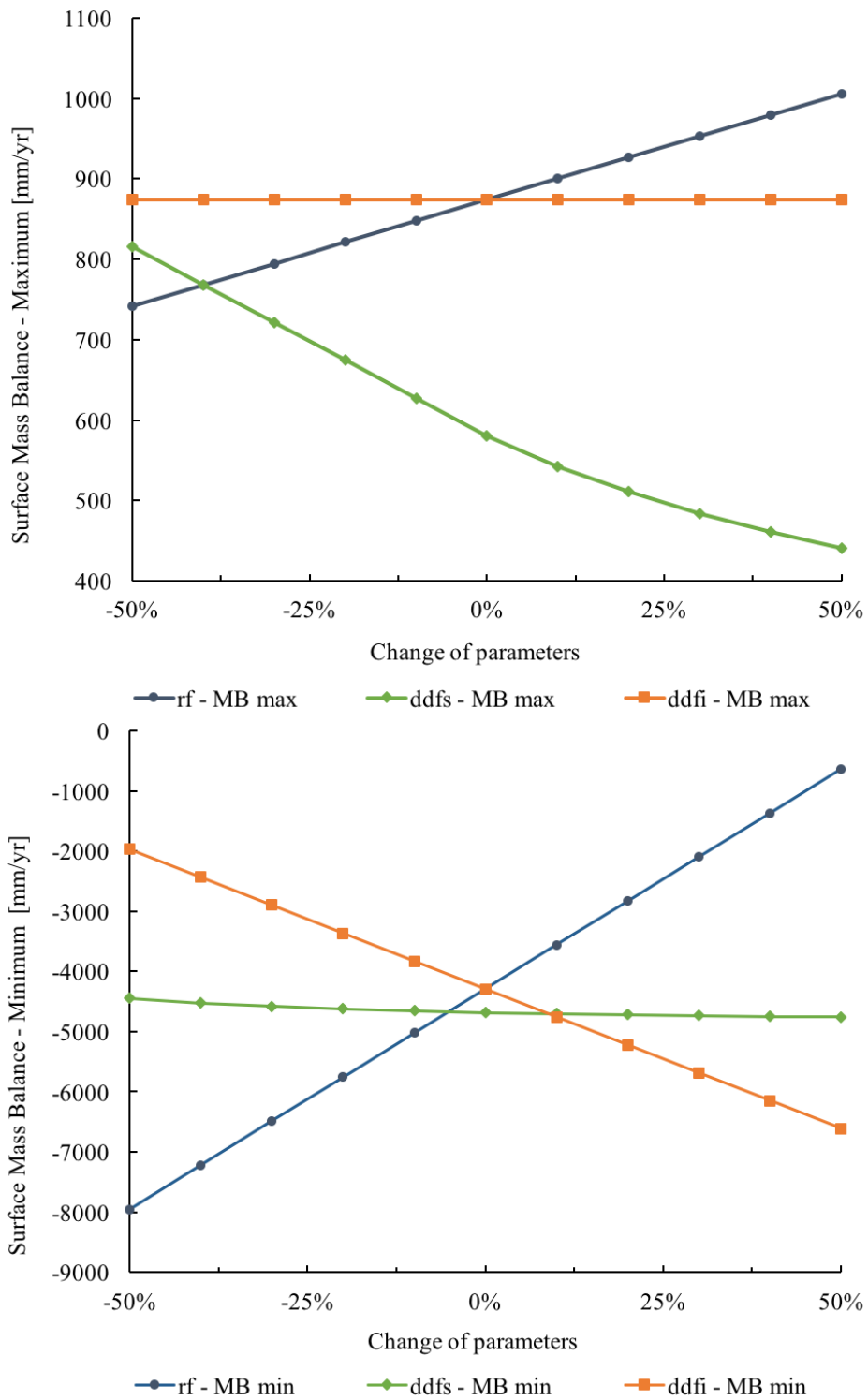
Figure 4.9 : The sensitivity of the parameters used in Surface Mass Balance. Paleoclimatic conditions are $\Delta T = 9°C$ and $\Delta P = +25\%$.

4.5 Comparison of Two-Dimensional Glacier Flow Model and PISM

The Two-Dimensional Glacier Flow Model was described in Section 2.3.6. It was also used to simulate the paleoglaciers. The comparison of it and PISM results were shown in Figure 4.10. Accordingly, the Two-Dimensional Glacier Flow Model produces a larger glacial area compared to the PISM results.
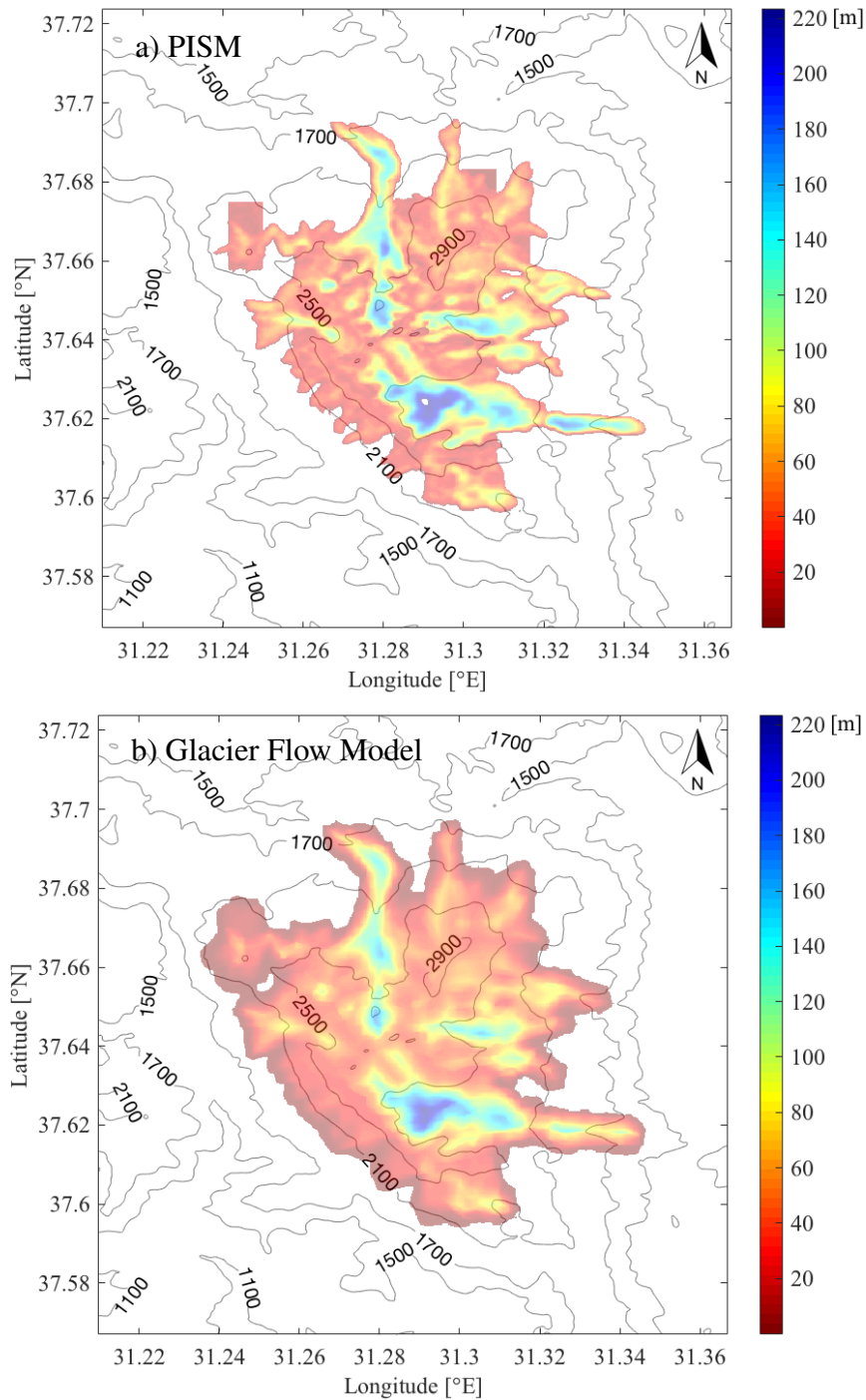
Figure 4.10 : Dedegöl Mountain paleoglaciation under climate condition ΔT = -9°C and ΔP = +25%. **a)** The thickness of paleoglacier obtained from PISM **b)** The thickness obtained from Two-Dimensional Glacier Flow Model.

5. DISCUSSIONS

Using numerical glacier model, a quantitative reconstruction of the temperature depression and precipitation increase from the present in the Dedegöl Mountain were provided. The reconstructed paleoglacial geometries are shown to match with the moraine deposits which are dated with cosmogenic dating methods. The sensitivity of these results to model was also examined. The main findings are as follows: (1) the Parallel Ice Sheet Model is suitable for use in modeling of relatively low resolution mountain glaciers, (2) a temperature depression of 9 to 10°C, accompanied by a 25% precipitation increase, is required for the remodeling of paleoglaciers existed during from the LGM to Early Holocene, (3) using the current digital elevation model can lead to some deterioration in the results due to the moraines blocking the glacier flow, (4) the simulations of different temperature and precipitation input values match with the moraine deposits in different valleys. This indicates that there has been more than one glaciation time in Dedegöl Mountain since the LGM.

In this study, the resolution of digital elevation model was 30 *m*. Although PISM is generally used for ice sheet (with 5-10 *km* resolution), the simulations of valley glaciers were sufficiently realistic. Especially, glacial thicknesses were consistent with the varying slopes through a valley. In addition to the changing of the thickness, the glacier velocity was changed properly in various elevation gradients.

The climate during the LGM was colder than the Early Holocene. This study showed that this difference was about 1°C. However, the precipitation is an important climatic factor. The models with 25% precipitation increase were very convenient with the temperature depressions. The moraine deposits dated to the Early Holocene and the LGM were well matched with the simulation results.

There were different sources of uncertainties. The climate data resolution was about 1 *km* in each direction. Digital elevation model's resolution is 30 *m*. This difference can cause some uncertainties in the mass balance calculation. It can affect the advance or retreat of the glacier in a certain area.

The erosion effect can also be considered as a source of uncertainty. This factor has continued to change the elevations since the LGM.

The moraine deposits in Dedegöl Mountain were matched with different precipitation and temperature change. This results showed that different glacial times occurred during the Late Quaternary in the area. For example, glaciers in Sayacak and Muslu valleys should be modeled with different climatic conditions. The cosmogenic dates of Sayacak Valley rock samples showed that a glacier retreat during the Early Holocene. Similarly, In Muslu Valley, the moraine crests were dated to the LGM.

5.1 Comparison of the Climate Data from WorldClim and the Weather Stations

The WorldClim data was compared with the measured weather stations' data from the Turkish Meteorological Network around the study area (Figure 5.1).
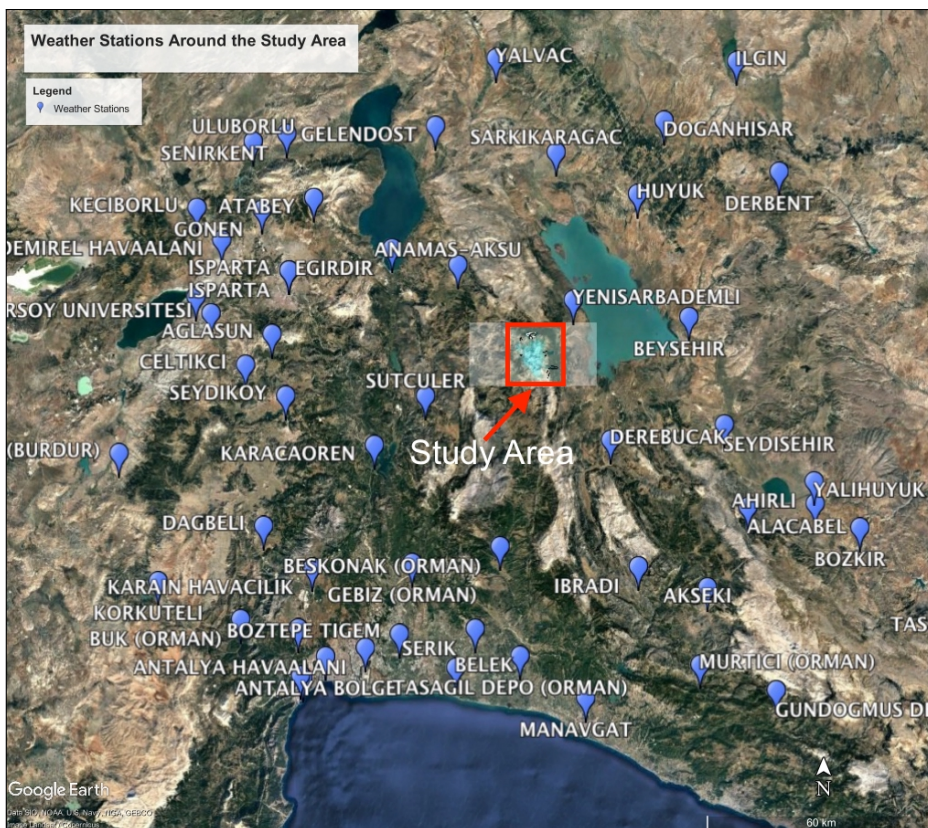
Figure 5.1 : Weather stations around the study area.

Firstly, yearly sum differences from the WorldClim and the station data were compared. The values were gathered from the same coordinates in Figure 5.2. It showed that the station data have higher values than the WorldClim. Near the study area the difference is somewhat minimal (i.e. Beyşehir and Seydişehir stations).

However, on the coastal Mediterranean and on Eğirdir stations the differences were up to about 230 *mm*.
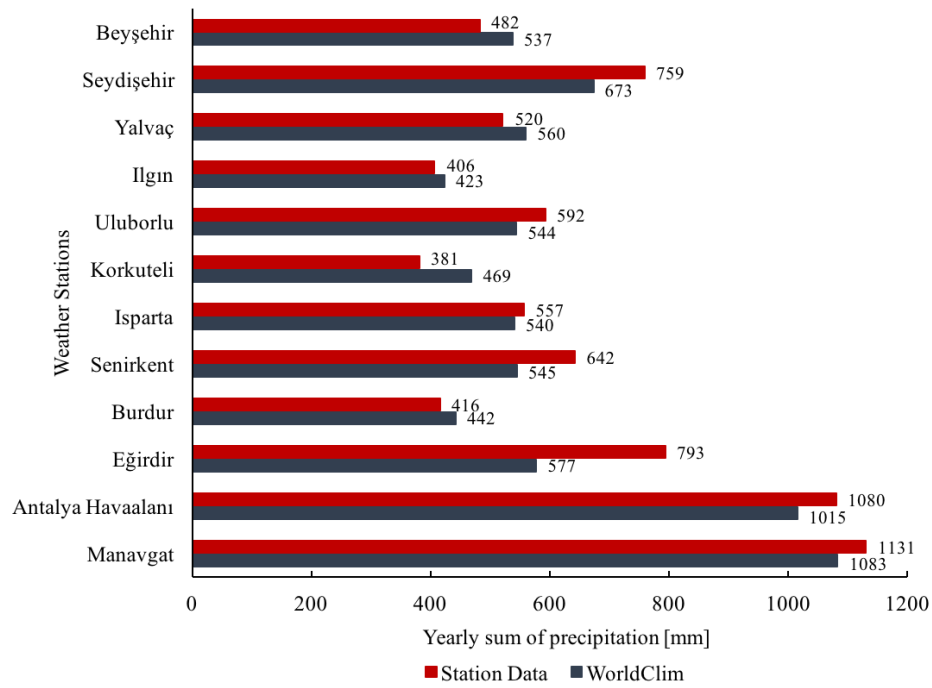
Figure 5.2 : Comparison of the yearly sum of precipitation from the WorldClim and station data around the study area.

On the other hand, if the temperature data were compared, the difference would be minimal. There was no significant differences in the annual average temperatures between the station data and the WorldClim data (Figure 5.3).
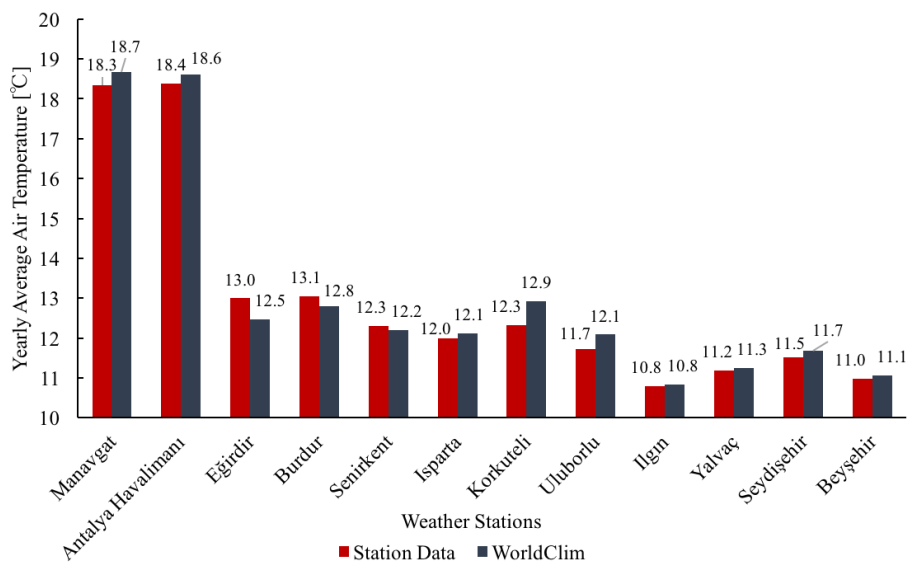
Figure 5.3 : Comparison of the average annual air temperatures from the WorldClim and station data around the study area.

When the temperature lapse rate from both data set was compared, there were no significant difference, either (Figure 5.4).
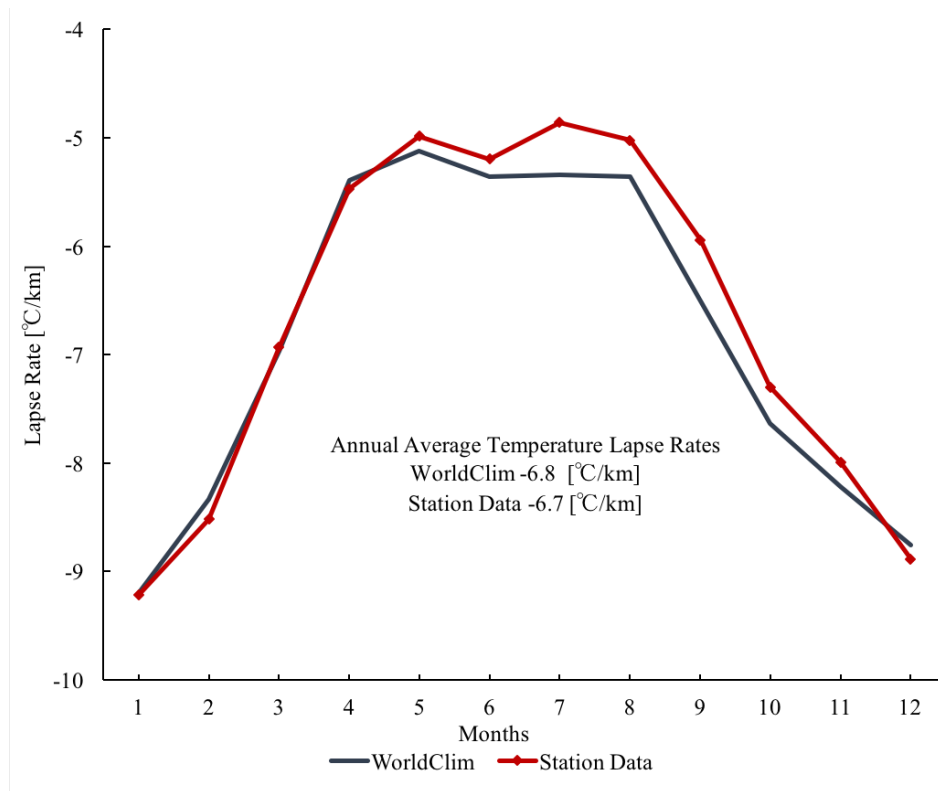
Figure 5.4 : Comparison of the average annual air temperatures from the WorldClim and station data around the study area.

The analysis showed that using the WorldClim data is reasonably suitable for the glacier modeling studies on the 1×1 *km* resolution grids. Other data sets might be tested as well. The differences in terms of the precipitation values can be tested for the future studies.

5.2 Comparison the Snow Accumulation from Brook90 Hydrological Model with the Mass Balance Calculations

Mass balance of the glacier model is calculated by a MATLAB code (APPENDIX B.2). An important outcome of the mass balance calculations is the accumulation of snow. Accumulation of snow calculated by the code was compared with the BROOK90 hydrological model [49]. BROOK90 simulates vertical soil water movement and daily evapotranspiration for all land surfaces at all times of year using a process-oriented approach with physically meaningful parameters [49, 50]. One of the outputs of the BROOK90 model is the monthly snowfall.

When the snow fall from the BROOK90 was compared with the MATLAB calculations, there were some differences in the spring months (Figure 5.5). During the winter months in which the glacier growth is substantial, there are no differences between the BROOK90 and MATLAB calculations. These analyses imply that the input data is accurate and acceptable for the glacial modeling work.
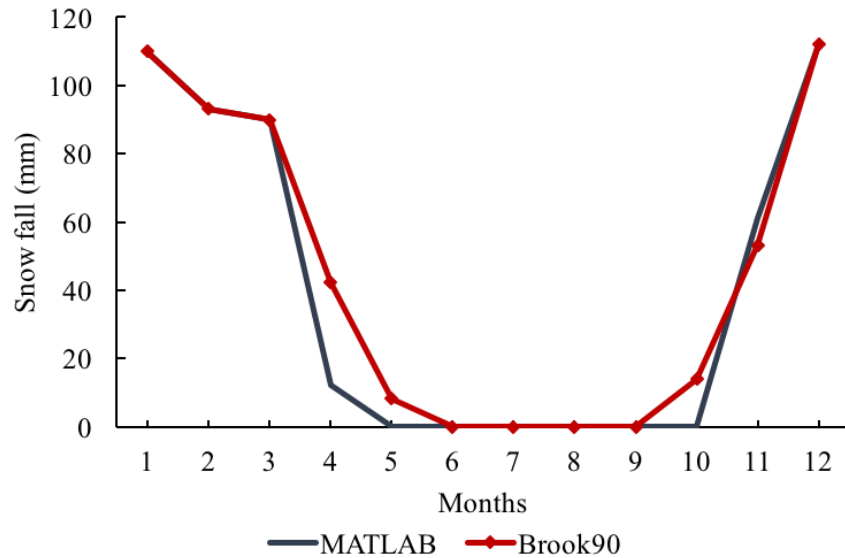
Figure 5.5 : Comparison of the snowfall modeled by the BROOK90 hydrological model and the Accumulation calculations by the MATLAB code.

5.3 Future Studies

Some further studies can be made about the variation of temperature and precipitation values used in palaeoclimate models according to today's values. Regarding this, the model established between present temperature values and paleoprecipitation values in this thesis is a preliminary study. In future studies, it will be useful to examine the variation of such model parameters.

The examination of paleoglacial sites, which were existed in the same area during the same period, is important for the confirmation of the palaeoclimatic reconstructions in the region. Although the results of the study comply with the results in other papers, the methods used in the models and the different parameters vary. For this reason, two dimensional numerical ice flow model and surface mass balance model can be used to model other paleoglacial areas in the southwestern Turkey.

It will be useful to examine the effects of the resolutions of the climate data and the digital elevation models (DEM) that will be used in future studies on the glacier reconstruction. The change in resolution values can change the interaction of the models with the elevation.

The monthly temperature standard deviation (σ) used in PDD calculations is an important factor. The changing of PDD affects the mass balance values and paleoclimatic conditions. The effect of this value on the climate models can be examined in further studies.

Finally, the removal of young moraines from the digital elevation data that are an obstacle in front of older moraine ridges in future studies may increase the accuracy of models. A model should be developed for the removal of moraines that exist in the digital elevation model. This will create a more accurate topography in the model of the valley glaciers that make up moraine deposits.

6. CONCLUSIONS

The paleoglacial modeling and paleoclimate reconstruction were carried out in the Dedegöl Mountain. The nine different climate simulations using a 2-D, coupled mass balance-ice flow model and the PISM showed that air temperatures were depressed by 9°C relative to present and precipitation were 25% more than present values during the Early Holocene. On the other hand, the valley glaciers extending to moraine deposits dated with the LGM age were in conformity with the 10°C temperature depression and 25% precipitation increase. These climate remodeling values are consistent with past studies in the region.

REFERENCES

[1] **Plummer, M.A. and Phillips, F.M.** (2003). A 2-D numerical model of snow/ice energy balance and ice flow for paleoclimatic interpretation of glacial geomorphic features, *Quaternary Science Reviews*, *22*(14), 1389–1406.

[2] **Sarıkaya, M.A.**, **Zreda, M.**, **Ciner, A. and Zweck, C.** (2008). Cold and wet Last Glacial Maximum on Mount Sandiras, SW Turkey, inferred from cosmogenic dating and glacier modeling, *Quaternary Science Reviews*, *27*(7-8), 769–780.

[3] **Sarıkaya, M.A.**, **Zreda, M. and Ciner, A.** (2009). Glaciations and paleoclimate of Mount Erciyes, central Turkey, since the Last Glacial Maximum, inferred from Cl-36 cosmogenic dating and glacier modeling, *Quaternary Science Reviews*, *28*(23-24), 2326–2341.

[4] **Sarıkaya, M.A.**, **Ciner, A. and Zreda, M.** (2011). Quaternary Glaciations of Turkey, *Quaternary Glaciations - Extent and Chronology: A Closer Look*, *15*, 393–403.

[5] **Zahno, C.**, **Akcar, N.**, **Yavuz, V.**, **Kubik, P.W. and Schluchter, C.** (2009). Surface exposure dating of Late Pleistocene glaciations at the Dedegol Mountains (Lake Beyşehir, SW Turkey), *Journal of Quaternary Science*, *24*(8), 1016–1028.

[6] **Akçar, N.**, **Yavuz, V.**, **Yeşilyurt, S.**, **Ivy-Ochs, S.**, **Reber, R.**, **Bayrakdar, C.**, **Kubik, P.W.**, **Zahno, C.**, **Schlunegger, F. and Schlüchter, C.** (2017). Synchronous Last Glacial Maximum across the Anatolian peninsula, *Geological Society, London, Special Publications*, *433*(1), 251–269.

[7] **Erinç, S.** (1952). Glacial evidences of the climatic variations in Turkey, *Geografiska Annaler*, *34*.

[8] **Bayrakdar, C.** (2012). Akdağ Kütlesi'nde (Batı Toroslar) Karstlaşma-Buzul İlişkisinin Jeomorfolojik Analizi, İstanbul University, *Ph.D. thesis*, İstanbul, Turkey.

[9] **Sarıkaya, M.A.** (2012). Kuvaterner Buzullaşmaları: Yayılımı ve zamanlaması [Quaternary glaciations: Extent and timing], *Kuvaterner Bilimi*, *350*, 41–58.

[10] **Monod, O.** (1977). Recherches geologigues dans le Taurus occidental au sud de Beyşehir (Turguie): These, Univ., *Ph.D. thesis*, Paris-Sud, Orsay.

[11] **Delannoy, J. and Maire, R.** (1983). Le massif du Dedegol dag (Taurus occidental, Turquie), *Bulletin de l'Association de Geographie Française*, *491*, 43–53.

[12] **Çılğın, Z.** (2012). Dedegöl Dağı (Batı Toroslar) Buzul Jeomorfolojisi Etüdü, İstanbul University, *Ph.D. thesis*, İstanbul, Turkey.

[13] **Çılğın, Z.** (2015). Dedegöl Dağı Kuvaterner buzullaşmaları, *Türk Coğrafya Dergisi*, *64*, 19–37.

[14] **Köse, O.** (2017). Late Quaternary glaciations and [36]Cl geochronology of the Mount Dedegöl, *M.Sc. Thesis*, Istanbul Technical University, Istanbul, Turkey.

[15] **Çiner, A.** (2004). Turkish glaciers and glacial deposits, *Quaternary Glaciations: Extent and Chronology, Part I: Europe*, 419–429.

[16] **Eaves, S.R.**, **Mackintosh, A.N.**, **Anderson, B.M.**, **Doughty, A.M.**, **Townsend, D.B.**, **Conway, C.E.**, **Winckler, G.**, **Schaefer, J.M.**, **Leonard, G.S. and Calvert, A.T.** (2016). The Last Glacial Maximum in the central North Island, New Zealand: palaeoclimate inferences from glacier modelling, *Climate of the Past*, *12*(4), 943–960.

[17] **Golledge, N.R.**, **Mackintosh, A.N.**, **Anderson, B.M.**, **Buckley, K.M.**, **Doughty, A.M.**, **Barrell, D.J.A.**, **Denton, G.H.**, **Vandergoes, M.J.**, **Andersen, B.G. and Schaefer, J.M.** (2012). Last Glacial Maximum climate in New Zealand inferred from a modelled Southern Alps icefield, *Quaternary Science Reviews*, *46*, 30–45.

[18] **Becker, P.**, **Seguinot, J.**, **Jouvet, G. and Funk, M.** (2016). Last Glacial Maximum precipitation pattern in the Alps inferred from glacier modelling, *Geogr. Helv.*, *71*(3), 173–187.

[19] **Oerlemans, J.** (1988). Simulation of Historic Glacier Variations with a Simple Climate Glacier Model, *Journal of Glaciology*, *34*(118), 333–341.

[20] **Oerlemans, J.** (1992). Climate Sensitivity of Glaciers in Southern Norway - Application of an Energy-Balance Model to Nigardsbreen, Hellstugubreen and Alfotbreen, *Journal of Glaciology*, *38*(129), 223–232.

[21] **Oerlemans, J.** (1997). Climate sensitivity of Franz Josef Glacier, New Zealand, as revealed by numerical modeling, *Arctic and Alpine Research*, *29*(2), 233–239.

[22] **Laabs, B.J.C.**, **Plummer, M.A. and Mickelson, D.M.** (2006). Climate during the last glacial maximum in the Wasatch and southern Uinta Mountains inferred from glacier modeling, *Geomorphology*, *75*(3-4), 300–317.

[23] **Tromp, S.W.** (1941). Notes on the geology and oil possibilities of the areas round, Beyşehir Gölü and Eğirdir Gölü, *Maden Tetkit ve Arama Dergisi*, *97-98*, 1–20.

[24] **Blumenthal, M.** (1951). Recherches geologigues dans le Taurus Occidental dans l'arriere-pays d'Alanya, *Maden Tetkit ve Arama Enstitüsü yayını D*, *5*, 134.

[25] **Türkünal, S.** (1969). Toros Dağları'nın kuzeyde Beyşehir ile güneyde Oymapınar (Homa) köyü enlemleri, doğuda Güzelsu bucağı, batıda Kırkkavak köyü boylamları arasında kalan kesimin jeolojisi, *Elektrik İşleri Etüd İdaresi Rapor, unpublished.*

[26] **Dumont, J.F.** (1976). Isparta kıvrımı ve Antalya naplarının orijini: Torosların Üst Kretase tektonojenezi ile oluşmuş yapısal düzenin büyük bir dekroşman, transtorik arıza ile ikiye ayrılması varsayımı, *Maden Tetkit ve Arama Dergisi, 86,* 56–67.

[27] **Özgül, N.**, **Bölükbaşı, S.**, **Alkan, H.**, **Öztaş, H. and Korucu, M.** (1991). Göller bölgesinin tektono-stratigrafik birlikleri, *Ozan Sungurlu Sempozyumu,* Bld. In: Turgut, S.

[28] **Robertson, A.H.F.** (1994). Mesozoik-Tertiary sedimentary and tectonic evolution of Neotethyan carbonate platforms margins and small ocean basin the Antalya complex of southwest Turkey.

[29] **MTA** (2010). 1/100,000 ölçekli Türkiye Jeoloji haritaları No 15 Isparta-M26 Paftası 2.

[30] **Şenel** (2002). 1/500,000 ölçekli Türkiye Jeoloji haritaları, Konya Paftası.

[31] **Kendrew, W.G.** (1961). *The Climates of the Continents, fifth ed.*, Oxford Press, London.

[32] **Stevens, L.**, **Jr., W.**, **H.E. and Ito, E.** (2001). Proposed changes in seasonality of climate during the Lateglacial and Holocene at Lake Zeribar, Iran, *Holocene, 11,* 747–755.

[33] **Wigley, T. and Farmer, G.** (1982). Climate of the Eastern Mediterranean and Near East. In: Bintliff, J.L., Van Zeist, W. (Eds.), *Paleoclimates, Paleoenvironments and Human Communities in the Eastern Mediterranean Region in Later Prehistory. B.A.R. International Series, 133,* 3–37.

[34] **Hijmans, R.J.**, **Cameron, S.E.**, **Parra, J.L.**, **Jones, P.G. and Jarvis, A.** (2005). Very high resolution interpolated climate surfaces for global land areas, *International Journal of Climatology, 25*(15), 1965–1978.

[35] WorldClim - Global Climate Data. Free climate data for ecological modeling and GIS., `http://www.worldclim.org`, date retrieved: 15.01.2017.

[36] **Wu, H.**, **Guiot, J.**, **Brewer, S. and Guo, Z.** (2007). Climatic changes in Eurasia and Africa at the last glacial maximum and mid-Holocene: reconstruction from pollen data using inverse vegetation modelling, *Climate Dynamics, 20*(2), 211–229, `http://dx.doi.org/10.1007/s00382-007-0231-3`.

[37] **Strandberg, G.**, **Bradegelt, J.**, **Kjellstrom, E. and Smith, B.** (2011). High-resolution regional simulation of last glacial maximum climate in Europe, *Tellus A, 63*(1), 107–125, `http://dx.doi.org/10.1111/j.1600-0870.2010.00485.x`.

[38] **Marshak, S.** (2009). *Essentials of Geology, 4th Edition*, volume 17, WW Norton & Company.

[39] **Ritter, D.F.**, **Kochel, R.C. and Miller, J.R.** (1995). *Process geomorphology*, Boston: McGraw-Hill.

[40] **Wake, L.M. and Marshall, S.J.** (2015). Assessment of current methods of positive degree-day calculation using in situ observations from glaciated regions, *Journal of Glaciology*, *61*(226), 329–344.

[41] **Braithwaite, R.J.** (1995). Positive Degree-Day Factors for Ablation on the Greenland Ice-Sheet Studied by Energy-Balance Modeling, *Journal of Glaciology*, *41*(137), 153–160.

[42] **Zweck, C. and Huybrechts, P.** (2005). Modeling of the northern hemisphere ice sheets during the last glacial cycle and glaciological sensitivity, *Journal of Geophysical Research-Atmospheres*, *110*(D7).

[43] **Shapiro, N.M. and Ritzwoller, M.H.** (2004). Inferring surface heat flux distributions guided by a global seismic model: particular application to Antarctica, *Earth and Planetary Science Letters*, *223*(1-2), 213–224.

[44] **Fastook, J.L. and Chapman, J.E.** (1989). A Map-Plane Finite-Element Model - 3 Modeling Experiments, *Journal of Glaciology*, *35*(119), 48–52.

[45] **Patankar, S.V.** (1980). *Numerical Heat Transfer and Fluid Flow*, Computational Methods in Mechanics and Thermal Sciences, Hemisphere Publishing Corporation, United States of America.

[46] **Greve, R. and Blatter, H.** (2009). *Dynamics of Ice Sheets and Glaciers*, Dynamics of Ice Sheets and Glaciers.

[47] **the PISM authors**, (2016), PISM, a Parallel Ice Sheet Model, `http://www.pism-docs.org`, date retrieved: 01.02.2017.

[48] **Boulder, C.U.P.C.**, (2017), Network Common Data Form (NetCDF), `https://www.unidata.ucar.edu/software/netcdf`, date retrieved: 01.03.2017.

[49] **Federer, C.**, A simulation model for evaporation, soil water, and streamflow., `http://www.ecoshift.net/brook/brook90.htm`, date retrieved: 01.03.2017.

[50] **Federer, C.**, **Vörösmarty, C. and Fekete, B.** (2003). Sensitivity of annual evaporation to soil and root properties in two models of contrasting complexity, *Journal of Hydrometeorology*, *4*(6), 1276–1290.

APPENDICES

APPENDIX A : 2-D Numerical Ice Flow Model (*gla.m*): It runs *function.smb_calc.m* and, simulates a glacier.

APPENDIX B : Codes for mass balance calculations and preparing data for PSIM

APPENDIX B.1 : Main Code: Climatic data importer (*data_importer.m*): It generates *x*, *y*, *topg*, *lat*, *lon*, *thk* variables, runs *function.smb_calc*, *function.bheatflx.m* and, *function.pism_in_gen.m* and, creates an input file for PISM.

APPENDIX B.2 : Surface Mass Balance function (*smb_calc.m*): It imports topography, temperature and precipitation data from *∗.txt* files, calculates positive degree days and surface mass balance.

APPENDIX B.3 : Basal Heat Flux function (*bheatflx.m*): File *hfmap.asc* contains global maps of the heat flow and its standard deviation predicted using the seismic model based extrapolation of the global dataset of heat flow measurements. The extrapolation method is described in [43]. The function *bheatflx.m* code extracts and plots heat flow from the *hfmap.txt* file.

APPENDIX B.4 : netCDF input file for PISM, function (*pism_in_gen.m*): It creates all dimensions, variables, attributes. It also imports *N*, *M*, *lat*, *lon*, *dem*, *mb*, *thk*, *bheatflx*, *prec*, *surtemp* and, writes variables and, generates an *.nc file: *pism_location_T{toffset}_P{pamp}.nc*

APPENDIX C : Parameters used in the study.

APPENDIX D : CD, including all input files, MATLAB codes and PISM outputs

APPENDIX A

```matlab
1  %% Start frompism
2
3  %% Glacier Modeling
4  % imports topography, temperature and precipitation data from ...
       *.txt files,
5  % generates x,y,topg,lat,lon,thk variables.
6  % runs function.smb_calc
7
8  %% Important Notes:
9  % Please add dem.txt, t(1,2,3...).txt and p(1,2,3...).txt files
10 % Input file names have to be:
11     % bed elevation......dem.txt
12     % temperature........t1.txt t2.txt ... (for each month)
13     % precipitation......p1.txt p2.txt ... (for each month)
14
15 % First indices          Second indices          Third indices
16 %  i-  input file       -dem-  bed elevation      -or    ...
       original file
17 %  o-  output           -lat-  latitude           -ml    ...
       matlab file
18 %  r-  results          -mb-   mass balance
19 %                       -h-    bed+glacier elev.
20 %                       -thk-  glacier thickness.
21
22 %-ml up down of -or
23
24 clc
25 clear
26 disp('This code calculates "Glacier Flow for a certain time')
27
28 %% 1- Defining the x,y axes grids distances
29 % disp('1- Defining the x,y axes grids distances.')
30 % disp('   Please enter the distance between two x axis grids')
31 %
32 % prompt = {'x axis [m]:',...
33 %           'y axis [m]:'};
34 % dlg_title = 'Grid distance';
35 % num_lines = 1;
36 % defaultans = {'30','30'};
37 % answer = inputdlg(prompt,dlg_title,num_lines,defaultans);
38 % dx = str2double(answer{1});
39 % dy = str2double(answer{2});
40 dx=30;
41 dy=30;
42
43 %% 2- Importing dem.txt file from the /input_files directory
44 disp('2- Importing dem.txt file from input_files directory')
45
46 topogtext='input_files/dem.txt';
47 delimiterIn=' ';
48 headerlinesIn=6;
49 topog=importdata(topogtext,delimiterIn,headerlinesIn);
50 i_dem_or=topog.data;
51 i_dem_ml=flipud(i_dem_or);
```

```matlab
52
53  for i=1:5
54      info=topog.textdata(i);
55      info2=cell2mat(info);
56      info3=strsplit(info2,' ');
57      info4(i)=info3(2);
58  end
59
60  dimcor=str2double(info4);   %first 5 row of dem file
61                              %1-y 2-x 3-leftdowncorner long ...
                                    [degree_east]
62                              %4-leftdowncorner lat  [degree_north]
63  M=dimcor(1);  %x axis grid number
64  N=dimcor(2);  %y axis grid number
65
66  %% 3- Latitude and longitude degrees
67  disp('3- Calculating latitude and longitude')
68  o_lat_or=zeros(N,M);             %latitude  [degree_north]
69  o_lon_or=zeros(N,M);             %longitude [degree_east]
70  o_lat_or(N,:)=dimcor(4);
71  o_lon_or(:,M)=dimcor(3);
72
73  for i=N:-1:2
74      o_lat_or(i-1,:)=o_lat_or(i,:)+dimcor(5);
75  end
76  for j=M:-1:2
77      o_lon_or(:,j-1)=o_lon_or(:,j)+dimcor(5);
78  end
79
80  o_lat_ml=flipud(o_lat_or);
81  o_lon_ml=fliplr(o_lon_or);
82
83
84  %% 6- Setting time step [s], steps in a year, model time [year]
85  disp('6- Setting time step [s], steps in a year, model time ...
        [year]')
86
87  prompt = {'Start year:',...
88            'End year:',...
89            'Time step - dt [year]:'}; %time step [year];
90  dlg_title = 'Model years';
91  num_lines = 1;
92  defaultans = {'-350','0','1/365'};
93  answer = inputdlg(prompt,dlg_title,num_lines,defaultans);
94  yearstart = str2double(answer{1});
95  yearend   = str2double(answer{2});
96  dt        = str2double(answer{3});
97
98  stepsinyear=1/dt;      %steps in a year
99  modelyear=yearend-yearstart;
100 modeltime=round(modelyear*stepsinyear);
101 showtimes=[' Time step: ' ,num2str(dt),' [year]',...
102           ' Model year: ',num2str(modelyear),' [years]',...
103           ' Count: ',      num2str(modeltime)];
104 disp(showtimes)
105
106 %% 7- Initial Thickness from PISM ex-files
107 disp('7- Getting initial thickness from PISM ex-files')
108 [i_thk_or, i_thk_ml, i_mask_or, i_mask_ml]=ncextracter();
```

```matlab
109
110  %% 8- Flow
111  disp('8- Flow')
112  %The proportionality constant k(x,y)
113  f=0.5;                  %f is the parameter (sliding - ...
         internal deformation)
114  rog=911*9.81;           %density of ice [kg/m^3] x ...
         acceleration due to gravity [m/s^2]
115  m=2;
116  n=3;
117  kx=zeros(N-1,M-1);
118  ky=zeros(N-1,M-1);
119
120  A=6e-16;
121  B=4e-9;
122
123  H=40;
124
125  for i=1:N-1
126      for j=1:M-1
127          kx(i,j)=  abs(f    *           (B)  * (rog^m) * ...
                 ((H)^(m+1))  * ...
                 (((i_dem_or(i+1,j+1)-i_dem_or(i,j+1))/dx)^(m-1))...
128                  +(1-f)*(2/(n+2))*(A/(3.154e7)) * (rog^n) ...
                    * ((H)^(n+2)) * ...
                    (((i_dem_or(i+1,j+1)-i_dem_or(i,j+1))/dx)^(n-1)));
129
130          ky(i,j)=  abs(f    *           (B)  * (rog^m) * ...
                 ((H)^(m+1))  * ...
                 (((i_dem_or(i+1,j+1)-i_dem_or(i+1,j))/dy)^(m-1))...
131                  +(1-f)*(2/(n+2))*(A/(3.154e7)) * (rog^n) ...
                    * ((H)^(n+2)) * ...
                    (((i_dem_or(i+1,j+1)-i_dem_or(i+1,j))/dy)^(n-1)));
132      end
133  end
134  at=zeros(N-2, M-2);
135  atmax=zeros(modeltime,1);
136  atmin=zeros(modeltime,1);
137
138  %flow iteration H
139  Hmodel=i_thk_or;
140  for t=1:modeltime
141      for i=2:N-1
142          for j=2:M-1
143              at(i-1,j-1)   =  (dt/(dx^2)) * ...
                    (kx(i-1,j-1)*(Hmodel(i-1,j)-Hmodel(i,j))  + ...
                    kx(i,j-1)*(Hmodel(i+1,j)-Hmodel(i,j)))...
144                      +(dt/(dy^2)) * ...
                          (ky(i-1,j-1)*(Hmodel(i,j-1)-Hmodel(i,j)) ...
                           + ...
                          ky(i-1,j)*(Hmodel(i,j+1)-Hmodel(i,j)));
145          end
146      end
147      atmax(t)=max(max(at));
148      atmin(t)=min(min(at));
149      Hmodel(2:N-1,2:M-1)=Hmodel(2:N-1,2:M-1)+at;
150  end
151
152  o_thk_or=Hmodel;
```

```matlab
153  o_thk_or(o_thk_or≤0.2)=NaN;
154  o_thk_ml=flipud(o_thk_or);
155  o_h_or=o_thk_or+i_dem_or;      % Final elevation
156  o_h_ml=flipud(o_h_or);
157
158  o_mask_ml=zeros(N,M);
159  i_mask_pos=0;
160  o_mask_pos=0;
161
162  %% i_mask and Area Calc
163  disp('Mask and Area Calc')
164  for i=1:N
165      for j=1:M
166          if i_thk_ml(i,j)>0
167              i_mask_ml(i,j)=2;
168              i_mask_pos=i_mask_pos+1;
169          else
170              i_mask_ml(i,j)=NaN;
171          end
172      end
173  end
174
175  GridArea=N*M;
176  i_area_perc=(i_mask_pos/GridArea)*100;
177  i_area_ml=(((N-1)*0.03)*((M-1)*0.03))*i_area_perc/100;
178
179  %% o_mask and Area Calc
180  disp('Mask and Area Calc')
181  for i=1:N
182      for j=1:M
183          if o_thk_ml(i,j)>0
184              o_mask_ml(i,j)=2;
185              o_mask_pos=o_mask_pos+1;
186          else
187              o_mask_ml(i,j)=NaN;
188          end
189      end
190  end
191
192  o_area_perc=(o_mask_pos/GridArea)*100;
193  o_area_ml=(((N-1)*0.03)*((M-1)*0.03))*o_area_perc/100;
194
195  %% 9- Results
196  disp('9- Writing result files. Please check r_ and o_ files.')
197  r_lon_east=max(max(o_lon_or));
198  r_lon_west=min(min(o_lon_or));
199  r_lat_north=max(max(o_lat_or));
200  r_lat_south=min(min(o_lat_or));
201
202  %% 9- Create some plots
203  disp(' ')
204  disp('9- Plotting')
205  close all
206  vi=[0 90];
207  ax_o_lat_ml=o_lat_ml(:,1)';
208  ax_o_lon_ml=o_lon_ml(1,:);
209
210  %A0 - Topography (i_dem_ML) + Glacier (i_thk_ml)
```

```matlab
211 figure('units','normalized','outerposition',[0.35 0.55 0.35 ...
       0.45])
212 ax3=axes;
213 [C1,h1]=contour(ax_o_lon_ml,ax_o_lat_ml,i_dem_ml,5,'EdgeColor',[0.5 ...
       0.5 0.5],'ShowText','On');
214 h1.LabelSpacing = 1000;
215 h1.LevelList = [1100 1500 1700 2100 2500 2900];
216 xlabel('Longitude [?E]')
217 ylabel('Latitude [?N]')
218
219 ax4=axes;
220 ax4surf=surf(ax_o_lon_ml,ax_o_lat_ml,i_thk_ml,'EdgeColor','none');
221 set(ax4surf,'facealpha',0.4)
222 hax=[ax3 ax4];
223 linkprop(hax,'view');
224
225 ax4.Visible = 'off';
226 ax4.XTick = [];
227 ax4.YTick = [];
228
229 colormap(ax3,flipud(winter))
230 colormap(ax4,flipud(jet))
231 set([ax3,ax4],'Position',[.15 .10 .700 .800]);
232 cb2=colorbar(ax4,'Position',[.90 .10 .025 .800]);
233 caxis(ax3,[min(min(i_dem_ml)) max(max(i_dem_ml))])
234 caxis(ax4,[min(min(o_thk_ml)) max(max(o_thk_ml))*1.01])
235 set(ax4, 'xlim',[r_lon_west r_lon_east],'ylim',[r_lat_south, ...
       r_lat_north], 'zlim', [min(min(o_thk_ml)) ...
       max(max(o_thk_ml))+1.01] );
236
237 %A1 - Topography (i_dem_ML) + Glacier (o_thk_ml)
238
239 figure('units','normalized','outerposition',[0.35 0.55 0.35 ...
       0.45])
240 ax3=axes;
241 [C2,h2]=contour(ax_o_lon_ml,ax_o_lat_ml,i_dem_ml,5,'EdgeColor',[0.5 ...
       0.5 0.5],'ShowText','On');
242 h2.LabelSpacing = 1000;
243 h2.LevelList = [1100 1500 1700 2100 2500 2900];
244 xlabel('Longitude [?E]')
245 ylabel('Latitude [?N]')
246
247 ax4=axes;
248 ax4surf=surf(ax_o_lon_ml,ax_o_lat_ml,o_thk_ml,'EdgeColor','none');
249 set(ax4surf,'facealpha',0.4)
250 hax=[ax3 ax4];
251 linkprop(hax,'view');
252
253 ax4.Visible = 'off';
254 ax4.XTick = [];
255 ax4.YTick = [];
256
257 colormap(ax3,flipud(winter))
258 colormap(ax4,flipud(jet))
259 set([ax3,ax4],'Position',[.15 .10 .700 .800]);
260 cb2=colorbar(ax4,'Position',[.90 .10 .025 .800]);
261 caxis(ax3,[min(min(i_dem_ml)) max(max(i_dem_ml))])
262 caxis(ax4,[min(min(o_thk_ml)) max(max(o_thk_ml))*1.01])
263
```

```matlab
264  set(ax4, 'xlim',[r_lon_west r_lon_east],'ylim',[r_lat_south, ...
         r_lat_north], 'zlim', [min(min(o_thk_ml)) ...
         max(max(o_thk_ml))+1.01] );
265
266  %% B0 - Topography (i_dem_ML) + Mask (i_mask_ml)
267  figure('units','normalized','outerposition',[0.35 0.55 0.35 ...
         0.45])
268  ax3=axes;
269  contour(ax_o_lon_ml,ax_o_lat_ml,i_dem_ml,5,'EdgeColor','cyan');
270  title('B0 - Topography (i-dem-ml) + Glacier Mask (i-mask-ml)');
271
272  ax4=axes;
273  ax4surf=surf(ax_o_lon_ml,ax_o_lat_ml,i_mask_ml,'EdgeColor','none');
274  set(ax4surf,'facealpha',0.4)
275  hax=[ax3 ax4];
276  linkprop(hax,'view');
277
278  ax4.Visible = 'off';
279  ax4.XTick = [];
280  ax4.YTick = [];
281
282  colormap(ax3,flipud(winter))
283  colormap(ax4,flipud(jet))
284  set([ax3,ax4],'Position',[.15 .10 .700 .800]);
285  cb2=colorbar(ax4,'Position',[.90 .10 .025 .800]);
286  caxis(ax3,[min(min(i_dem_ml)) max(max(i_dem_ml))])
287  caxis(ax4,[min(min(o_mask_ml)) max(max(o_mask_ml))*1.01])
288
289  xlabel('Latitude [degree_north]')
290  ylabel('Longitude [degree_east]')
291  set(ax4, 'xlim',[r_lon_west r_lon_east],'ylim',[r_lat_south, ...
         r_lat_north], 'zlim', [min(min(o_mask_ml)) ...
         max(max(o_mask_ml))+1.01] );
292
293  %B1 - Topography (i_dem_ML) + Mask (o_mask_ml)
294  figure('units','normalized','outerposition',[0.35 0.55 0.35 ...
         0.45])
295  ax3=axes;
296  contour(ax_o_lon_ml,ax_o_lat_ml,i_dem_ml,5,'EdgeColor','cyan');
297  title('B1 - Topography (i-dem-ml) + Glacier Mask (o-mask-ml)');
298
299  ax4=axes;
300  ax4surf=surf(ax_o_lon_ml,ax_o_lat_ml,o_mask_ml,'EdgeColor','none');
301  set(ax4surf,'facealpha',0.4)
302  hax=[ax3 ax4];
303  linkprop(hax,'view');
304
305  ax4.Visible = 'off';
306  ax4.XTick = [];
307  ax4.YTick = [];
308
309  colormap(ax3,flipud(winter))
310  %colormap(ax4,flipud(jet))
311  set([ax3,ax4],'Position',[.15 .10 .700 .800]);
312  cb2=colorbar(ax4,'Position',[.90 .10 .025 .800]);
313  caxis(ax3,[min(min(i_dem_ml)) max(max(i_dem_ml))])
314  caxis(ax4,[min(min(o_mask_ml)) max(max(o_mask_ml))*1.01])
315
316  xlabel('Latitude [degree_north]')
```

```matlab
317  ylabel('Longitude [degree_east]')
318  set(ax4, 'xlim',[r_lon_west r_lon_east],'ylim',[r_lat_south, ...
         r_lat_north], 'zlim', [min(min(o_mask_ml)) ...
         max(max(o_mask_ml))+1.01] );
319
320  % B- Convergance
321  figure('units','normalized','outerposition',[0.8 0.5 0.2 0.5])
322  plot(1:modeltime,atmax)
323  title('atmax & atmin - Difference in each iteration')
324  hold on
325  plot(1:modeltime,atmin)
326  xlabel('Iteration number')
327  ylabel('Difference')
328  grid on
329
330  % C- Stability control
331  format short g
332  kxminmax=[min(min(kx)) max(max(kx))];
333  kyminmax=[min(min(ky)) max(max(ky))];
334  hetx=(dx^2)/(4*kxminmax(2));
335  diffx=hetx-dt;
336  if diffx>0
337      OKx='pass';
338  else
339      OKx='fail';
340  end
341  hety=(dy^2)/(4*kyminmax(2));
342  diffy=hety-dt;
343  if diffy>0
344      OKy='pass';
345  else
346      OKy='fail';
347  end
348  diffxy=[diffx diffy]
349  OKpassxy=[OKx; OKy];
350
351  thkminmax=[min(min(o_thk_or)); max(max(o_thk_or))]
352
353  disp('OK. All done!')
```

APPENDIX B.1

```matlab
1  %% data_importer.m
2  % imports topography, temperature and precipitation data from ...
       *.txt files,
3  % generates x,y,topg,lat,lon,thk variables.
4  % runs function.smb_calc, function.bheatflx.m and, ...
       function.pism_in_gen
5
6  %% Important Notes:
7  % Please add dem.txt, t(1,2,3...).txt and p(1,2,3...).txt files
8  % (exported from ArcGis) and, hfmap.txt to "input_files" ...
       directory.
9  % Input file names have to be:
10     % bed elevation......dem.txt
11     % temperature........t1.txt t2.txt ... (for each month)
12     % precipitation......p1.txt p2.txt ... (for each month)
13     % basal heat flux ...hfmap.txt
14
15 % First indices        Second indices          Third indices
16 %   i-  input file      -dem-  bed elevation     -or    ...
       original file
17 %   o-  output          -lat-  latitude          -ml    ...
       matlab file
18 %   r-  results         -mb-   mass balance      -pism  pism ...
       file
19
20 %-ml up down of -or; -pism transpose of -ml
21
22 clc
23 clear
24 disp('This code calculates "Basal Heat Flux, Surface Mass ...
       Balance; creates pism input file (*.nc)')
25
26 %% 1- Defining the x,y axes grids distances
27 disp('1- Defining the x,y axes grids distances.')
28 disp('   Please enter the distance between two x axis grids, ...
       Study Area')
29
30 prompt = {'Study Area:','x axis [m]:','y axis [m]:',...
31           'Temperature offset [C]:','Precipitation ...
               multiplier:',...
32           'Model start year:', 'Model end year:'};
33 %temperature depression value [oC]
34 %precipitation multiplier  (default x2) (Use 0-1 drier ...
       conditions, >1 wetter conditions)
35 dlg_title = 'Input variables';
36 num_lines = 1;
37 defaultans = {'dedegol','30','30','-10','1','-500','0'};
38 answer = inputdlg(prompt,dlg_title,num_lines,defaultans);
39
40 locationname = answer{1};
41 dx = str2double(answer{2});
```

63

```matlab
42  dy = str2double(answer{3});
43  i_toffset = str2num(answer{4});    %#ok<ST2NM>
44  i_pamp = str2num(answer{5});       %#ok<ST2NM>
45  ys = answer{6};
46  ye = answer{7};
47
48  %% 2- Importing dem.txt file from the /input_files directory
49  disp('2- Importing dem.txt file from input_files directory')
50
51  topogtext='/input_files/dem.txt';
52  delimiterIn=' ';
53  headerlinesIn=6;
54  topog=importdata(topogtext,delimiterIn,headerlinesIn);
55  for i=1:5
56      info=topog.textdata(i);
57      info2=cell2mat(info);
58      info3=strsplit(info2,' ');
59      info4(i)=info3(2); %#ok<SAGROW>
60  end
61
62  dimcor=str2double(info4);  %first 5 row of dem file
63                             %1-y 2-x 3-leftdowncorner long ...
64                                 [degree_east]
65                             %       4-leftdowncorner lat  ...
                                   [degree_north]
65  M=dimcor(1);
66  N=dimcor(2);
67
68  o_dem_or=topog.data;
69  o_dem_ml=flipud(o_dem_or);
70  o_dem_pism=o_dem_ml';
71
72  %% 3- Latitude and longitude degrees
73  disp('3- Calculating latitude and longitude')
74  o_lat_or=zeros(N,M);            %latitude  [degree_north]
75  o_lon_or=zeros(N,M);            %longitude [degree_east]
76  o_lat_or(N,:)=dimcor(4);
77  o_lon_or(:,M)=dimcor(3);
78
79  for i=N:-1:2
80      o_lat_or(i-1,:)=o_lat_or(i,:)+dimcor(5);
81  end
82
83  for j=M:-1:2
84      o_lon_or(:,j-1)=o_lon_or(:,j)+dimcor(5);
85  end
86
87  o_lat_ml=flipud(o_lat_or);
88  o_lon_ml=fliplr(o_lon_or);
89  o_lat_pism=o_lat_ml';
90  o_lon_pism=o_lon_ml';
91
92  %% 4- Calculating x and y variables
93  disp('4- Calculating x and y variables')
94  o_x_pism=0:dx:(N-1)*dx;
95  o_y_pism=0:dy:(M-1)*dy;
96
97
98  %% 5- Generate initial glacier area
```

```matlab
99  disp('5- Generating initial glacier area. Default thk=0')
100 o_thk_pism=zeros(N,M);
101
102 %% 6- Generate basal heat flux
103 disp('6- Running Basal Heat Flux Calculator (bheatflx.m)')
104 disp(' ')
105 [r_bheatflx_ml,r_bheatflx_sigma_ml,o_bheatflx_pism] = ...
        bheatflx(); %[W/m2]
106
107 %% 7- Generate basal melt rate
108 disp(' ')
109 disp('7- Generating Basal Melt Rate. Default bmelt=0 m/year')
110 o_bmelt_pism(1:N,1:M)=0; %[m/year]
111
112 %% 8- Results
113 disp('8- Writing result files. Please check r_ and o_ files.')
114 r_lon_east=max(max(o_lon_or));
115 r_lon_west=min(min(o_lon_or));
116 r_lat_north=max(max(o_lat_or));
117 r_lat_south=min(min(o_lat_or));
118
119 %% 9- Surface Mass Balance
120 disp('9- Running Surface Mass Balance Calculator (smb_calc.m)')
121 disp(' ')
122         [o_mb_pism,...
123          r_mb_max,r_mb_min,...
124          r_t_month_mean,r_tt_month_mean,r_tt_year_mean,...
125          r_tt_year_mean_ml,o_tt_year_mean_pism,...
126          r_p_month_mean,r_pp_month_mean,r_pp_year_sum,...
127          r_pp_year_sum_ml,o_pp_year_sum_pism,...
128          r_snow_data_or, r_snow_data_ml,...
129          toffset, pamp] = smb_calc();
130
131 %% 10- Generate ice surface temperature
132 disp(' ')
133 disp('10- Generating Ice Surface Temperature. Default ...
        ice_surf_temp=273.15 K')
134 o_surtemp_pism=o_tt_year_mean_pism; %[C]
135
136 %% 11- Generate ice surface precipitation (Just for pism SMB ...
        calculation.)
137 disp(' ')
138 disp('11- Generating Yearly Precipitation [m/year]')
139 o_prec_pism=o_pp_year_sum_pism/1000; %[C]  %converting ...
        mm/year to m/year
140
141 %% 12- Run Pism input file generator
142 disp('12- Running Pism Input Generator (pism_in_gen.m)')
143 disp(' ')
144         [CheckData_x,CheckData_y,...
145           CheckData_time,CheckData_lat,...
146           CheckData_lon,CheckData_topg,...
147           CheckData_mb,CheckData_prec,...
148           CheckData_surtemp,CheckData_bheatflx,...
149           CheckData_bmelt, CheckData_thk] = pism_in_gen();
150
151 %% 13- Create some plots
152 close all
153 disp(' ')
```

```matlab
154  disp('13- Please choose "Plotting topg and mb with lat and ...
         long axes" or "No"')
155  nextchoise2 = questdlg('Do you want to plot graphics?', ...
156      'Plot graphics', ...
157      'Yes','No','No');
158  % Handle response
159  switch nextchoise2
160      case 'Yes'
161  close all
162  vi=[0 90];
163  ax_o_lat_ml=o_lat_ml(:,1)';
164  ax_o_lon_ml=o_lon_ml(1,:);
165
166  %Bed Topography [m] and Surface Mass Balance [kg/m.year]
167  figure('units','normalized','outerposition',[0 0.55 0.35 0.45])
168  ax1=axes;
169  contour(ax_o_lon_ml,ax_o_lat_ml,o_dem_ml,15,'EdgeColor','cyan');
170  title('Bed Topography [m] and Surface Mass Balance [kg/m.year]');
171
172  ax2=axes;
173  ax2surf=surf(ax_o_lon_ml,ax_o_lat_ml,o_mb_ml,'EdgeColor','none');
174  set(ax2surf,'facealpha',0.4)
175  hax=[ax1 ax2];
176  linkprop(hax,'view');
177
178  ax2.Visible = 'off';
179  ax2.XTick = [];
180  ax2.YTick = [];
181
182  colormap(ax1,flipud(winter))
183  colormap(ax2,flipud(jet))
184  set([ax1,ax2],'Position',[.15 .10 .700 .800]);
185  %cb1=colorbar(ax1,'Position',[.05 .10 .025 .800]);
186  cb2=colorbar(ax2,'Position',[.90 .10 .025 .800]); %#ok<NASGU>
187  caxis(ax1,[min(min(o_dem_ml)) max(max(o_dem_ml))])
188  caxis(ax2,[min(min(o_mb_ml)) max(max(o_mb_ml))])
189
190  xlabel('Latitude [degree_north]')
191  ylabel('Longitude [degree_east]')
192  set(ax2, 'xlim',[r_lon_west r_lon_east],'ylim',[r_lat_south, ...
         r_lat_north], 'zlim', [min(min(o_mb_ml)) ...
         max(max(o_mb_ml))] );
193
194  %Bed Topography [m] and Basal Heat Flux sigma [W/m^2]
195  figure('units','normalized','outerposition',[0.35 0.55 0.35 ...
         0.45])
196  ax3=axes;
197  contour(ax_o_lon_ml,ax_o_lat_ml,o_dem_ml,15,'EdgeColor','cyan');
198  title('Bed Topography [m] and Basal Heat Flux sigma [W/m^2]');
199
200  ax4=axes;
201  ax4surf=surf(ax_o_lon_ml,ax_o_lat_ml,r_bheatflx_ml,'EdgeColor',...
202  'none');
203  set(ax4surf,'facealpha',0.4)
204  hax=[ax3 ax4];
205  linkprop(hax,'view');
206
207  ax4.Visible = 'off';
208  ax4.XTick = [];
```

```matlab
209  ax4.YTick = [];
210
211  colormap(ax3,flipud(winter))
212  colormap(ax4,flipud(jet))
213  set([ax3,ax4],'Position',[.15 .10 .700 .800]);
214  %cb1=colorbar(ax1,'Position',[.05 .10 .025 .800]);
215  cb2=colorbar(ax4,'Position',[.90 .10 .025 .800]); %#ok<NASGU>
216  caxis(ax3,[min(min(o_dem_ml)) max(max(o_dem_ml))])
217  caxis(ax4,[min(min(r_bheatflx_ml)) max(max(r_bheatflx_ml))*1.01])
218
219  xlabel('Latitude [degree_north]')
220  ylabel('Longitude [degree_east]')
221  set(ax4, 'xlim',[r_lon_west r_lon_east],'ylim',[r_lat_south, ...
         r_lat_north], 'zlim', [min(min(r_bheatflx_ml)) ...
         max(max(r_bheatflx_ml))+1.01] );
222
223  %Bed Topography [m] and Temperature (+ toffset) [C]
224  figure('units','normalized','outerposition',[0 0.1 0.35 0.45])
225  ax5=axes;
226  contour(ax_o_lon_ml,ax_o_lat_ml,o_dem_ml,15,'EdgeColor','cyan');
227  title('Bed Topography [m] and Temperature (+ toffset) [C]');
228
229  ax6=axes;
230  ax6surf=surf(ax_o_lon_ml,ax_o_lat_ml,r_tt_year_mean_ml,...
231  'EdgeColor','none');
232  set(ax6surf,'facealpha',0.4)
233  hax=[ax5 ax6];
234  linkprop(hax,'view');
235
236  ax6.Visible = 'off';
237  ax6.XTick = [];
238  ax6.YTick = [];
239
240  colormap(ax5,flipud(winter))
241  colormap(ax6,flipud(jet))
242  set([ax5,ax6],'Position',[.15 .10 .700 .800]);
243  cb2=colorbar(ax6,'Position',[.90 .10 .025 .800]); %#ok<NASGU>
244  caxis(ax5,[min(min(o_dem_ml)) max(max(o_dem_ml))])
245  caxis(ax6,[min(min(r_tt_year_mean_ml)) ...
         max(max(r_tt_year_mean_ml))])
246
247  xlabel('Latitude [degree_north]')
248  ylabel('Longitude [degree_east]')
249  set(ax6, 'xlim',[r_lon_west r_lon_east],'ylim',[r_lat_south, ...
         r_lat_north], 'zlim', [min(min(r_tt_year_mean_ml)) ...
         max(max(r_tt_year_mean_ml))] );
250
251  %Bed Topography [m] and Precipitation (* pamp) [mm/year]
252  figure('units','normalized','outerposition',[0.35 0.1 0.35 0.45])
253  ax7=axes;
254  contour(ax_o_lon_ml,ax_o_lat_ml,o_dem_ml,15,'EdgeColor','cyan');
255  title('Bed Topography [m] and Precipitation (* pamp) [mm/year]');
256
257  ax8=axes;
258  ax8surf=surf(ax_o_lon_ml,ax_o_lat_ml,r_pp_year_sum_ml,...
259  'EdgeColor','none');
260  set(ax8surf,'facealpha',0.4)
261  hax=[ax7 ax8];
262  linkprop(hax,'view');
```

```matlab
263
264 ax8.Visible = 'off';
265 ax8.XTick = [];
266 ax8.YTick = [];
267
268 colormap(ax7,flipud(winter))
269 colormap(ax8,flipud(jet))
270 set([ax7,ax8],'Position',[.15 .10 .700 .800]);
271 cb2=colorbar(ax8,'Position',[.90 .10 .025 .800]);
272 caxis(ax7,[min(min(o_dem_ml)) max(max(o_dem_ml))])
273 caxis(ax8,[min(min(r_pp_year_sum_ml)) ...
        max(max(r_pp_year_sum_ml))])
274
275 xlabel('Latitude [degree_north]')
276 ylabel('Longitude [degree_east]')
277 set(ax8, 'xlim',[r_lon_west r_lon_east],'ylim',[r_lat_south, ...
        r_lat_north], 'zlim', [min(min(r_pp_year_sum_ml)) ...
        max(max(r_pp_year_sum_ml))] );
278
279 % Temperature (+ toffset) [C] and Precipitation (* pamp) ...
        [mm/year]
280 figure('units','normalized','outerposition',[0.7 0.1 0.3 0.45]);
281 monthnum = 1:12;
282 yyaxis left
283 plot(monthnum,r_pp_month_mean,'*-')
284
285 xlabel('Months')
286 ylabel('Precipitation [mm/year]')
287 hold on
288 plot(monthnum,r_p_month_mean,'*--')
289 hold off
290
291 title('Monthly Climate Data')
292 yyaxis right
293 plot(monthnum,r_tt_month_mean,'^-')
294 ylabel('Temperature [C]')
295 hold on
296 plot(monthnum,r_t_month_mean,'^--')
297 legend('Precipitation (Paleo)','Precipitation ...
        (Present)','Temperature (Paleo)','Temperature (Present)')
298 axis([1,12,-inf,inf])
299 hold off
300 grid on
301
302 disp(' ')
303 disp('OK. All done!')
304     case 'No'
305         disp(' ')
306         disp('  OK. All done!')
307 end
```

APPENDIX B.2

```matlab
 1  %% Surface Mass Balance
 2  % Input file names have to be:
 3      %temperature.....t1.txt t2.txt ... (for each month)
 4      %precipitation...p1.txt p2.txt ... (for each month)
 5
 6  % First indices   Second indices     Third indices
 7  %  i- input file  -mb- mass balance  -or   original file
 8  %  o- output                         -ml   matlab file
 9  %  r- results                        -pism pism file
10
11  %-ml up down of -or; -pism transpose of -ml
12
13  function [o_mb_pism,...
14          r_mb_max,r_mb_min,...
15          r_t_month_mean,r_tt_month_mean,r_tt_year_mean,...
16          r_tt_year_mean_ml,o_tt_year_mean_pism,...
17          r_p_month_mean,r_pp_month_mean,r_pp_year_sum,...
18          r_pp_year_sum_ml,o_pp_year_sum_pism,...
19          r_snow_data_or, r_snow_data_ml,...
20          toffset, pamp] = smb_calc()
21  %% 1- Importing the climate values from txt files
22  disp('      This code calculates Surface Mass Balance')
23  disp('      Inputs: t1.txt, t2.txt ... p1.txt...')
24  disp('      Outputs: o_mb_pism,r_mb_max,r_mb_min,...
25  r_tt_month_mean,r_tt_year_mean,r_tt_year_mean_ml,...
26  o_tt_year_mean_pism,r_pp_month_mean,r_pp_year_sum,...
27  r_pp_year_sum_ml,o_pp_year_sum_pism,toffset, pamp')
28
29  toffset=evalin('base','i_toffset');
30  pamp=evalin('base','i_pamp');
31
32  disp('  1- Importing temperature and pricipitation values ...
33      from text files')
34  delimiterIn=' ';
35  headerlinesIn=6;
36  puff=importdata('input_files/t1.txt',delimiterIn,headerlinesIn);
37
38  for i=1:5
39      info5=puff.textdata(i);
40      info6=cell2mat(info5);
41      info7=strsplit(info6,' ');
42      info8(i)=info7(2);
43  end
44
45  dimcor2=str2double(info8);  %first 5 row of t1.txt file
46                             %1-y 2-x 3-leftdowncorner long ...
47                               [degreeE]
48                             %4-leftdowncorner lat  [degreeN]
49  MM=dimcor2(1);
50  NN=dimcor2(2);
51
52  t=zeros(NN,MM,12);          %temperature - all year
53  p=zeros(NN,MM,12);          %precipitation - all year
54  r_t_month_mean=zeros(12,1); %temperature montly mean (1x12)
```

```matlab
53  r_p_month_mean=zeros(12,1);   %precipitation montly mean (1x12)

54

55  for j=1:12                    %12 months

56

57      d_1=strcat('t',num2str(j));
58      file_t=strcat('input_files/',d_1,'.txt');
59      temp=importdata(file_t,delimiterIn,headerlinesIn);
60      t(:,:,j)=temp.data(:,:)./10;
61      r_t_month_mean(j)=mean(mean(t(:,:,j)));

62

63      d_2=strcat('p',num2str(j));
64      file_p=strcat('input_files/',d_2,'.txt');
65      prec=importdata(file_p,delimiterIn,headerlinesIn);
66      p(:,:,j)=prec.data(:,:);
67      r_p_month_mean(j)=mean(mean(p(:,:,j)));
68  end

69

70  %Temp dist. monthly
71  TT=toffset*12;
72  kat= [0.55 0.55 0.65 0.75 0.8 0.9 1 1 0.9 0.8 0.75 0.65];
73  y=TT/sum(kat);
74  month=[y*kat(1)  y*kat(2) y*kat(3) y*kat(4) y*kat(5)...
75          y*kat(6)  y*kat(7) y*kat(8) y*kat(9) y*kat(10)...
76          y*kat(11) y*kat(12)]';
77  tt=t;
78  for i=1:12
79  tt(:,:,i)=t(:,:,i)+month(i);
80  end

81

82  %tt=t+toffset;           % adding toffset to temperature [C]
83  pp=p.*pamp;             % multiplying precipitation with pamp ...
        [mm/month]
84  r_tt_month_mean=r_t_month_mean+toffset; %temperature montly ...
        mean (1x12) + t offset
85  r_pp_month_mean=r_p_month_mean.*pamp;   %precipitation montly ...
        mean (1x12) * p amp

86

87

88  %% 2- Calculate the accumulation of ice and positive degree days
89  disp('   2- Calculating positive degree days and accumulation')
90  rhoi=911;                  %density of ice [kg/m^3]
91  rhow=1000;                 %density of water [kg/m^3]
92  ddfs=3;          %degree day factor for snow [mm/day/C]
93  ddfi=8;          %degree day factor for ice [mm/day/C]
94  sigma=2;         %standart deviations of monthly temp [C]
95  rf=0.6;          %refreeze factor. it is 0.6 from pism ...
        climate forcing manual p.19

96

97  macc=zeros(NN,MM,12);      %monthly accumulation of ice ...
        [mm/month]
98  snow_data=zeros(NN,MM,12); %monthly accumulation of snow ...
        [mm/month]
99  empds=zeros(NN,MM,12);     %expected montly positive degree ...
        day [day.C]
100 pdd=zeros(NN,MM);          %expected yearly positive degree ...
        day [day.C]
101 acc=zeros(NN,MM);          %yearly accumulation of ice  [mm/yr]

102

103 for i=1:NN
```

```matlab
104     for j=1:MM
105         for mo=1:12          %12 months
106             if tt(i,j,mo) ≤0
107                 snow=pp(i,j,mo);
108             elseif tt(i,j,mo)<2
109                 snow=pp(i,j,mo)*abs(tt(i,j,mo)/2-1);
110             else
111                 snow=0;
112             end
113             snow_data(i,j,mo)=snow;
114             macc(i,j,mo)=snow/(rhoi/rhow);
115             %expected monthly positive degree day sum(empds)
116 empds(i,j,mo)=30.4*(0.3989*exp(-1.58*(abs(tt(i,j,mo)/,...
117 sigma))^1.1372)+max(0,tt(i,j,mo)/sigma));
118         end
119             %calculate positive degree days (eq.9 in Zweck ...
                    and Huybrechts, 2005)
120             pdd(i,j)=sum(empds(i,j,:)).*sigma;
121             acc(i,j)=sum(macc(i,j,:));
122     end
123 end
124
125 r_snow_data_or=snow_data;
126 r_snow_data_ml=flipud(r_snow_data_or);
127
128
129 %% 3- Calculate mass balance
130 disp('   3- Calculating mass balance')
131 abl=zeros(NN,MM);            %ablation of ice [mm/yr]
132 meltsnow=zeros(NN,MM);       %melt of snow    [mm/yr]
133 meltice=zeros(NN,MM);        %melt of ice     [mm/yr]
134 pddexcess=zeros(NN,MM);      %pdd excess      [day.C]
135 o_mb_or=zeros(NN,MM);        %mass balance    [mm/a]
136
137 for i=1:NN
138     for j=1:MM
139         if pdd(i,j)*ddfs>acc(i,j) %check if max possible snow ...
                melt is bigger than acc
140             meltsnow(i,j)=acc(i,j); %melt all available snow
141         else
142             meltsnow(i,j)=pdd(i,j)*ddfs; %melt some of the snow
143         end
144         %calculate pddexcess
145         pddexcess(i,j)=pdd(i,j)-meltsnow(i,j)/ddfs;
146         %melt some ice too
147         meltice(i,j)=pddexcess(i,j)*ddfi;
148
149         %refreeze melted ice and compute total abblation
150         abl(i,j)=meltsnow(i,j)+meltice(i,j)-(meltsnow(i,j)+,...
151         meltice(i,j))*rf;
152         o_mb_or(i,j)=acc(i,j)-abl(i,j);
153     end
154 end
155
156 o_mb_ml=flipud(o_mb_or);
157 o_mb_pism=o_mb_ml';
158
159 %% 4- Results
160 disp('   4- Writting result files. Exiting smb_calc.m function')
```

```matlab
161  r_mb_max=max(max(o_mb_or));
162  r_mb_min=min(min(o_mb_or));
163
164  r_tt_year_mean=mean(r_tt_month_mean);
165  r_tt_year_mean_ml=flipud(mean(tt,3));
166  o_tt_year_mean_pism=r_tt_year_mean_ml';
167
168  r_pp_year_sum=sum(r_pp_month_mean);
169  r_pp_year_sum_ml=flipud(mean(pp,3));
170  o_pp_year_sum_pism=r_pp_year_sum_ml';
171
172  assignin('base', 'pamp', pamp);
173  assignin('base', 'toffset', toffset);
174
175  assignin('base', 'o_mb_ml', o_mb_ml);
176  assignin('base', 'o_mb_pism', o_mb_pism);
177  assignin('base', 'r_mb_max', r_mb_max);
178  assignin('base', 'r_mb_min', r_mb_min);
179
180  assignin('base', 'r_tt_month_mean', r_tt_month_mean);
181  assignin('base', 'r_tt_year_mean', r_tt_year_mean);
182  assignin('base', 'r_tt_year_mean_ml', r_tt_year_mean_ml);
183  assignin('base', 'o_tt_year_mean_pism', o_tt_year_mean_pism);
184
185  assignin('base', 'r_pp_month_mean', r_pp_month_mean);
186  assignin('base', 'r_pp_year_sum', r_pp_year_sum);
187  assignin('base', 'r_pp_year_sum_ml', r_pp_year_sum_ml);
188  assignin('base', 'o_pp_year_sum_pism', o_pp_year_sum_pism);
189
190  assignin('base', 'r_snow_data_or', r_snow_data_or);
191  assignin('base', 'r_snow_data_ml', r_snow_data_ml);
192  end
```

APPENDIX B.3

```matlab
1   %File hfmap.asc contains global maps of the
2   %heat flow and its standard deviation predicted using
3   %the seismic model based extrapolation of the
4   %global dataset of heat flow measurements.
5   %Format: lon   lat   HF (mW/m**2)   sigmaHF(mW/m**2)
6   %The extrapolation method is described by Shapiro
7   %and Ritzwoller (2004):
8   %http://ciei.colorado.edu/¬nshapiro/PUBS/,...
9   %Shapiro_Ritzwoller_epsl2004.pdf
10
11  %This function (bheatflx.m) code plots heat flow from ...
        hfmap.txt file
12
13  function [r_bheatflx_ml,r_bheatflx_sigma_ml,o_bheatflx_pism] ...
        = bheatflx()
14
15  %% This code generates a pism_input.nc file.
16  disp('     This code calculates Geothermal Heat Flux. ...
        Shapiro and Ritzwoller (2004)')
17  disp('     Inputs: N,M,o_lat_or, o_lon_or')
18  disp('     Outputs: ...
        bhflux.mat,r_bheatflx_ml,r_bheatflx_sigma_ml,o_bheatflx_pism')
19
20  %% 1- Importing latitude and longitude values from dem.txt
21  disp('   1- Importing latitude and longitude values from ...
        dem.txt')
22  lat_or = round(evalin('base', 'o_lat_or'));
23  lon_or = round(evalin('base', 'o_lon_or'));
24  N = evalin('base', 'N');
25  M = evalin('base', 'M');
26  lat_coor=lat_or+91;
27  lon_coor=lon_or+181;
28
29  %% 2- Loading heat flux from hfmap.mat
30  disp('   2- Loading hfmap.mat')
31  load /hfmap.mat
32
33  lon=0:359;
34  lat=-90:90;
35  bheatflx_ml=zeros(length(lat),length(lon));
36  r_bheatflx_sigma_ml=zeros(length(lat),length(lon));
37
38  %% 3- Generating beheatflx_ml files
39  disp('   3- Generating beheatflx_ml files')
40  for j=1:181
41      bheatflx_ml(j,:)=hfmap(((j-1)*360)+1:j*360,3);
42  end
43
44  for j=1:181
45      r_bheatflx_sigma_ml(j,:)=hfmap(((j-1)*360)+1:j*360,4);
46  end
47
48  hf_ordered=zeros(length(lat),length(lon));
49  hf_ordered(:,181:360)=bheatflx_ml(:,1:180);
```

73

```matlab
50  hf_ordered(:,1:180)=bheatflx_ml(:,181:360);
51  r_bheatflx_ml=zeros(N,M);
52
53  %% 4- Editing lat_coor, lon_coor, o_bheatflx_ml and, ...
       o_bheatflx_pism
54  disp('   4- Editing lat_coor, lon_coor and, o_bheatflx')
55  for i=1:N
56      for j=1:M
57          lat_val=lat_coor(i,j);
58          lon_val=lon_coor(i,j);
59          r_bheatflx_ml(i,j)=hf_ordered(lat_val,lon_val)/1000; ...
               %W/m2
60      end
61  end
62  o_bheatflx_pism=r_bheatflx_ml'; %W/m2
63
64  %% 5- Writing results and output files
65  disp('   5- Writing results and outputfiles and Exiting ...
       bheatflx.m function')
66  assignin('base', 'r_bheatflx_ml', r_bheatflx_ml);
67  assignin('base', 'r_bheatflx_sigma_ml', r_bheatflx_sigma_ml);
68  assignin('base', 'o_bheatflx_pism', o_bheatflx_pism);
69  end
```

APPENDIX B.4

```matlab
1  %% pism_in_gen.m
2  % creates all dimensions, variables, attributes in netcdf file.
3  % imports N,M,lat,lon,dem,mb,thk,bheatflx,prec,surtemp,
4  % writes variables
5  % generates a *.nc file: pism_{location}_T{toffset}_P{pamp}.nc
6
7  function [CheckData_x, CheckData_y,...
8            CheckData_time, CheckData_lat,...
9            CheckData_lon, CheckData_topg,...
10           CheckData_mb, CheckData_prec,...
11           CheckData_surtemp, CheckData_bheatflx,...
12           CheckData_bmelt, CheckData_thk] = pism_in_gen()
13
14 %% This code generates a pism_input.nc file.
15 disp('       This code generates a ...
       pism_{location}_T{toffset}_P{pamp}_thk{initial_thk}.nc file')
16 disp('       Inputs: o_dem_pism, o_lat_pism, o_lon_pism, ...
       o_x_pism, o_y_pism, o_thk_pism, o_mb_pism')
17 disp('       Outputs: ...
       pism_{location}_T{toffset}_P{pamp}_thk{initial_thk}.nc file')
18
19 %% 1- Inputs should be defined before run: N,M
20 disp('   1- Importing N, M, lat, lon, dem, mb, thk, bheatflx, ...
       bmelt, prec, surtemp')
21 N=evalin('base', 'N');
22 M=evalin('base', 'M');
23 o_x_pism = evalin('base', 'o_x_pism');
24 o_y_pism = evalin('base', 'o_y_pism');
25 o_lat_pism = evalin('base', 'o_lat_pism');
26 o_lon_pism = evalin('base', 'o_lon_pism');
27 o_dem_pism = evalin('base', 'o_dem_pism');
28 o_mb_pism = evalin('base', 'o_mb_pism');
29 o_thk_pism = evalin('base', 'o_thk_pism');
30 o_surtemp_pism = evalin('base', 'o_surtemp_pism');
31 o_bheatflx_pism = evalin('base', 'o_bheatflx_pism');
32 o_bmelt_pism = evalin('base', 'o_bmelt_pism');
33
34 toffset=evalin('base', 'toffset');
35 pamp=evalin('base', 'pamp');
36
37 locationname=evalin('base','locationname');
38
39 ys=evalin('base','ys');
40 ye=evalin('base','ye');
41
42 %% 2- Create pism_input.nc file
43 disp('   2- Creating a *.nc file')
44
45 toffsetabs=abs(toffset);
46
47 ffilename=[locationname,'_T',num2str(toffsetabs),...
48            '_P',num2str(pamp)];
49 filename=['pism_',ffilename,'.nc'];
50
```

```matlab
51  cmode = netcdf.getConstant('NETCDF4');          % Define file ...
        type netcdf4
52  ncid = netcdf.create(filename, cmode);
53
54  %% 3- Define x, y and, time dimensions
55  disp('    3- Defining dimensions x, y and, time')
56  dimid_time = netcdf.defDim(ncid,'time',1);
57  dimid_x = netcdf.defDim(ncid,'x',N);
58  dimid_y = netcdf.defDim(ncid,'y',M);
59
60
61  %% 4- Define variables
62  disp('    4- Defining variables x, y, time, lat, lon, mapping, ...
        topg, mb, prec, surtemp, bheatflx, bmelt thk')
63  varid_x       =netcdf.defVar(ncid,'x','NC_FLOAT',dimid_x);%1
64  varid_y       =netcdf.defVar(ncid,'y','NC_FLOAT',dimid_y);%2
65  varid_time    ...
        =netcdf.defVar(ncid,'time','NC_FLOAT',dimid_time);%3
66  varid_lat     ...
        =netcdf.defVar(ncid,'lat','NC_FLOAT',[dimid_y,dimid_x]);%4
67  varid_lon     ...
        =netcdf.defVar(ncid,'lon','NC_FLOAT',[dimid_y,dimid_x]);%5
68  varid_mapping =netcdf.defVar(ncid,'mapping','NC_CHAR',[]);%6
69  varid_topg    ...
        =netcdf.defVar(ncid,'topg','NC_FLOAT',[dimid_y,dimid_x]);%7
70  varid_mb      ...
        =netcdf.defVar(ncid,'climatic_mass_balance','NC_DOUBLE',...
71  [dimid_time,dimid_y,dimid_x]);%8
72  varid_prec    =netcdf.defVar(ncid,'precipitation','NC_DOUBLE',...
73  [dimid_time,dimid_y,dimid_x]);%9
74  varid_surtemp ...
        =netcdf.defVar(ncid,'ice_surface_temp','NC_FLOAT',...
75  [dimid_time,dimid_y,dimid_x]);%10
76  varid_bheatflx=netcdf.defVar(ncid,'bheatflx','NC_FLOAT',...
77  [dimid_time,dimid_y,dimid_x]);%11
78  varid_bmelt   =netcdf.defVar(ncid,'bmelt','NC_FLOAT',...
79  [dimid_time,dimid_y,dimid_x]);%12
80  varid_thk     =netcdf.defVar(ncid,'thk','NC_FLOAT',...
81  [dimid_time,dimid_y,dimid_x]);%13
82  varid_global  =netcdf.getConstant('GLOBAL');
83
84  %% 5- Create global attributes.
85  disp('    5- Creating and define global attributes')
86  netcdf.putAtt(ncid,varid_global,'Title','Pism input Data Set');
87  netcdf.putAtt(ncid,varid_global,'Comments','Created at EIES, ...
        Istanbul Technical University');
88  netcdf.putAtt(ncid,varid_global,'input_code_example','mpiexec ...
        -n 4 pismr -i ...
        pism_{location}_T{toffset}_P{pamp}_thk{initial_thk}.nc ...
        -bootstrap -Mx 565 -My 565 -Mz 11 -Lz 1000 ...
        -bed_smoother_range 0 -ys -100 -ye 0 -extra_file ...
        ex_dedegol_T_P_thk.nc -extra_times -100:1:0 -o ...
        output_dedegol_T_P_thk.nc &> out.output_dedegol_T_P_thk &');
89
90  %% 6- Create attributes associated with the variables.
91  disp('    6- Creating and define attributes associated with ...
        the variables')
92  %6
93  netcdf.putAtt(ncid,varid_mapping,'ellipsoid','WGS84');
```

```matlab
94  netcdf.putAtt(ncid,varid_mapping,'false_easting',0.0);
95  netcdf.putAtt(ncid,varid_mapping,'false_northing',0.0);
96  netcdf.putAtt(ncid,varid_mapping,'grid_mapping_name',...
97  'polar_stereographic');
98  netcdf.putAtt(ncid,varid_mapping,...
99  'latitude_of_projection_origin',90.0);
100 netcdf.putAtt(ncid,varid_mapping,'standard_parallel',71.0);
101 netcdf.putAtt(ncid,varid_mapping,...
102 'straight_vertical_longitude_from_pole',-39.0);
103 %1
104 netcdf.putAtt(ncid,varid_x,'long_name','Cartesian x-coordinate');
105 netcdf.putAtt(ncid,varid_x,...
106 'standard_name','projection_x_coordinate');
107 netcdf.putAtt(ncid,varid_x,'units','meters');
108 %2
109 netcdf.putAtt(ncid,varid_y,'long_name','Cartesian y-coordinate');
110 netcdf.putAtt(ncid,varid_y,'standard_name',...
111 'projection_y_coordinate');
112 netcdf.putAtt(ncid,varid_y,'units','meters');
113 %3
114 netcdf.putAtt(ncid,varid_time,'calender','none');
115 netcdf.putAtt(ncid,varid_time,'long_name','Time');
116 netcdf.putAtt(ncid,varid_time,'standard_name','time');
117 netcdf.putAtt(ncid,varid_time,'units','year since 1-1-1 0:0:0');
118 %4
119 netcdf.putAtt(ncid,varid_lat,'grid_mapping','mapping');
120 netcdf.putAtt(ncid,varid_lat,'long_name','Latitude');
121 netcdf.putAtt(ncid,varid_lat,'standard_name','latitude');
122 netcdf.putAtt(ncid,varid_lat,'units','degree_north');
123 %5
124 netcdf.putAtt(ncid,varid_lon,'grid_mapping','mapping');
125 netcdf.putAtt(ncid,varid_lon,'long_name','Longitude');
126 netcdf.putAtt(ncid,varid_lon,'standard_name','longitude');
127 netcdf.putAtt(ncid,varid_lon,'units','degree_east');
128 %7
129 netcdf.putAtt(ncid,varid_topg,'reference','ArcGIS');
130 netcdf.putAtt(ncid,varid_topg,'comment','30x30m grid size');
131 netcdf.putAtt(ncid,varid_topg,'grid_mapping','mapping');
132 netcdf.putAtt(ncid,varid_topg,'long_name','Bedrock Topography');
133 netcdf.putAtt(ncid,varid_topg,'standard_name','bedrock_altitude');
134 netcdf.putAtt(ncid,varid_topg,'units','meters');
135 netcdf.putAtt(ncid,varid_topg,'coordinates','lat lon');
136 %8
137 netcdf.putAtt(ncid,varid_mb,'reference','model_input file');
138 netcdf.putAtt(ncid,varid_mb,'grid_mapping','mapping');
139 netcdf.putAtt(ncid,varid_mb,'long_name','Surface Mass Balance');
140 netcdf.putAtt(ncid,varid_mb,'standard_name',...
141 'land_ice_surface_specific_mass_balance_flux');
142 netcdf.putAtt(ncid,varid_mb,'units','kg m-2 year-1');
143 netcdf.putAtt(ncid,varid_mb,'coordinates','lat lon');
144 %9
145 netcdf.putAtt(ncid,varid_prec,'reference','WorldClim');
146 netcdf.putAtt(ncid,varid_prec,'grid_mapping','mapping');
147 netcdf.putAtt(ncid,varid_prec,'long_name','Present ...
       Precipitation');
148 netcdf.putAtt(ncid,varid_prec,'standard_name',...
149 'lwe_precipitation_rate');
150 netcdf.putAtt(ncid,varid_prec,'units','meters/year');
151 netcdf.putAtt(ncid,varid_prec,'coordinates','lat lon');
```

```matlab
152 %10
153 netcdf.putAtt(ncid,varid_surtemp,'reference','NaN');
154 netcdf.putAtt(ncid,varid_surtemp,'grid_mapping','mapping');
155 netcdf.putAtt(ncid,varid_surtemp,'long_name',...
156 'Annual Mean Air Temperature (2 meter)');
157 netcdf.putAtt(ncid,varid_surtemp,'standard_name',...
158 'air_temperature');
159 netcdf.putAtt(ncid,varid_surtemp,'units','Celsius');
160 netcdf.putAtt(ncid,varid_surtemp,'coordinates','lat lon');
161 %11
162 netcdf.putAtt(ncid,varid_bheatflx,'reference','NaN');
163 netcdf.putAtt(ncid,varid_bheatflx,'grid_mapping','mapping');
164 netcdf.putAtt(ncid,varid_bheatflx,'long_name','Basal Heat Flux');
165 netcdf.putAtt(ncid,varid_bheatflx,'standard_name',...
166 'basal_heat_flux');
167 netcdf.putAtt(ncid,varid_bheatflx,'units','watts/meter^2');
168 netcdf.putAtt(ncid,varid_bheatflx,'coordinates','lat lon');
169 %12
170 netcdf.putAtt(ncid,varid_bmelt,'reference','NaN');
171 netcdf.putAtt(ncid,varid_bmelt,'grid_mapping','mapping');
172 netcdf.putAtt(ncid,varid_bmelt,'long_name','Ice Basal Melt ...
        Rate');
173 netcdf.putAtt(ncid,varid_bmelt,'standard_name',...
174 'land_ice_basal_melt_rate');
175 netcdf.putAtt(ncid,varid_bmelt,'short_name','bmelt');
176 netcdf.putAtt(ncid,varid_bmelt,'units','m/year');
177 netcdf.putAtt(ncid,varid_bmelt,'coordinates','lat lon');
178 %13
179 netcdf.putAtt(ncid,varid_thk,'reference','Initial. Cond.');
180 netcdf.putAtt(ncid,varid_thk,'grid_mapping','mapping');
181 netcdf.putAtt(ncid,varid_thk,'long_name','Ice Thickness');
182 netcdf.putAtt(ncid,varid_thk,'standard_name',...
183 'land_ice_thickness');
184 netcdf.putAtt(ncid,varid_thk,'units','meters');
185 netcdf.putAtt(ncid,varid_thk,'coordinates','lat lon');
186
187 %% 7- Set variable's default values NaN
188 disp('   7- Setting variables default values NaN')
189
190 netcdf.defVarFill(ncid,varid_x,false,NaN);          %1
191 netcdf.defVarFill(ncid,varid_y,false,NaN);          %2
192 netcdf.defVarFill(ncid,varid_time,true,0);          %3
193 netcdf.defVarFill(ncid,varid_lat,false,NaN);        %4
194 netcdf.defVarFill(ncid,varid_lon,false,NaN);        %5
195 netcdf.defVarFill(ncid,varid_topg,false,NaN);       %7
196 netcdf.defVarFill(ncid,varid_mb,false,NaN);         %8
197 netcdf.defVarFill(ncid,varid_prec,false,NaN);       %9
198 netcdf.defVarFill(ncid,varid_surtemp,false,NaN);    %10
199 netcdf.defVarFill(ncid,varid_bheatflx,false,NaN);   %11
200 netcdf.defVarFill(ncid,varid_bmelt,false,NaN);      %12
201 netcdf.defVarFill(ncid,varid_thk,false,NaN);        %13
202
203 %% 8- Leave define mode and enter data mode to write data
204 disp('   8- Leaving define mode and enter data enter mode')
205 netcdf.endDef(ncid)
206
207 %% 9- Write 'model input' data to variables.
208 disp('   9- Writing model input data to variables')
209 netcdf.putVar(ncid,varid_x,o_x_pism);
```

78

```matlab
210  netcdf.putVar(ncid,varid_y,o_y_pism);
211  % netcdf.putVar(ncid,varid_time,null);
212  netcdf.putVar(ncid,varid_lat,o_lat_pism);
213  netcdf.putVar(ncid,varid_lon,o_lon_pism);
214  netcdf.putVar(ncid,varid_topg,o_dem_pism);
215  netcdf.putVar(ncid,varid_mb,o_mb_pism);
216  % netcdf.putVar(ncid,varid_prec,null);
217  netcdf.putVar(ncid,varid_surtemp,o_surtemp_pism);
218  netcdf.putVar(ncid,varid_bheatflx,o_bheatflx_pism);
219  netcdf.putVar(ncid,varid_bmelt,o_bmelt_pism);
220  netcdf.putVar(ncid,varid_thk,o_thk_pism);
221
222  %% 10- Writing CheckData_ files
223  disp('   10- Writing CheckData_ files')
224  netcdf.close(ncid)
225  CheckData_x=ncread(filename,'x'); %1
226  CheckData_y=ncread(filename,'y'); %2
227  CheckData_time=ncread(filename,'time'); %3
228  CheckData_lat=ncread(filename,'lat');    %4
229  CheckData_lon=ncread(filename,'lon');    %5
230  CheckData_topg=ncread(filename,'topg'); %7
231  CheckData_mb=ncread(filename,'climatic_mass_balance'); %8
232  CheckData_prec=ncread(filename,'precipitation');       %9
233  CheckData_surtemp=ncread(filename,'ice_surface_temp'); %10
234  CheckData_bheatflx=ncread(filename,'bheatflx'); %11
235  CheckData_bmelt=ncread(filename,'bmelt'); %12
236  CheckData_thk=ncread(filename,'thk'); %13
237
238  %% 11- Closing the ...
         pism_{location}_T{toffset}_P{pamp}_thk{initial_thk}.nc.nc ...
         file')
239  disp('   11- Closing the ...
         pism_{location}_T{toffset}_P{pamp}_thk{initial_thk}.nc.nc ...
         file')
240
241  %% 12- Pism Run Code
242  disp('   12- Here is a pism run code:')
243  pism_runner=['mpiexec -n 8 pismr -i ',filename,' -bootstrap ...
244  -Mx ',num2str(N),' -My ',num2str(M),' -Mz 11 -Lz 600 ...
245   -bed_smoother_range 0 -ys ',ys,' -ye ',ye,' -surface given ...
246    -ts_file ts_',ffilename,'.nc -ts_times ',ys,':yearly:',ye, ...
247    ' -extra_file ex_',ffilename,'.nc -extra_times ...
         ',ys,':5:',ye, ...
248    ' -extra_vars tempicethk_basal,bmelt,velsurf_mag,mask,thk, ...
249    topg,lat,lon,usurf -o output_',ffilename,'.nc &> run_', ...
250    ffilename,'.txt &'];
251  disp(pism_runner)
252
253  disp('13- Run command file generation')
254  file=['runner_',ffilename,'.txt'];
255  fid = fopen(file,'w');
256  fprintf(fid, pism_runner);
257  fclose(fid);
258
259  % assignin('base', 'pism_runner', pism_runner);
260  % assignin('base', 'filename', filename);
261  disp('   13- Exiting pism_in_gen.m function')
262  end
```

APPENDIX C

Table A.1 : Parameters used in the study.

A	6e-16 $yr^{-1}Pa^{-3}$
B	4e-9 $myr^{-1}Pa^{-2}$
ddfi	8 $d^{-1}°C^{-1}$
ddfs	3 $d^{-1}°C^{-1}$
g	9.81 m/s^2
ρ	911 kg/m^3
rf	0.6
ye	500 yr
ys	0

APPENDIX D

CD

CURRICULUM VITAE

Name Surname: Adem Candaş

Place and Date of Birth: Dinar, 4 April 1988

E-Mail: candas@itu.edu.tr

EDUCATION:

- **M.Sc.:** 2017, Istanbul Technical University, Eurasia Institute of Earth Sciences, Geodynamics.

- **M.Sc.:** 2013, Istanbul Technical University, Mechanical Engineering Faculty, Mechanical Design.

- **B.Sc.:** 2013, Anadolu University (Open Education), Public Administration.

- **B.Sc.:** 2010, Istanbul Technical University, Mechanical Engineering Faculty, Mechanical Engineering.

PROFESSIONAL EXPERIENCE AND REWARDS:

- 2010-... Istanbul Technical University at Mechanical Engineering Faculty, Research Assistant

- 2009 TOFAS, Turk Otomobil Fabrikaları, Bursa, Turkey

PUBLICATIONS, PRESENTATIONS AND PATENTS ON THE THESIS:

- Candaş A., Sarıkaya M. A., 2017. A new attempt of 2-D numerical ice flow model to reconstruct paleoclimate from mountain glaciers, Poster, *EGU 2017, European Geosciences Union General Assembly*, Apr 23-28, 2017 Vienna, Austria.

- Candaş A., Sarıkaya M. A., 2016. Two Dimensional Numerical Ice Flow Modeling: a New Approach to Reconstruct the Paleoclimate from Glacial Recors, Poster, *TURQUA 2016, Turkey Quaternary Symposium*, May 08-11, 2016 Istanbul, Turkey.

OTHER PUBLICATIONS, PRESENTATIONS AND PATENTS:

- Atay S., Kayaoğlu E., Candaş A., İmrak C. E., 2014. Determination of Loads Acting on Guide Rail Fixing Under Certain Loading Condition, Poster, *ELEVCON 2014, The 20th International Congress on Vertical Transportation Technologies*, Jul 08-10, 2014 Paris, France.

- Candaş A., Kayaoğlu E., 2013. FEM and Experimental Stress analysis of a Jib Crane, Presentation, *ADME 2013, The 3rd International Conferance on Advanced Design and Manufacutring Engineering*, Anshan, China.

- Elmalı S., Candaş A., Kayaoğlu E., İmrak C. E., Targıt S., 2012. Modeling and Analysis of Guide Rail Brackets and Attaching Parts, Presentation, *ELEVCON 2012, The 19th International Congress on Vertical Transportation Technologies*, May 22-24, 2012 Miami, USA.

- Gerdemeli İ., Çotur A. E., Kayaoğlu E., Candaş A., 2011. Computer Aided Valve Design of Shock Absorbers Used in Vehicles, Presentation, *Advanced Design and Manufacture IV 2011*, 2011 Kunming, China.